

Interactive comment on “Iron budgets for three distinct biogeochemical sites around the Kerguelen archipelago (Southern Ocean) during the natural fertilisation experiment KEOPS-2” by A. R. Bowie et al.

Anonymous Referee #1

Received and published: 20 January 2015

General comments:

I found this to be a well-written synthesis paper bringing together many aspects of the other manuscripts in this special issue to produce a set of comprehensive iron budgets from the data collected. The paper combines dissolved and particulate iron concentration measurements made during the KEOPS-2 cruise with export fluxes, iron uptake and regeneration rates and estimates of lateral, upwelling, vertical diffusive and entrainment processes measured during the same study to synthesize biogeochemical iron budgets at three contrasting sites within the Kerguelen archipelago region: over the plateau, downstream of the islands and at a reference site upstream of the Kerguelen plateau. There are very few examples of such budgets available in the literature and so this study represents an important addition to our understanding of the relative importance of various supply terms in the biogeochemical cycle of iron in the ocean. The inclusion of an estimate of the vertical entrainment of iron in this case suggests an overlooked but significant supply term in the surface ocean iron budget. Similarly, the relatively low contribution calculated to be supplied by bacterial regeneration and zooplankton grazing in this study compared to the other iron budgets available highlights the variability of this term. My recommendation is that this manuscript be published in Biogeosciences after a few minor points are addressed.

We thank the reviewer for his/her very positive comments.

Specific comments:

There is no reference made to blanks measured during the description of particulate iron sampling (page 17872, section 2.3.2). I appreciate that this part of the study is described in more detail in an accompanying paper, but I think it would be worthwhile to include something to the effect that blanks were carried out and were low compared to sample measurements (which I assume was the case).

Procedures for determining blanks for particulate iron were reported in the companion paper (Table A1 in van der Merwe et al., 2015) following methods previously documented in Bowie et al. (2010). Blanks were typically 2-3% and <1% of the pFe sample concentrations for the ISP deployments and

P-trap deployments, respectively. The following sentence has been added to the manuscript (page 17872, lines 16-).

“Blanks from replicate analysis of filters treated identically to the sample filters, but without large volumes of seawater passed through them, were typically 2-3% and <1% of the pFe sample concentrations for the ISP deployments and P-trap deployments, respectively.”

In comparing the two dFe profiles at stations A3-1 and A3-2 (page 17877, lines 7-8), the authors state that “below the mixed layer, similar profiles were observed during both visits to A3”. However, it appears that the profile below the mixed layer during A3-1 consists of two points. Whilst the both profiles do show an increase in dFe concentration with depth below the mixed layer, based upon interpolation between the data points available, I feel the fact that only two data points contribute to the A3-1 profile makes the statement a little misleading.

As noted on page 17877 line 9, operational constraints (bad weather) prevented us from sampling deeper than 340 m at station A3-1. We agree that we only have 2 dFe datapoints below the mixed layer (123m) at A3-1 (Figure 3b, page 17919), but still contend that the profile shows an increasing trend towards the seafloor. Our statement is supported by the profile at A3-2 (5 datapoints below the mixed layer; Figure 3c), the KEOPS-1 dFe profiles at station A3 (Figure 4b, page 17920) and our knowledge of plateau shelf sedimentary supply process for dissolved iron in the ocean. We have changed the sentence to (page 17877, line 10-):

“Such enrichments at depth were also observed in dissolved Mn and Co profiles (F. Quéroué, personal communication, 2014; data not shown) and dFe profiles from the occupations of station A3 during the KEOPS-1 study (Fig. 4b), indicative of plateau sedimentary supply.”

During the discussion of export measurements (page 17880, line 26 and Section 3.2.4) it should be mentioned that as the value calculated at station R-2 was derived from Th measurements it reflects integrated export over the previous 30 days, rather than instantaneous vertical flux at the time of sampling. As this was the reference site, with low phytoplankton abundance, the longer time period probably has a minimal effect upon interpretation of the data.

We agree with the reviewer and did note on page 17889 line 16 of our original manuscript the following:

“estimates based on ^{234}Th at this time, reflecting the previous ~30 days of export”.

We have added the sentence to note 4 of Table 1, which we think is the most appropriate place:

“This method will reflect the integrated Fe export over the previous ~30 days, rather than an instantaneous flux at the time of sampling. Since this was a reference site, with low phytoplankton abundance, the longer time period probably has a minimal effect upon interpretation of the data.”

The authors estimate the amount of the winter dFe stock that had been used by the time of sampling during KEOPS-1 based on the observed decrease in concentration during the current study and with the assumption that annual variability is low (Page 17881 Line 28 – Page 17882 Line 2). Obviously there is limited additional dFe data available to comment on the validity of this assumption, but is it possible to do so based on indirect methods (e.g. interannual variation of bloom progression from satellite imagery)? The assumption of low inter-annual variability is mentioned again at Page 17890 Line 10, but with the caveat included that this may not be so (citing Grenier et al., 2014) and I think that this caveat should also be included during the earlier comparison to KEOPS-1.

We agree with the reviewer that this is a data sparse region and estimates of winter stocks based on the assumption of low interannual variability may have inherent uncertainties. We earlier examined interannual variability in bloom development and progression in the study region (Mongin et al., 2008), but believe that extrapolating this analysis to dissolved Fe is problematic as concentrations are dependent on a number of factors not determinable via satellite. We have modified the sentence to include this possible caveat (page 17882, line 1):

“If annual variability is low, which may not always be the case (Grenier et al., 2014), by late summer >90% of the winter stock had been used with only 4.7 $\mu\text{mol dFe m}^{-2}$ remaining in the surface mixed layer at A3 (KEOPS-1 data; Blain et al., 2007).”

The estimates of biogenic iron are calculated from particulate phosphorus data with the assumption that all particulate phosphorus collected has a biogenic origin. Can this assumption be validated from elemental composition of the local rocks (i.e. that they do not contribute a significant amount to the particulate P pool)?

This concern is valid and was pointed out in a review of our companion paper (van der Merwe et al., 2015). In response to that reviewer, van der Merwe et al. modified their text to:

“If we assume that all particulate phosphorus (pP) is of biogenic origin, we can calculate the biogenic Fe fraction of the total Fe concentration by normalising to pP and comparing with published elemental ratios of Southern Ocean diatoms (Planquette et al., 2013). For the calculations we used the upper limit of Fe:P (1.93 mmol mol^{-1}) reported by Twinning et al. 1 (2004) for Southern Ocean diatom assemblages. Given that pP and POC are remineralised throughout the water column and are generated within the surface mixed layer, calculations of biogenic trace metals will only be valid within the surface mixed layer, as the concentration of pP and POC decreases strongly with depth. It should also be noted that Kerguelen Island basalts and upper continental crust can contribute particulate phosphorus concomitantly with pFe to the particulate pool. However the Fe:P ratio found within Kerguelen Island basalts and the continental crust is 12.8 and 25.8 (mol:mol) respectively (Gautier et al., 1990; Wedepohl, 1995). Thus, the factor of 1000 increase in pP within suspended particles compared to these rock sources indicates that this pP is likely produced insitu within the mixed layer from dissolved PO_4^- rather than supplied from rock weathering. Furthermore, within the upper 200 m of the water column, biogenic Fe correlates significantly with both fluorescence (Spearmans RHO $R = 0.518$, $P < 0.05$, $n = 30$) and dissolved oxygen (Spearmans RHO $R =$

0.507, $P < 0.05$, $n = 30$) confirming the autotrophic composition of the particles identified as high in biogenic Fe.”

In this paper, we cite the modified van der Merwe et al. text and have added a sentence (page 17882 line 8):

“These calculations follow methods reported in Planquette et al. (2013), and assume particulate P is not in part derived from local rock weathering. van der Merwe et al. (2015) have tested this assumption using Fe/P ratios in Kerguelen Island basalts and the upper continental crust, and note that the ~1000-fold increase in pP within suspended particles can only be explained by pP produced in situ within the mixed layer from dissolved PO₄-.”

There are several references to Fe/C ratios of “suspended” particles on Pages 17892 and 17893, but the authors state on Page 17871 that particulate Fe data reported in this manuscript is the sum of 1-53µm and >53µm size fractions collected by in situ pumps. As such, the particulate material collected undoubtedly consists of both suspended and sinking pFe and POC. The references on pages 17892 and 17893 should be reworded, or an explanation included on page 17871 that the measured particles are included as a “suspended” term, while acknowledging that there is some sinking material included in that term.

We have changes the text on page 17892 line 14 to acknowledge that some sinking particles may be included in that term:

“We also note that pFe data is the sum of 1-53µm and >53µm size fractions collected by ISPs and thus may also include some sinking particles. This may affect the suspended Fe/C ratios.”

In the comparison between mixed layer Fe/C ratios and those of phytoplankton intracellular uptake (page 17892, lines 1-13), I feel that the current paragraph structure may be interpreted as suggesting that the contribution of lithogenic and detrital Fe to the suspended material Fe/C is a relatively minor factor. I would argue that this would be the most important factor in explaining the much higher values for Fetot/C of suspended material and should be emphasized more - looking at the lithogenic and total pFe concentrations in Table 1, the lithogenic fraction alone contributes 15-66% of the total pFe. Also, the following paragraph (line 14) starts with the statement that Fetot/C was also calculated – is this not the same as described in the paragraph before? In explaining the surface-to-deep increases in Fetot/C, the authors state that scavenging drives the Fetot/C ratio (page 17892, line 22). Is it possible that a greater lithogenic contribution to particles is also a factor? This is later mentioned as a reason for the higher Fetot/C observed in sinking particles over the plateau (page 17893, line 29)

We have changed the text on page 17892- of the article as follows. We have also changed the term Fe/Ctot to Fe/C throughout the manuscript for consistency.

“Suspended mixed layer Fe/C ratios (Table 1) were significantly higher than phytoplankton intracellular uptake ratios. This finding is likely the result of the contribution of lithogenic and

detrital Fe to suspended material Fe/C ratios, and is consistent with the removal of C at a faster rate than that of Fe, and for Fe to be added through new sources after phytoplankton uptake. Differences may also arise because of luxury uptake, the timescale of integration in deckboard experiments compared to Fe/C ratios in ocean suspended and sinking particles (which are broadly similar – see below), and/or that our system was not in steady-state. Also, since a Ti-citrate-EDTA wash was used to remove extracellular surface Fe during the incubation experiments, but not on particles collected in the ISPs and P-traps, our suspended and sinking pFe concentrations include Fe present within cells, adsorbed to cell walls, detrital Fe and lithogenic Fe. This would tend to increase Fe/C in suspended particles. Differences between intracellular and suspended mixed layer Fe/C ratios may also derive from the C term, since the ISP sampling includes detrital material as well as living cells.

In addition to the ratio of “total” particulate (biogenic+lithogenic) Fe over POC (Fe/C) in suspended particles discussed above, we also calculated the ratio of biogenic Fe over POC (i.e., Fe_{bio}/C) following methods discussed in section 3.2.1. Profiles are shown in Figure 5.”

Although the text states “a comparison of Fe supply and demand at the three sites around the Kerguelen archipelago in spring was possible (Fig. 7). . .” the figure only includes budgets for the plateau and plume sites. As there are a limited number of detailed biogeochemical iron budgets published and the reference site does after all represent a different variation of the upper ocean iron cycle (in terms of the magnitude of iron supply), I feel that it would be worthwhile including the third budget here. Also relating to Figure 7, the way it is set out makes it appear that the lateral advection input to the plume also represents an output term from the plateau station. Was this intentional? Although the plateau and plume certainly do seem to be linked by a lateral export of Fe from one to the other, the source of this plume Fe is discussed in the manuscript (Page 17886 Line 1) as being from the northern part of the plateau, rather than from the area of station A3. This being the case, the current spacing between Figure 7a and 7b could be misleading.

These are valuable comments. We have added a third budget in Figure 7 (panel a) for reference site R-2. We have also modified the figure (three separate panels) so that the lateral advection into plume station E does not appear to be a direct output term from station A3 (this was not our intention).

Additional comments (with page and line numbers):

Page 17868, Line 23: change “. . .were taken tracking. . .” to “. . .were taken as tracking. . .”

Done

Page 17869, Line 7: replace “passes” with “pass”.

Done

Page 17879, Lines 22-24 and Figure 3d-f: The pFe concentrations given in the text in reference to the profiles of stations E-1, E-3 and E-5 appear to be lower than the concentrations shown in Figure 3d-f. Perhaps the numbers quoted refer to the 1-53 μm size fraction only and the data in the figure is for material $>1\mu\text{m}$. As far as I could tell the values stated for the reference and plateau stations did match the figure.

Thank you for pointing that out. Figure 3 plots correctly used $>1\mu\text{m}$ pFe data, whereas the original text referred to the 1-53 μm size fraction only. We have modified the text for A3 and E stations (station R-2 was okay).

Page 17881, Line 12: Suggest changing “. . .on plateau A3 compared to the plume E. . .” to “. . .on the plateau (station A3) compared to the plume station, E. . .”.

Done

Page 17883, Line 23: Italicize “w” and include the “ek” subscript.

Done

Page 17889, Line 7: Replace “and” with “at”.

Done

Page 17890, Line 14 and Table 3: The range of mesoplankton Fe regeneration rates given in the text (0.04-0.08 pmol Fe/L/d) does not match that in the table that it refers to (0.02-0.08 pmol Fe/L/d).

Sorry, incorrect text. Fixed

Page 17893, Lines 24, 25: Change “conversation” to “conversion”

Done

Figure 2: Polar Front is shown as a white dashed line and labeled in the first panel.

The caption could be changed from “The polar front is shown as a black dashed line” to “The polar front is shown as a black dashed line in panels b and c”.

Done

Figure 4: Change “Note difference scale for . . .” to “Note difference in scale for . . .”.

Done

Anonymous Referee #2

Received and published: 18 March 2015

“Iron budgets for three distinct biogeochemical sites around the Kerguelen archipelago (SO) during the natural fertilization experiment Keops-2” by Bowie et al. This is a very good manuscript, well written, clear and above all very interesting. It describes the multiple sources of Fe for phytoplankton on three different sites close to the Kerguelen Islands in the Southern Ocean. Budgets are made of sources and sinks in which fluxes are compared with the needs of phytoplankton at the three sites. These budgets differ per site.

We thank the reviewer for his/her very positive comments, and for the very useful comments below which have improved our manuscript.

I have only minor comments. Three comments are relatively important: the influence of error estimates on the budget are not discussed. Information on certain calculations and assumptions is missing or difficult to find, since it is given in the discussion instead of methods (see below). The references used are not always correct.

We have modified the text to make it easier for the reader to understand the budget calculations (and associated assumptions) and updated the references, as detailed in our response below. We have included estimates of the error bound where available in Table 1.

The title: In the title and whole manuscript the word experiment is used. This word implies manipulations whereas it is essential here that it is a natural fertilization. I suggest research or study.

We have modified the text, and changed the word “experiment” to “study” in both the title and manuscript text.

Abstract line 7: introduce the term new here, so that it is clear below which supplies are considered new, and which are not.

We have changed the sentence to:

“Iron supply from ‘new’ sources (diffusion, upwelling, entrainment, lateral advection, atmospheric dust) to surface waters of the plume was double that above the plateau and 20 times greater than at the reference site, whilst iron demand (measured by cellular uptake) in the plume was similar to the plateau but 40 times greater than the reference.”

Introduction P 17864 Line 2 add “marine” to carbon cycle.

Done

Line 17: add de Baar et al., 2005 to the Boyd reference.

Done

Line 22-24: what about wind mixed layer depth and differences in estimated or assumed Fe/C ratios of the cells?

We have modified the sentence to:

“This is due to a number of factors, including rapid grazing of phytoplankton in surface waters, loss of the added Fe by its precipitation and scavenging onto sinking particles, differences in estimated or assumed Fe/C ratios of the cells, and changes in wind mixed layer depth.”

P17866, line 23: In Cullen et al a lot of text is on particulate Fe however, the subject of the paper is DFe, thus this reference is not correct here.

We have removed the Cullen et al. reference.

P 17867 Line 15: abbreviations ISP and P-trap are not explained yet

We have changed the sentence to:

“Our observations also include particulate measurements in both suspended water column (in situ pump; ‘ISP’) and sinking export (free-floating sediment trap; ‘P-trap’) particles below the mixed layer, with linkage to food web processes via discussion of iron-to-carbon (Fe/C) ratios.”

Methods P17869 Line 19-20: as closely as possible: Has anything been treated differently? If so then specify. The data of KEOPS-1 and 2 are compared in this manuscript. Is this data obtained in the same way, with the same analytical methods?

We have changes this paragraph to:

“All trace metal sampling and analytical procedures followed recommended protocols in the cookbook² published by the international program GEOTRACES (Bishop et al., 2012; Cutter and Bruland, 2012; Planquette and Sherrell, 2012). All methods have been successfully used previously by this team during the KEOPS-1 (Blain et al., 2008b) and SAZ-Sense projects (Bowie et al., 2009). Subtle differences in methods employed during the earlier KEOPS-1 and SAZ-Sense projects are described in those papers and/or later in this manuscript.”

P17872 line 18: please use capital P and D to indicate particulate and dissolved. PFe for particulate Fe cannot be confused with the negative logarithm of 'free' iron as pFe clearly can.

The terms dFe (for dissolved iron) and pFe (for particulate iron) have been used by many groups and widely reported in the literature previously. We thus prefer to keep these terms in our paper. They are clearly defined on page 17864 line 10 (for dFe) and page 17871 line 8 (for pFe), so I do not think there will be confusion with the negative logarithm of 'free' iron (which isn't discussed at all in the manuscript). We have added this sentence to that start of section 2.3.2 (page 17872 line 11):

"Particulate Fe (pFe) was determined as follows."

P17874, line 16: instead of estimated use assumed to be equal to

Done

P17875, line 6. I am glad that the description is given, it is essential for understanding the discussion.

OK

P17875 which temperature is used, is it corrected for pressure, is it conservative temperature (in θ_{θ})? For st R and E this is important with depths to 2500 and 2000 m.

Thanks for the clarification. Potential temperature is used and has now been defined in the caption to Figure 3.

17877 line 26 Planquette et al 2011 Frew et al. 2006 : Are Planquette et al et al really discussing the size change for small to large particles, they did not discriminate between sizes didn't they, for that they referred to Lam et al 2006. No idea whether these cover the microbial aspect. Frew et al, 2006 do not, it is an extremely interesting paper but as far as I understood they describe that the lithogenic part of PFe increases with increasing particle size. They only mention microbial dissolution of biogenic particles. Lam, P. J., J. K. B. Bishop, C. C. Henning, M. A. Marcus, G. A. Waychunas, and I. Y. Fung (2006), Wintertime phytoplankton bloom in the subarctic Pacific supported by continental margin iron, *Global Biogeochem. Cycles*, 20, GB1006, doi:10.1029/2005GB002557.

Noted, we have changed the text to:

"This may have been due to either: (i) physical aggregation of the particles onto diatom aggregates; and/or (ii) microbially-driven conversion of small lithogenic Fe (1-53 μm) to bioavailable forms and incorporation into the large (>53 μm) diatoms as biogenic Fe, with potentially some fraction of these larger particles exported to depths below the mixed layer, as previously discussed by Lam et al. (2006), (Frew et al., (2006) and ; Planquette et al., (2011)."

17878 lines 1-10: The comparison between Keops 1 and 2 cannot be done so easy, seasonal difference occur as said in the text but can the biological uptake be the cause of the differences below 400 m? How do other stations compare in Fe between KEOPS 1 and 2? Can that support the comparison here?

The only exact station that was visited on both KEOPS-1 and KEOPS-2 was A3, which we compare here. We had other reference stations (C11 on KEOPS-1 and R-2 on KEOPS-2) and stations east of Kergulen (A11 on KEOPS-1 and E stations on KEOPS-2), which we compared on page 17876 (lines 7-14) and page 17880 (lines 4-9), respectively. We agree that biological uptake cannot explain the differences between Fe concentrations in waters deeper than 400 m at station A3. We did note in our original text that biological uptake must be combined with seasonal changes in the strength of the supply mechanisms to A3 (discussed in van der Merwe et al., 2014) to explain the differences. Thus we have changed the text as follows:

“The lower values during KEOPS-1 were likely the result of biological uptake in surface waters and export of Fe during the spring bloom prior to our arrival at the study site, combined with seasonal changes in the strength of the supply mechanisms to deeper waters at A3 (discussed in van der Merwe et al., 2014).”

Pages 17879 lines 25-30 and 17880 lines 25-28. Data treatment like using P and Al for biogenic and lithogenic fractions and Th fluxes on page 80 should be in a separate methods section, then it is not necessary to refer to information later in the text

We prefer to leave these descriptions of how the data was treated and the validity of such approaches in the Results and Discussions section (and with reference to other manuscripts who have adopted similar approaches) to minimise repetition and improve the flow of the text.

3.21 Iron Pools Line 26-29: Is it correct to assume that A3-1 is representative for winter stock, it might be prebloom, but both DFe and nitrate are lower than below the mixed layer (fig 3b), why not use the concentration just below the MLD for integration? Or perhaps mention that this winter stock is possibly (probably) an underestimation.

This is a valid point. Unfortunately, there are no wintertime dFe profiles at A3 to use in our calculations, and for these reasons it is problematic to try to estimate the integrated winter pool. We still think this seasonal comparison is strong and therefore prefer to include a note of caution in our text. We have added this sentence:

“We note this drawdown is probably a conservative estimate since the winter dFe stock was probably an underestimation (as evidenced by lower dFe in the mixed layer compared to deep waters at A3-1; Queroue et al., 2015).

Page 17882: lines 15-24, what is the range, what is the influence on the budget of the choices made here?

We believe that text on page 17882 lines 8-24 adequately explains the rationale for our chosen Fe/Al ratio (of 0.36) and how this value is representative of basaltic rocks in the region. We prefer not to use a range of Fe/Al ratios as we will then have to do the same for our Fe/P ratios (to estimate biogenic Fe), and this will over-complicate the budget and make it extremely difficult for the reader to compare biogenic vs lithogenic particulate iron stocks. As we note, there is some plasticity in the chosen Fe/Al and Fe/P ratios (which we discuss in the text). Nevertheless, our estimates of biogenic and lithogenic Fe provide a perspective on the relative contributions to the total pFe pool (page 17882, lines 22-24)".

3.2.2 Lines 9 and 11 give original references of Shih and Osborn, 1980 Osborn, T.R., 1980. Estimates of the local rate of vertical diffusion from dissipation measurements. *Journal of Physical Oceanography* 10, 83–89. Shih, L. H., J. R. Koseff, G. N. Ivey, and J. H. Ferziger, 2005: Parameterization of turbulent fluxes and scales using homogeneous sheared stably stratified turbulence simulations. *Journal of Fluid Mechanics*, 525, 193–214, doi:10.1017/S0022112004002587.

Done

P 17884: line 5: Indeed used by de Baar but from Gordon et al. 1977 Gordon, A.L., Taylor, H.W., Georgi, D.T., 1977. Antarctic oceanography zonation. In: *Proceedings of SCOR/SCAR Polar Oceans Conference, Montreal, Canada, May 5–11, 1974*,. Dunbar, M.J.(Ed.), Arctic Institution of North America. McGill University, Montreal.

We have changed the sentence to:

"...and a conservative value of $w_{ek} = 0.13 \text{ m d}^{-1}$ for the open Southern Ocean (used by de Baar et al. (1995); originally reported in Gordon et al., 1977) was chosen for our reference station."

Line 19: here WW values are used, why indeed not do the same in A3-1 to calculate winter stock (see above).

We have addressed this point above for station A3-1.

Lines 15-18: interesting, however, it is not clear how this was derived, can you explain in a few words? I realize that I probably ask too much here. However, reading on line 22: this value, causes the reader to wonder which value??

The method for calculating vertical supply due to entrainment at station A3 and E is described in full in the Supplement, so we do not wish to describe it again in the main body of the paper. For the 'detrainment' calculations for station R-2 (line 22), we have revised the text to:

“‘Detrainment’ at R-2 was accounted for by multiplying this new entrainment flux by the summer-to-winter MLD ratio.”

Lines 18-20: how does the simplification applied to A and E compares with the detrainment-derived value?

We performed the same ‘simplified’ calculations (used to determine entrainment at R-2) for stations A3 and E. This resulted in an entrainment of 240 and 222 nmol m⁻² d⁻¹ for A3-1 and A3-2, and 25 and 15 nmol m⁻² d⁻¹ for E-3 and E-5. Thus the simplified method gives lower entrainment values than the more robust calculations based on mixed layer depth excursions and their frequency (Supplement), although the relative magnitude of the fluxes between A3 and E stations were the same.

Page 17885: from line 3 onwards: the lateral fluxes: at which depth(s) are the lateral flux calculations applied to?

For the plateau, lateral Fe supply (difference between inflowing and outflowing lateral fluxes of dissolved iron) was estimated in the 0-150 surface depth band (refer to Fig 3b in Chever et al., 2010 for details). We have changed the text as follows:

“On plateau Fe supply at station A3 was taken from the steady-state box model of Chever et al. (2010) which used the horizontal dFe gradient and current velocities from Park et al. (2008a) to calculate the lateral flux of 180 nmol m⁻² d⁻¹ in the 0-150 m depth band above the plateau; noting this model used KEOPS-1 data.”

For the plume, we also used a depth band of 0–150 m, considered as the winter mixed layer in the plume over the season. This text has been added to the manuscript.

Lines 10-20: I do not understand how these calculations are done, and since it is interesting it would be good to either explain more extensively or add an explanation in the supplement.

The calculations are explained fully in the KEOPS-2 companion paper, to which the reader is referred to (d’Ovidio et al., 2014).

Line 18 is it allowed to use the Keops 1 data, since this paper shows quite some differences between the two studies?

We have added this caveat to the text:

“On plateau Fe supply at station A3 was taken from the steady-state box model of Chever et al. (2010) which used the horizontal dFe gradient and current velocities from Park et al. (2008a) to

calculate the lateral flux of $180 \text{ nmol m}^{-2} \text{ d}^{-1}$ in the 0-150 m depth band above the plateau; noting this model used KEOPS-1 data.”

Page 17891: line 5: Refer to Brussaard et al 2008. Brussaard, C.P.D., Timmermans, K.R., Uitz, J., Veldhuis, M.J.W., 2008. Virioplankton dynamics and virally induced phytoplankton lysis versus microzooplankton grazing southeast of the Kerguelen (Southern Ocean). *Deep-Sea Research II* 55, 752–765

Done

P 17895: any idea why regeneration differs so much between the KEOPS studies?

We believe this is largely due the stage of phytoplankton bloom development, in other words seasonality. Our estimates of iron regeneration rates are based on biomass and activity of heterotrophic bacteria and mesozooplankton. Biomass and activity of heterotrophic bacteria and mesozooplankton are both a response to the phytoplankton bloom and the associated DOC and POC production. This response is more pronounced during the peak-decline of the bloom as compared to the early stage of the bloom.

We note this on page 17891 lines 9-11 and thereafter:

“Importantly, Fe regeneration was much lower during the early compared to late bloom stage and was dominated by bacterial regeneration in spring (60-90% of total Fe regeneration).”

Other possible reasons are discussed on page 17895.

End of page 17895 and start 17896: One can only conclude that a flux is missing if the other fluxes and calculations are assumed to be correct within the estimated errors. One sentence is needed is here to make the assumption or discuss the errors.

We have changed the text to:

“Assuming all flux calculations to be correct within the estimated error bounds in Table 1, this implies there is a missing flux term in the budget at A3 and this is likely lithogenic pFe from the Kerguelen plateau and/or Heard Island (and this may be converted to biogenic Fe).”

Line 11: Shaked and Lis have written an excellent paper on Fe availability, however the dissolution of PFe by organic ligands is only briefly mentioned by them, add Thuroczy et al 2012 as reference; they measured complexation in Antarctic waters and discussed the role of ligands in transporting and dissolving PFe into DFe and refer to the more theoretical work of Borer. Thuróczy, C-E, Alderkamp, A.-C. Laan, P, Gerringa, L.J.A., de Baar H.J.W., Arrigo, K.R., 2012. Key role of organic complexation of iron in sustaining phytoplankton blooms in the Pine Island and Amundsen Polynyas (Southern

Ocean). DSR II, 71-76, 49-60. Borer, P.M., Sulzberger, B., Reichard, P., and Kraemer, S.M. (2005). Effect of siderophores on the light-induced dissolution of colloidal iron(III)(hydr)oxides. *Mar. Chem.* 93, 179–193.

Thanks for the extra references. We have changed the text to:

“This will vary largely with the mineralogy (Schroth et al., 2009), provenance of the particles, and seawater characteristics (e.g., organic complexation; Shaked and Liset al., 2012). Indeed, Thuroczy et al. (2012) previously measured complexation in Antarctic waters and discussed the role of ligands in transporting and dissolving pFe into dFe, using theoretical data provided by Borer et al. (2005).”

Page 17898, lines 16-18: It is not clear what the meaning is of this sentence.

We have changed the text to:

“This coupling has important implications for geoengineering schemes that propose to increase the supply of Fe to surface waters by pumping waters from below.”

1 **Iron budgets for three distinct biogeochemical sites around**
2 **the Kerguelen archipelago (Southern Ocean) during the**
3 **natural fertilisation study KEOPS-2**

4
5 **Andrew R. Bowie^{1,2,3}, Pier van der Merwe¹, Fabien Qu  rou  ^{1,2,3}, Tom Trull^{1,4},**
6 **Marion Fourquez^{2,5}, Fr  d  ric Planchon³, G  raldine Sarthou³, Fanny Chever^{3,*},**
7 **Ashley T. Townsend⁶, Ingrid Obernosterer⁵, Jean-Baptiste Sall  e^{7,8,9}, St  phane**
8 **Blain⁵**

9 [1] {Antarctic Climate and Ecosystems Cooperative Research Centre (ACE CRC), Private
10 Bag 80, Hobart, Tasmania, Australia}

11 [2] {Institute for Marine and Antarctic Studies (IMAS), University of Tasmania, Private Bag
12 129, Hobart, Tasmania, Australia}

13 [3] {Laboratoire des Sciences de l'Environnement Marin (LEMAR), UMR6539
14 UBO/CNRS/IRD/IFREMER, Institut Universitaire Europ  en de la Mer (IUEM), Technopole
15 Brest Iroise, 29280 Plouzan  , France}

16 [4] {CSIRO Marine and Atmospheric Research, Castray Esplanade, Hobart, Tasmania,
17 Australia}

18 [5] {Universit   Pierre et Marie, Laboratoire d'Oc  anographie Microbienne (LOMIC), UMR
19 7621 CNRS UPMC, Avenue du Fontaul  , 66650 Banyuls sur mer, France}

20 [6] {Central Science Laboratory (CSL), University of Tasmania, Private Bag 74, Hobart, TAS
21 7001, Australia}

22 [7] {Sorbonne Universit  s, UPMC Univ., Paris 06, UMR 7159, LOCEAN-IPSL, F-75005,
23 Paris, France}

24 [8] { CNRS, UMR 7159, LOCEAN-IPSL, F-75005, Paris, France}

25 [9] {British Antarctic Survey, High Cross, Cambridge, CB3 0ET, United Kingdom}

26 [*] {now at: National Oceanography Centre, University of Southampton Waterfront Campus,
27 European Way, Southampton SO14 3ZH, United Kingdom }

28 Correspondence to: A. R. Bowie (Andrew.Bowie@utas.edu.au)

29

1 **Abstract**

2 Iron availability in the Southern Ocean controls phytoplankton growth, community
3 composition and the uptake of atmospheric CO₂ by the biological pump. The KEOPS-2
4 project, a GEOTRACES ‘Process Study’, took place around the Kerguelen plateau in the
5 Indian sector of the Southern Ocean. This is a region naturally fertilised with iron at the scale
6 of hundreds to thousands of square kilometres, producing a mosaic of spring blooms which
7 show distinct biological and biogeochemical responses to fertilization. This paper presents
8 biogeochemical iron budgets (incorporating vertical and lateral supply, internal cycling, and
9 sinks) for three contrasting sites: an upstream high-nutrient low-chlorophyll reference, over
10 the plateau, and in the offshore plume east of Kerguelen Island. These budgets show that
11 distinct regional environments driven by complex circulation and transport pathways are
12 responsible for differences in the mode and strength of iron supply, with vertical supply
13 dominant on the plateau and lateral supply dominant in the plume. Iron supply from ‘new’
14 sources (diffusion, upwelling, entrainment, lateral advection, atmospheric dust) to surface
15 waters of the plume was double that above the plateau and 20 times greater than at the
16 reference site, whilst iron demand (measured by cellular uptake) in the plume was similar to
17 the plateau but 40 times greater than the reference. ‘Recycled’ iron supply by bacterial
18 regeneration and zooplankton grazing was a relative minor component at all sites (<8% of
19 ‘new’ supply), in contrast to earlier findings from other biogeochemical iron budgets in the
20 Southern Ocean. Over the plateau, a particulate iron dissolution term of 2.5% was invoked to
21 balance the budget; this approximately doubled the standing stock of dissolved iron in the
22 mixed layer. The exchange of iron between dissolved, biogenic particulate and lithogenic
23 particulate pools was highly dynamic in time and space, resulting in a decoupling of iron
24 supply and carbon export and, importantly, controlling the efficiency of fertilization.

25

26 **1 Introduction**

27 The concentration of carbon dioxide in earth’s atmosphere and therefore earth’s climate is
28 highly sensitive to modification of the marine carbon (C) cycle due to the growth of
29 phytoplankton in the Southern Ocean (Sarmiento and Gruber, 2006). These single-cell plants
30 remove inorganic carbon from surface seawater during photosynthesis, which can be directly
31 transferred into the deep sea when they die and sink, or indirectly through the food web. The
32 Southern Ocean is responsible for 30% of global ocean carbon export (Schlitzer, 2002). As

1 first demonstrated over 20 years ago, phytoplankton growth in the Southern Ocean is limited
2 by the availability of the micro-nutrient trace element iron (Fe; Martin, 1990). Low dissolved
3 iron (dFe) availability limits the annual uptake of atmospheric carbon dioxide (CO₂) by the
4 Southern Ocean (Boyd et al., 2000), shapes phytoplankton species composition and
5 physiology (Assmy et al., 2013), the cycling of other nutrient elements (Moore and Doney,
6 2007) and thus the structure of the entire marine ecosystem (Boyd and Ellwood, 2010).

7 Artificial mesoscale ocean iron fertilisation experiments have unequivocally demonstrated the
8 role of Fe in setting phytoplankton productivity, biomass and community structure in high
9 nutrient low chlorophyll (HNLC) regions (de Baar et al., 2005; Boyd et al., 2007). However,
10 the ‘carbon sequestration efficiency’ of ocean fertilisation as a means to sequester
11 atmospheric CO₂ (calculated as the additional (net) C that is exported from surface waters into
12 the deep (>1000 m) ocean for a given addition of Fe) varies widely between experiments and
13 is considerably less than estimates from the early iron fertilisation experiments (see discussion
14 in de Baar et al., 2008). This is due to a number of factors, including rapid grazing of
15 phytoplankton in surface waters, loss of added Fe by its precipitation and scavenging onto
16 sinking particles, differences in estimated or assumed Fe/C ratios of the cells, and changes in
17 wind mixed layer depth.

18 The natural resupply of iron to Fe-depleted waters is a more efficient process (Blain et al.,
19 2007), although in part this depends on the mode of Fe delivery (e.g., from above, laterally or
20 from below), the ability of organic ligands to keep the supplied Fe in solution (Gerringa et al.,
21 2008), and for continued ocean fertilisation is in part reliant on the concurrent supply of other
22 major nutrients. In the Indian sector of the subantarctic Southern Ocean, natural Fe supply
23 from the Kerguelen plateau (Blain et al., 2007) and Crozet Islands (Pollard et al., 2009)
24 results in increased phytoplankton biomass during summer, with chlorophyll levels increasing
25 to more than an order of magnitude above background; as revealed by NASA MODIS
26 satellite chlorophyll climatology for January (2003-2010) (Westberry et al., 2013). Previous
27 research of blooms in these localised ‘natural laboratories’ have provided invaluable insights
28 into mechanisms linking iron fertilisation and carbon cycling in the Southern Ocean,
29 especially since they can address the effects of persistent, varying and multiple Fe sources
30 that are not accessible through deliberate artificial mesoscale fertilisation experiments.

31 The KEOPS-1 (KErguelen: compared study of Ocean and Plateau in Surface waters) project
32 which took place in the late austral summer of January – February 2005 demonstrated that

1 this natural fertilisation of the Southern Ocean resulted in dramatic changes in the functioning
2 of the ecosystem with large impacts on marine biogeochemical cycles (Blain et al., 2007,
3 2008a). These observations of the bloom were largely confined to the plateau region, where
4 vertical upwelled supply from the plateau sediments (Blain et al., 2008b; Zhou et al., 2014)
5 and lateral advection of water that had been in contact with the continental shelf of Heard
6 Island to the south (Chever et al., 2010), were the dominant sources of dissolved and
7 particulate Fe (as confirmed using REE and Ra isotope tracers; van Beek et al., 2008; Zhang
8 et al., 2008). The interaction of waters, islands and plateau of the Kerguelen archipelago with
9 several circumpolar fronts of the Southern Ocean allowed us to make a first attempt at placing
10 our regional KEOPS-1 observations within a broader basin scale context (Blain et al., 2007).

11 The KEOPS-2 project was designed to improve the spatial and temporal coverage of the
12 Kerguelen region. During KEOPS-2, which was approved as a GEOTRACES Process Study¹,
13 we studied the region above and downstream of the plateau and observed a massive natural
14 iron fertilisation at the scale of hundreds of thousands of square kilometres. This produced a
15 patchwork of blooms with diverse biological and biogeochemical responses, as detailed in the
16 multiple studies in this special issue of Biogeosciences (volume 11). KEOPS-2 was also
17 carried out in the austral spring to document the early stages of the bloom and to complement
18 results of KEOPS-1 obtained in late summer during the start of the decline of the bloom, with
19 a principal aim to better constrain the mechanism of Fe supply to surface waters earlier in the
20 season.

21 Since Fe is actively taken up into phytoplankton, and transferred throughout the food-web,
22 including removal by particle settling and remineralisation in deep waters, the assessment of
23 its availability is quite complex and cannot be judged from dFe levels in surface waters alone
24 (Breitbarth et al., 2010). Advances in chemical oceanographic techniques for trace elements
25 through the GEOTRACES program (SCOR Working Group, 2007) now allow the
26 measurement of Fe associated with different phases (dissolved and particulate), internal
27 biological recycling and Fe export from surface waters. The results from earlier iron
28 biogeochemical budgets for FeCycle-I (Boyd et al., 2005; Frew et al., 2006), KEOPS-1 (Blain
29 et al., 2007; Chever et al., 2010), CROZEX (Planquette et al., 2007, 2009) and SAZ-Sense
30 (Bowie et al., 2009) have highlighted that the dominant 'new' Fe fluxes are associated with

¹ <http://www.geotraces.org/cruises/cruise-summary/68-science/process-studies/206-geotraces-process-studies>

1 the particulate phase. Particles thus represent an important transport vector for trace metals in
2 the marine ecosystem, although their bioavailability or transfer into a bioavailable fraction
3 remains uncertain. Suspended particles have also been shown to be important aspects of
4 sedimentary, boundary layer Fe sources and export processes (Tagliabue et al. 2009; Homoky
5 et al., 2013; Marsay et al., 2014; Wadley et al., 2014), with particles being transported
6 laterally over hundreds of kilometres in the ocean (Lam et al., 2006; Lam and Bishop, 2008).
7 The biological cycling of particulate Fe may therefore be the most important aspect of the
8 complete Fe biogeochemical cycle especially since earlier budgets have demonstrated that
9 biological Fe ‘demand’ cannot be satisfied by the ‘new’ Fe supply (Boyd et al., 2005; Blain et
10 al., 2007; Sarthou et al., 2008; Bowie et al., 2009; de Jong et al., 2012). A simple one
11 dimensional vertical model that correctly represented the input of dFe to surface waters
12 during KEOPS-1 did not accurately represent the supply of other geochemical tracers or
13 particulate Fe (Blain et al., 2007; van Beek et al., 2008; Zhang et al., 2008), and the role of
14 dissolved and particulate Fe earlier in the season (winter stock) in the Kerguelen region has
15 yet to be quantified.

16 This paper presents a short-term (days-weeks) Fe budget for the period of the KEOPS-2 study
17 for each of three process sites: (i) a “Plateau” bloom site (A3) on the central Kerguelen
18 plateau studied during late summer on KEOPS-1 and reoccupied during spring on KEOPS-2;
19 (ii) a “Plume” bloom site (E) east of Kerguelen Island which was located within a quasi-
20 stationary, bathymetrically trapped recirculation feature near the Polar Front; and (iii) a
21 “Reference” site (R-2) south of the Polar Front (PF) and upstream (southwest) of Kerguelen
22 in HNLC waters. We focus on mixed layer integrated pools of dissolved Fe and particulate Fe
23 (which we further separate into biogenic and lithogenic fractions using elemental
24 normalisers), estimate the fluxes of Fe associated with ‘new’ and ‘recycled’ Fe sources, and
25 compare Fe supply and demand with implications for bloom duration and magnitude. Our
26 observations also include particulate measurements in both suspended water column (in situ
27 pump; ‘ISP’) and sinking export (free-floating sediment trap; ‘P-trap’) particles below the
28 mixed layer, with linkage to food web processes via discussion of iron-to-carbon (Fe/C)
29 ratios. Finally, we present a seasonal comparison of our springtime budget for KEOPS-2 with
30 late summer observations from KEOPS-1, and also make comparison with findings from
31 other sectors of the Southern Ocean subjected to natural Fe fertilisation (e.g., Frew et al.
32 (2006) and Boyd et al. (2005) for ‘FeCycle-I’, and Ellwood et al. (2014) for ‘FeCycle-II’ east
33 of New Zealand; Bowie et al. (2009) for ‘SAZ-Sense’ south of Tasmania; Planquette et al.

1 (2011) for ‘CROZEX’ near the Crozet Islands; and Zhou et al. (2010) for ‘Blue Water Zone’
2 near the western Antarctic Peninsula). The observations of dFe (Qu  rou   et al., 2015) and
3 particulate trace metals (van der Merwe et al., 2015) are detailed in companion papers in this
4 special issue, to allow the current paper to focus explicitly on construction of iron budgets;
5 however the three papers should be seen as a collective whole.

6

7 **2 Material and methods**

8 **2.1 Study area**

9 The KEOPS-2 (KErguelen: compared study of Ocean and Plateau in Surface waters)
10 expedition was carried out in the Indian sector of the Southern Ocean in the vicinity of the
11 Kerguelen plateau between 7 October and 30 November 2011 on the M.D. *Marion Dufresne*
12 (Figure 1a). The plateau of the Kerguelen archipelago is a northwest-southeast seafloor
13 feature approximately 500 m deep and is constrained by the Kerguelen Islands to the north
14 and the smaller volcanic Heard/McDonald Islands to the south. Our study was conducted in
15 early austral spring when phytoplankton biomass was developing rapidly and forming a
16 mosaic of phytoplankton blooms in the region (Trull et al., 2015; Lasbleiz et al., 2014). Since
17 sampling at the different stations took place at different times over the ~7 week study, our
18 observations also provide a temporal sequence relative to the development of surface
19 biomass.

20 The Kerguelen bloom has two main features, a northern branch that extends northeast of the
21 island into waters both south and north of the PF, and a larger bloom covering ~45,000 km²
22 south of the PF and largely constrained to the shallow bathymetry of the Kerguelen plateau
23 (<700m) (Mongin et al., 2008; Supplementary Material in Trull et al., 2015) (Figures 1(b) and
24 2). Thirty-two stations were sampled during KEOPS-2, often with repeat visits. Here we focus
25 on three study sites, namely: plateau A3, plume E and reference R-2 (Figure 1). Two visits
26 were made to A3 at the start (A3-1) and end (A3-2) of the voyage (28 days apart), and five
27 visits were made to site E (over 21 days) to document the bloom development. Based on the
28 trajectories of surface drifters, stations E-1, E-3 and E-5 were taken as tracking the middle of
29 a recirculation region (d'Ovidio et al., 2015), so that they can be considered as pseudo-
30 Lagrangian and their succession in time can be considered a first order time series. Full details
31 of other stations and sampling designed to document the meridional and zonal extensions of

1 the blooms on the plateau and to the east of Kerguelen are contained in companion papers in
2 this special issue of Biogeosciences.

3 The hydrology and circulation around and above the Kerguelen plateau have been described
4 by Park et al. (2008a, 2008b, 2014a), van Beek et al. (2008), Zhang et al. (2008) and Zhou et
5 al. (2014). The mean circulation is shown in Figure 1(b). Briefly, the Kerguelen plateau
6 constitutes a barrier to the eastward flowing Antarctic Circumpolar Current (ACC), the main
7 jets of which are the Sub-Antarctic Front (SAF) and PF. Most of the ACC is deflected north
8 of the Kerguelen Islands as Sub-Antarctic Surface Water (SASW) but some filaments pass
9 between the Kerguelen Islands and Heard Island (as the PF) and further south between Heard
10 Island and Antarctica (Roquet et al., 2009). Above the plateau, the remainder of the ACC
11 comes from the western part of the plateau. Currents of AASW travelling along the western
12 flank of the plateau are deflected south and east of Heard Island as a branch of the Fawn
13 Trough Current (FTC) (Sokolov and Rintoul, 2009), before travelling in a broadly northwest
14 direction up along the eastern shelf-break. The water flow is then deflected toward the east of
15 Kerguelen Island, where there is an intense mixing zone consisting of mesoscale eddies which
16 travel many thousands of kilometres in the ACC towards the Australian sector of the Southern
17 Ocean.

18

19 **2.2 Sampling**

20 All trace metal sampling and analytical procedures followed recommended protocols in the
21 cookbook² published by the international program GEOTRACES (Bishop et al., 2012; Cutter
22 and Bruland, 2012; Planquette and Sherrell, 2012). All methods have been successfully used
23 previously by this team during the KEOPS-1 (Blain et al., 2008b) and SAZ-Sense projects
24 (Bowie et al., 2009). Subtle differences in methods employed during the earlier KEOPS-1 and
25 SAZ-Sense projects are described in those papers and/or later in this manuscript.

26

² <http://www.geotraces.org/libraries/documents/Intercalibration/Cookbook.pdf>

1 **2.2.1 Trace metal rosette (TMR)**

2 Water column samples were collected using 10 L externally-closing, Teflon-lined Niskin-
3 1010X bottles deployed on an autonomous 1018 intelligent rosette system ('TMR', specially
4 adapted for trace metal work, General Oceanics Inc.). The polyurethane-powder-coated
5 aluminium rosette frame was suspended on Kevlar rope which passed through a clean block
6 with a plastic sheave (General Oceanics) and was lowered to a maximum depth of 1300 m.
7 Bottles were tripped at pre-programmed depths using a pressure sensor as the TMR was being
8 raised through the water column at approximately 0.5 m s^{-1} .

9 All sample processing was carried out under an ISO class 5 trace-metal-clean laminar flow
10 bench in a HEPA filtered-air clean container, with all materials used for sample handling
11 thoroughly acid-washed. Samples were drawn through C-Flex tubing (Cole Parmer) and
12 filtered in-line through $0.2 \text{ }\mu\text{m}$ pore-size acid-washed capsules (Pall Supor membrane
13 Acropak 200 or Sartorius Sartobran 300 filters). The dissolved fraction is thus likely to
14 contain colloids and small particles $<0.2 \text{ }\mu\text{m}$ in diameter (Bowie and Lohan, 2009). All
15 transfer tubes, filtering devices and sample containers were rinsed liberally with sample
16 before final collection in 125 mL Nalgene LDPE bottles. Seawater samples were acidified
17 within 24 h of collection using 2 mL of concentrated ultrapure hydrochloric acid (HCl,
18 Seastar BASELINE grade) per L of sample, resulting in an approximate final pH of 1.8,
19 double bagged and stored for at least 24 h at ambient temperature until analysis.

20 **2.2.2 In situ pumps (ISPs)**

21 Suspended particles for trace elemental analysis were collected using 11 large-volume in situ
22 pumps (McLane Research Laboratories WTS6-1-142LV and Challenger Oceanics pumps),
23 suspended simultaneously at pre-chosen depths, following methods reported in Bowie et al.
24 (2009). Up to 2000 L of seawater was filtered across a 142 mm diameter stack (134 mm
25 diameter active area) consisting of a $53 \text{ }\mu\text{m}$ nylon pre-filter screen (NYTEX) followed by a
26 QMA quartz fibre filter ($1 \text{ }\mu\text{m}$ nominal pore size; Sartorius). The QMA filter was supported
27 by a $350 \text{ }\mu\text{m}$ polyester mesh which was placed on top of the Teflon PFA grid of the pump
28 housing. Prior to use, NYTEX screens were conditioned by soaking in 5% H_2SO_4 , rinsed 3x
29 with Milli-Q grade water, dried at ambient temperature under a laminar flow hood and stored
30 in clean plastic Ziploc[®] bags. QMA filters were conditioned for trace-metal analysis (pre-
31 combustion and acid cleaning) following Bowie et al. (2010). Upon recovery of the pumps,

1 sub-samples were taken from the QMA filters using a circular plastic punch (14 mm
2 diameter) and by cutting the nylon mesh using ceramic scissors. Filters were dried under a
3 laminar flow bench and stored at -18 °C in acid-washed PCR trays until further analysis in the
4 home laboratory. The 1-53 µm and >53 µm size fractions were digested and analysed
5 separately, and the particulate iron (pFe) reported here is the sum of both fractions. The ISPs
6 were shown to be efficient in capturing large (>53 µm) particles (Planchon et al., 2014).

7 **2.2.3 Free-floating traps (P-trap)**

8 Sinking particles for trace elemental analysis were collected using PPS3/3 free-floating
9 sediment traps (Technicap, France), specially adapted for trace metals, deployed at 200 m.
10 Traps were deployed for 5.3, 5.1, 1.9 and 1.5 days at stations E-1, E-3, A3-2 and E-5,
11 respectively. The trap deployed at station R-2 was lost and not recovered. Traps drifted
12 between 10 and 43 km over the course of the deployment. Full details of the trap deployments
13 are given in Laurenceau-Cornec et al. (2015) and Planchon et al. (2014). Samples for trace
14 elemental analysis were collected in three separate acid-washed cups (dedicated for trace
15 metals) containing a low trace metal brine solution (salinity ~60), each opened for either 1, 3,
16 8 or 12 h (depending on the station). Upon recovery, cups were taken to a clean room and
17 particles filtered off-line onto a 47 mm diameter, 2 µm porosity polycarbonate filter under
18 gentle vacuum using a Teflon PFA unit (Savillex Corp., USA), equipped with a 350 µm pre-
19 screen (to exclude zooplankton).

20

21 **2.3 Analysis**

22 **2.3.1 Dissolved iron**

23 Dissolved Fe (dFe) was determined shipboard by flow injection analysis with
24 chemiluminescence detection (FI-CL) using in-line preconcentration on an 8-
25 hydroxyquinoline chelating resin (adapted from Obata et al. (1993), de Jong et al. (1998) and
26 Sarthou et al. (2003)). Dissolved Fe data were quality controlled against the SAFe (“Sampling
27 and Analysis of Fe”) standard reference materials (Johnson et al., 2007). Full data including
28 certification results and analytical figures of merit are reported in Quéro   et al. (2015).

1 **2.3.2 Particulate iron**

2 Particulate Fe (pFe) was determined as follows. Sampled particles were acid extracted in 1
3 mL concentrated HNO₃ (Seastar Baseline) for 12 h on a DigiPREP HP Teflon hotplate
4 supplied with HEPA filtered air (SCP Science) at 120 °C using 15 mL Teflon PFA Savillex
5 vials. Digest solutions were diluted with 10 mL ultra-high purity water to 10 % HNO₃ and
6 spiked with 10 ppb indium as internal standard prior to analysis by sector field inductively
7 coupled plasma mass spectrometry (Finnigan ELEMENT 2, Thermo Scientific), following
8 Bowie et al. (2010). Blanks from replicate analysis of filters treated identically to the sample
9 filters, but without large volumes of seawater passed through them, were typically 2-3 % and
10 <1 % of the pFe sample concentrations for the ISP deployments and P-trap deployments,
11 respectively. Recoveries from the analysis of the Community Bureau of Reference plankton
12 certified reference material BCR-414 were excellent, with a 101 % recovery (n=3) for pFe.
13 Full data are reported in van der Merwe et al. (2015).

14 **2.3.3 Particulate organic carbon and nitrogen**

15 For particulate organic carbon (POC) and particulate nitrogen (PN) analyses, QMA quartz
16 filters from the ISPs were sub-sampled in a flow-bench using a 14 mm diameter plastic punch
17 and transferred to silver foil cups (Sercon brand p/n SC0037). Samples were also collected
18 from the P-traps for POC and PN analyses (see Laurenceau-Cornec et al., 2015). Samples
19 were treated with a 40 µL aliquot of 2 N HCl to remove carbonates (King et al., 1998), dried
20 at 60 °C for 48 h, and stored in a desiccator until analysis using a Thermo-Finnigan Flash
21 EA1112 elemental analyzer (using sulfanilamide standards) at the Central Science
22 Laboratory, University of Tasmania. The >53 µm fraction was treated in the same way at the
23 Vrije Universiteit Brussel, after first transferring the material from one fourth of the screen
24 using pre-filtered seawater onto 25 mm diameter, 1.0 µm pore size silver membrane filters
25 (Sterlitech, Concord). Blank corrections for the pump samples were estimated from filters
26 prepared identically but not deployed on the ISPs, and for the trap samples by re-filtering the
27 pre-filtered seawater. All blank corrections were less than 2 % for all samples. The sub-
28 sampling introduces uncertainties of 5-10 % from inhomogeneous filter coverage that exceeds
29 the analytical uncertainty of the POC analysis of ~1 % (Trull et al., 2015).

30

1 **2.4 Biological iron cycling**

2 **2.4.1 Iron uptake**

3 Trace metal clean seawater was collected from the mixed layer (20-40 m) using the TMR,
4 transferred into acid-washed polycarbonate bottles and 0.2 nmol L⁻¹ (final concentration) of
5 enriched ⁵⁵Fe as FeCl₃ added (1.83 x 10³ Ci mol⁻¹ of specific activity, Perkin Elmer). Bottles
6 were placed at in situ temperature in on-deck incubators continuously fed by surface seawater.
7 Incubations were conducted for 24 h (sunrise to sunrise) at several light intensity levels (75,
8 45, 25, 16, 4, and 1 % of photosynthetically-active radiation; PAR). For stations R-2, A3-1, E-
9 1 and E-3, seawater was prefiltered on a 25 µm mesh size before ⁵⁵Fe was added. After
10 incubation, 300 mL of seawater was passed through 0.2 µm pore-size nitrocellulose filters (47
11 mm diameter, Nuclepore). To determine intracellular Fe uptake rates, ⁵⁵Fe not incorporated by
12 cells was removed immediately after filtration using 6 mL of a Ti-citrate-EDTA washing
13 solution for 2 min., followed by rinsing 3 times with 5 mL of 0.2 µm filtered-seawater for 1
14 min. (Hudson and Morel, 1989; Tang and Morel, 2006). The filters were placed into plastic
15 vials and 10 mL of the scintillation cocktail 'Filtercount' (Perkin Elmer) added. Vials were
16 agitated for 24 hours before the radioactivity on filters was counted with the Tricarb[®]
17 scintillation counter (precision <10 %). Controls were obtained with 300 mL of microwave-
18 sterilized seawater (750 W for 5 min.) incubated and treated the same way. Sub-samples for
19 enumeration by flow cytometry were collected from each bottle just before the filtration step.
20 Cells were fixed in glutaraldehyde (1 %) and kept frozen (-80 °C) until processing and
21 analysis. Data were corrected by blank subtraction and Fe uptake rates normalised to the
22 concentration of Fe in each incubation (in situ dFe and ⁵⁵Fe added). Further details are given
23 in Fourquez et al. (2015).

24 **2.4.2 Iron remineralisation**

25 Since iron regeneration was not measured directly by experiment during KEOPS-2, we used
26 the following approach to calculate iron regeneration fluxes. Bacterial Fe regeneration was
27 estimated from bacterial turnover times determined from bacterial production and biomass
28 (Christaki et al., 2014), assuming all loss of bacterial biomass through viral lysis and
29 flagellate grazing resulted in the regeneration of Fe (Strzepek et al., 2005), and using a
30 bacterial iron quota of 7.5 µmol Fe (mol C)⁻¹ (Tortell et al. 1996). The mesozooplankton
31 grazing contribution to Fe regeneration was assumed to be equal to the experimentally

1 determined Fe regeneration during KEOPS-1 (Sarhou et al., 2008). The regeneration rates
2 per mesozooplankton individual determined in Sarhou et al. (2008), were then multiplied by
3 mesozooplankton abundance, calculated from the number of cells captured in a daily haul
4 over 200 m during KEOPS-2 (Carlotti et al., 2015; values reported in Table 6 in Laurenceau-
5 Cornec et al., 2015).

6

7 **3 Results and Discussion**

8 **3.1 Biogeochemical settings at our three study sites**

9 Full descriptions of the dFe and pFe distributions can be found in Qu erou e et al. (2015) and
10 van der Merwe et al. (2015), respectively, with further presentation of the distributions of
11 other micronutrient trace elements (Mn, Co, Ni, Cu, Cd, Pb) from KEOPS-2 to be presented
12 elsewhere. However, briefly our subset of stations used for the iron budgets can be described
13 as follows.

14 **3.1.1 Reference station R-2**

15 In the upper 100 m, we observed a salinity minimum (33.8) and temperature maximum (2.2
16  C) characteristic of Antarctic surface water (AASW) overlying a layer of winter water (WW)
17 at 180-200 m (T_{\min} of 1.6  C) (Figure 3a). Deeper in the water column, a T_{\max} of 2.5 C at 500
18 m (associated with an oxygen minimum; not shown) was indicative of upper circumpolar
19 deep water (UCDW) overlying a salinity maximum of 34.8 at 1830 m in lower circumpolar
20 deep water (LCDW). Phytoplankton abundance was low (0.2 $\mu\text{g Chl-a L}^{-1}$; Lasbleiz et al.,
21 2014) and dominated by diatoms, in waters with relatively high surface nitrate concentrations
22 ($>25 \mu\text{mol L}^{-1}$; Blain et al., 2015), typical of Southern Ocean HNLC conditions (Lasbleiz et
23 al., 2014).

24 Dissolved Fe concentrations were very low at the surface ($<0.1 \text{ nmol L}^{-1}$) and increased with
25 depth averaging 0.3 nmol L^{-1} in LCDW, broadly tracking the nitrate profile. The pFe profile
26 showed similar structure to the dFe profile, but with surface and deep water concentrations
27 between 0.3 and 1.1 nmol L^{-1} (the deepest sample was 148 m above the seafloor). The
28 exception was at 500 m where interestingly we observed a dFe and pFe peak of 0.4 and 1.6
29 nmol L^{-1} , respectively. Whilst this maximum may have arisen due to enrichment of Fe in
30 UCDW delivered from further south, we hypothesise that the Fe supply may have originated

1 from subsurface sediments of the nearby Leclaire Rise (also known as Skiff Bank; Kieffer et
2 al., 2002), a large seamount which rises to 250 m at 49°50'S 65°00'E (approximately 140 km
3 northwest of station R-2). Similar lithogenic inputs were also observed for other dissolved
4 (Mn; Fabien Quérroué, pers. comm., data not shown) and particulate (Mn, Al; van der Merwe
5 et al., 2015) trace elements.

6 The dFe profile at the KEOPS-2 reference station R-2 is similar to the KEOPS-1 reference
7 station C11 (with the exception of the R-2 enrichment in the 200-700 m depth strata; Figure
8 4a), noting that the location of C11 was quite different - in HNLC waters to the southeast of
9 the Kerguelen plateau (51°39'S, 78°00'E) - and we had only 1 dFe data point in UCDW at
10 C11. In contrast to the similarity of the dFe profiles, the pFe profile at C11 was generally
11 lower than R-2, with mean values through the water column of $0.2 \pm 0.14 \text{ nmol L}^{-1}$ (Andrew
12 Bowie, unpublished data) compared to $0.53 \pm 0.35 \text{ nmol L}^{-1}$ for station R-2.

13 **3.1.2 Plateau station A3**

14 Stations A3-1 (Figure 3b) and A3-2 (Figure 3c) were in relatively shallow waters on the
15 central plateau, and were impacted by plateau sediments and possibly fluvial and glacial
16 runoff from basaltic rocks of Heard Island ~300 km upstream (van der Merwe et al., 2015;
17 Melanie Grenier, pers. comm.). A pycnocline was observed at ~190 m, above which the
18 salinity (33.9) and nitrate (~29 $\mu\text{mol L}^{-1}$) were relatively constant. The mixed layer shoaled
19 (from 165 to 123 m) and increased in temperature (from 1.7 to 2.2 °C) between the two visits
20 to A3, consistent with springtime warming of surface waters. We believe the water masses at
21 A3-1 and A3-2 are comparable since surface waters move slowly in this region (Park et al.,
22 2008, 2014a; Zhou et al., 2014); this was confirmed by rare earth element (REE) data which
23 indicated similar waters at both stations marked with fresh continental supplies, only modified
24 by biological processes (Melanie Grenier, pers. comm.).

25 Surface chlorophyll images revealed that during the 28 days between the first and second
26 visits to A3, a large diatom spring bloom developed mostly dominated by lightly silicified
27 *Chaetoceros* spp. (surface Chl-a increasing from 0.2 $\mu\text{g L}^{-1}$ at A3-1 to 1.3 $\mu\text{g L}^{-1}$ at A3-2;
28 Lasbleiz et al., 2014), which likely resulted in the drawdown of dFe (mean mixed layer values
29 decreasing from 0.3-0.4 nmol L^{-1} at A3-1 to 0.1-0.2 nmol L^{-1} at A3-2). The peak of biomass
30 had passed by the time we sampled at A3-2, with the bloom starting to fade (Trull et al.,
31 2015). Below the mixed layer, similar dFe profiles were observed during both visits to A3,

1 with expected significant increases at depth towards the plateau floor (e.g., to 1.30 nmol L⁻¹ at
2 480 m at A3-2; note, due to operational constraints, there was no dFe data deeper than 340 m
3 at A3-1). Such enrichments at depth were also observed in dissolved Mn and Co profiles (F.
4 Qu  rou  , pers. comm., 2014; data not shown) and dFe profiles from the occupations of station
5 A3 during the KEOPS-1 study (Fig. 4b), indicative of plateau sedimentary supply.

6 The pFe profiles at A3 showed similar structure to the dFe profile, with lower values at the
7 surface (<10 nmol L⁻¹ at A3-1 and <4 nmol L⁻¹ at A3-2), increasing with depth due to
8 enrichment from bottom sediments (up to 33 and 14 nmol L⁻¹ at 440 m at A3-1 and A3-2,
9 respectively), and were on average 10 times greater than dissolved concentrations through the
10 water column. The mixed layer pFe concentrations changed remarkably between the two
11 visits, and the full water column integrated pool was ~70% lower at A3-2 compared to A3-1.
12 Interestingly, this change was also associated with a shift of particles from the 1-53 μ m size
13 range to the >53 μ m size range, with the larger size class tripling in size (van der Merwe et al.,
14 2015). The development of the large bloom between our two visits to A3, which consisted of
15 a diatom community 50-210 μ m in size (Trull et al., 2015) was likely responsible for
16 converting the pFe within the surface mixed layer from the smaller size class to the larger size
17 class. This may have been due to either: (i) physical aggregation of the particles onto diatom
18 aggregates; and/or (ii) microbially-driven conversion of small lithogenic Fe (1-53 μ m) to
19 bioavailable forms and incorporation into the large (>53 μ m) diatoms as biogenic Fe, with
20 potentially some fraction of these larger particles exported to depths below the mixed layer, as
21 previously discussed by Lam et al. (2006), Frew et al. (2006) and Planquette et al. (2011).

22 The spring (Oct-Nov) KEOPS-2 Fe profiles at station A3 showed a similar structure to those
23 from the late summer (Jan-Feb) KEOPS-1 study, with surface depletion, concentrations
24 increasing with depth and enrichment just above the plateau seafloor (Figure 4b). Through the
25 water column, dFe was between 2-5 times greater during KEOPS-2 compared to KEOPS-1
26 and pFe was ~10 times greater during KEOPS-2 (with the exception of the deepest samples).
27 The lower values during KEOPS-1 were likely the result of biological uptake in surface
28 waters and export of Fe during the spring bloom prior to our arrival at the study site,
29 combined with seasonal changes in the strength of the supply mechanisms to deeper waters at
30 A3 (discussed in van der Merwe et al., 2015).

1 3.1.3 Plume E stations

2 The E stations within the bathymetrically trapped complex recirculation system showed
3 similar hydrographic and nutrient distributions below the mixed layer (Figures 3d, 3e and 3f),
4 which shoaled from 64 m at E-1 to 32 m at E-3 to 39 m at E-5, with some internal variability
5 in water column structure at mid-depths. Surface waters warmed from 2.7 to 3.4 °C between
6 the occupations of E-1 and E-5, although no significant nitrate drawdown was observed
7 (Blain et al., 2015). Below AASW, a subsurface temperature minimum (T_{\min} , ~1.7 °C) was
8 observed between 180 m (E1) and 220 m (E5), characteristic of WW. The T_{\min} feature is
9 associated with waters south of the PF, although the recirculation feature probably also
10 received SAZ waters mixed in from the north (d'Ovidio et al., 2015). T, S and O₂
11 characteristics indicated the presence of UCDW (~600-700 m) and LCDW (deeper than
12 ~1300 m) deeper in the water column above the seafloor (Qu  rou   et al., 2015). Water parcel
13 trajectories calculated from altimetry based geostrophic currents indicated that it took
14 generally >2 months for Fe-rich waters from the plateau to travel to the downstream plume
15 site associated with the recirculation feature (E stations) (d'Ovidio et al., 2015). However
16 shorter transport times are also possible due to episodic transport across the PF (Sanial et al.,
17 2015).

18 Waters at the plume stations showed the largest spatial heterogeneity in surface biomass as
19 revealed by the evolution of a mosaic of complex blooms seen in satellite images (see
20 Supplementary Material in Trull et al., 2015). We observed moderate surface Chl-a levels
21 ranging from 0.3-0.4 $\mu\text{g L}^{-1}$ at E-1 and E-3 to 0.5-0.9 $\mu\text{g L}^{-1}$ at E-5 (Lasbleiz et al., 2014),
22 noting that as much as 50 % of the chlorophyll was below the mixed layer at the plume
23 stations due to stratification of the upper water column in the warm, spring conditions. Unlike
24 the plateau bloom dominated by large cells >53 μm , the community in the plume E stations
25 was more mixed (Laurenceau-Cornec et al., 2015), with cells present in both the 5-20 and 50-
26 200 μm size classes (Trull et al., 2015). The E stations showed the highest C export fluxes of
27 all regions as estimated from Th deficits, nitrate depletions, and free-drifting sediment trap
28 observations (Planchon et al., 2014; Trull et al., 2015; Laurenceau-Cornec et al., 2015).

29 Due to operational constraints, no dFe data was available at station E-1. The dFe vertical
30 profiles at E-3 and E-5 were quite different, with a distinct surface enrichment to 0.4 nmol L^{-1}
31 at E-3 above a minimum of 0.2 nmol L^{-1} at 100 m. This feature was absent at station E-5,
32 where dFe was depleted to <0.1 nmol L^{-1} at the surface, likely due to biological Fe uptake,

1 which was highest at E-5 ($1745 \text{ nmol m}^{-2} \text{ d}^{-1}$) compared to A3-2 ($1120 \text{ nmol m}^{-2} \text{ d}^{-1}$) (Table 1)
2 and E-4E ($880 \text{ nmol m}^{-2} \text{ d}^{-1}$; data not shown), despite lower POC and primary production (see
3 discussion below and Fourquez et al., 2015). Deeper in the water column ($>500 \text{ m}$) at E
4 stations, dFe was broadly uniform ($0.3\text{-}0.5 \text{ nmol L}^{-1}$).

5 The pFe distributions at the three E stations were similar with a surface (35-40 m) enrichment
6 ($1.6\text{-}1.9 \text{ nmol L}^{-1}$), a minimum at $\sim 100\text{-}200 \text{ m}$ below the mixed layer ($0.7\text{-}0.9 \text{ nmol L}^{-1}$;
7 broadly consistent with the T_{min} layer), above a maximum at 280-600 m ($1.7\text{-}2.4 \text{ nmol L}^{-1}$),
8 and with evidence of enrichment near the seafloor at depths $>1800 \text{ m}$ (up to $1.5\text{-}2.3 \text{ nmol L}^{-1}$).
9 By applying biogenic (using P) and lithogenic (using Al) normalisers to the data (see
10 ‘Construction of iron budgets’ section below), surface pFe enrichment was roughly equally
11 composed of biogenic and lithogenic Fe, whilst the 300-600 m maximum was predominantly
12 composed of lithogenic Fe (>100 -fold greater than biogenic Fe at these depths). This
13 lithogenic Fe was most likely from waters enriched from sediments and transported laterally
14 eastward off the Kerguelen plateau which sits at $\sim 530 \text{ m}$ below the sea surface. There was no
15 obvious change in pFe in surface or deep waters during the bloom evolution at the pseudo-
16 Lagrangian E stations.

17 The KEOPS-1 study only occupied one station in the plume east of Kerguelen (A11 at
18 $49^{\circ}09'S$ $74^{\circ}00'E$). Dissolved Fe at A11 ranged from 0.09 nmol L^{-1} at the surface to 0.17 nmol
19 L^{-1} at 1500 m (Blain et al., 2008b), and pFe ranged from 0.07 nmol L^{-1} at the surface to 0.81
20 nmol L^{-1} at 1500 m (Andrew Bowie, unpublished data); thus much lower than our KEOPS-2
21 observations at the E site (noting different sampling and digestion methods for pFe were used
22 for the two cruises).

23

24 **3.2 Construction of iron budgets**

25 The primary aim of this work was to use our observations of Fe pools and fluxes to
26 understand the sources, sinks and biological Fe cycling, and evaluate if Fe supply could meet
27 demand in both the high-Fe and low-Fe environments in the vicinity of the Kerguelen
28 archipelago during the KEOPS-2 study. Iron budgets have been constructed for previous
29 studies in waters fertilized with Fe both naturally (Sarhou et al., 2008; Bowie et al., 2009;
30 Chever et al., 2010; Ellwood et al., 2014) and artificially (Bowie et al., 2001) as well as low-
31 Fe conditions (Price and Morel, 1998; Boyd et al., 2005). These budgets have combined

1 geochemical and chemical components to demonstrate that the dominant long-term fluxes of
2 Fe are associated with the particulate pool (dust supply and particle export), whilst studies on
3 Fe uptake and microbial cycling have shown that short-term fluxes within the ‘ferrous wheel’
4 are dominated by biological uptake and remineralisation (Strzepek et al., 2005). Here, we
5 follow a similar approach to that used by Bowie et al. (2009) for the SAZ-Sense study south
6 of Tasmania (Australia) at our three study sites. Since all parameters in our iron budget
7 calculations were only measured at stations R-2, A3-2 and E-5, discussion will focus on these
8 stations. Data for stations A3-1, E-1 and E-3 are given to provide a context for spatial and
9 temporal changes in the Fe pools and fluxes during KEOPS-2, and are collated in Table 1.

10 **3.2.1 Iron pools**

11 Iron and carbon pools were calculated by integrating the dissolved and particulate profiles
12 down to the base of the surface mixed layer, defined as the depth where the potential density
13 equalled the potential density at 10 m + 0.02 kg m⁻³ (Park et al., 2014a). The mixed layer
14 varied from 165 m at station A3-1 to 32 m at station E-3, consistent with the seasonal
15 shoaling as surface waters warmed, but remained deep (>120 m) on the plateau throughout
16 the study due to deep mixing as a result of several passing storms.

17 Integrated pools of both dissolved (~5x) and particulate (~10x) Fe were significantly greater
18 on the plateau (station A3) compared to the plume (station E), with stocks at the reference
19 station R-2 lower still. Horizontal dFe supply from the plateau to the plume was either or both
20 via: (i) a geostrophic path looping along the northern side of the PF and then back into the
21 recirculation feature (d’Ovidio et al., 2015), or (ii) direct Ekman flux transport of Fe-rich
22 coastal water across the polar front driven by westerly winds, as indicated by radium (Ra)
23 tracers (Sanial et al., 2015). The latter process is supported by Lagrangian trajectories of water
24 parcels derived from altimetry, which showed the polar front was not a strong barrier to water
25 mass movement, with transport of waters across the front taking place on timescale of days-
26 weeks but being highly variable in space and time (d’Ovidio et al., 2015). The pFe pool
27 showed the same variability as the dissolved pool at our three study sites and exceeded the
28 dFe stocks at all sites by factors of approximately 19-26 (A3), 31 (E) and 6 (R-2), although it
29 is estimated that only ~2-3 % of the particulate pool can be converted into bioavailable forms
30 by physically or biologically-mediated dissolution (Schroth et al., 2009). If we assume that
31 station A3-1 represented pre-bloom conditions and the integrated mixed layer pool of 54
32 $\mu\text{mol dFe m}^{-2}$ was a good estimate of the winter stock, observations show that only 4 weeks

1 later at station A3-2, almost 60 % of the winter stock had been drawn down to 21 $\mu\text{mol m}^{-2}$. If
2 annual variability is low, which may not always be the case (Grenier et al., 2015), by late
3 summer >90% of the winter stock had been used with only 4.7 $\mu\text{mol dFe m}^{-2}$ remaining in the
4 surface mixed layer at A3 (KEOPS-1 data; Blain et al., 2007). We note this drawdown is
5 probably a conservative estimate since the winter dFe stock was probably an underestimation
6 (as evidenced by lower dFe in the mixed layer compared to deep waters at A3-1; Qu  rou   et
7 al., 2015). Biogenic iron (defined as the Fe associated with living phytoplankton and
8 phytoplankton biodetritus) was calculated by assuming that all particulate phosphorus (P) was
9 of biogenic origin, and multiplying the mean particulate P concentration in the mixed layer at
10 each station by a maximum intracellular Fe/P ratio of 1.9 mmol mol^{-1} for natural
11 phytoplankton assemblages measured by Twining et al. (2004) for Fe-replete conditions.
12 These calculations follow methods reported in Planquette et al. (2013), and assume particulate
13 P is not (in part) derived from local rock weathering. van der Merwe et al. (2015) have tested
14 this assumption using Fe/P ratios in Kerguelen Island basalts and the upper continental crust,
15 and note that the ~1000-fold increase in pP within suspended particles can only be explained
16 by pP produced in situ within the mixed layer from dissolved PO_4^- . Lithogenic Fe was
17 calculated by assuming that all particulate aluminium (pAl) was of lithogenic origin and by
18 multiplying the mean pAl concentration in the mixed layer by a lithogenic Fe/Al ratio of 0.36
19 mol mol^{-1} , which is the mean value based on basaltic rocks from the Crozet region (0.51;
20 Gunn et al., 1970) and crustal materials (0.2; Wedephol, 1995). A chosen Fe/Al ratio of 0.36
21 mol mol^{-1} is also very similar to that of 0.33 used extensively in earlier calculations (Taylor
22 and McLennan, 1985) and reported for the deep Atlantic Ocean (Sherrell and Boyle, 1992).
23 This approach is dependent not only on the chosen Fe/Al ratio, but also assumes that
24 processes other than biological assimilation, such as adsorption and scavenging onto organic
25 particles, photo-reduction, surface precipitation, and chemically and biologically driven
26 dissolution, are not significant (Measures et al., 2008; Planquette et al., 2011, 2013; Ellwood
27 et al., 2014). Since biogenic and lithogenic Fe were calculated independently, their sum may
28 be less than the observed total particulate Fe concentration. This is likely due to plasticity in
29 the chosen Fe/Al and Fe/P ratios and differential remineralisation rates for Fe, Al and P.
30 Nevertheless, our estimates of biogenic and lithogenic Fe provide a perspective on the relative
31 contributions to the total pFe pool.

32 Reference and plume waters contained roughly an equal fraction of biogenic and lithogenic
33 Fe. The origin of this biogenic Fe pool will be a combination of biological uptake of dFe,

1 physical adsorption onto suspended biological particles, and conversion from the lithogenic
2 fraction (likely driven by microbes), with these processes operating on different timescales
3 (Boyd et al., 2005; Frew et al., 2006; Planquette et al., 2011). On the contrary, the plateau
4 stations contain 19-69 times more lithogenic Fe than biogenic Fe, consistent with the supply
5 from the nearby sediments of the plateau and Heard Island, as suspected by Zhang et al.
6 (2008), van Beek et al. (2008) and discussed in Chever et al. (2010). Measurement of other
7 geochemical ‘fingerprint’ particulate tracers (such as Al, Mn) on the plateau confirmed the
8 provenance of Fe supplied from the Kerguelen shelf sediments in the particulate phase (van
9 der Merwe et al., 2015).

10 **3.2.2 Internal iron supply**

11 Vertical fluxes were calculated as follows. A vertical diffusivity (K_z) at the base of mixed
12 layer of $10^{-5} \text{ m}^2 \text{ s}^{-1}$ was used for the plume and reference site, and a K_z of $3 \times 10^{-4} \text{ m}^2 \text{ s}^{-1}$ was
13 used for the plateau site, estimated from the Shih parameterisations (Shih et al., 2005) using
14 the Thorpe scale method (Park et al., 2014b). These values are comparable to K_z values
15 estimated for KEOPS 1 using the Osborn model ($4 \times 10^{-4} \text{ m}^2 \text{ s}^{-1}$; Osborn, 1980) (Park et al.,
16 2008a). Vertical diffusivity was multiplied by the vertical dFe gradient for each profile, which
17 was determined using the linear part of the vertical profiles corresponding to the 150-200 m
18 depth strata in Figures 3a-3f, consistent with calculations for KEOPS-1 (Blain et al., 2007).
19 Vertical diffusivity of Fe was negligible at reference and plume sites, but significant on the
20 plateau due to both the higher vertical diffusivity and the steeper Fe gradient between 150 and
21 200 m.

22 Upwelling was defined as the vertical velocity (w_{ek}) multiplied by the dFe concentration at
23 200 m, which corresponds to the depth of the remnant winter water. The magnitude of vertical
24 velocity in this region has recently been studied by Rosso et al. (2014) who used the MIT
25 general circulation model to examine the sensitivity of the vertical velocity to the horizontal
26 resolution. They found clear differences in w_{ek} due to the development of near surface sub-
27 mesoscale frontal structures that only their highest resolution model was able to resolve.
28 Rosso et al. (2014) reported vertical velocities for individual water parcels in excess of 100 m
29 day^{-1} in the Kerguelen region, with w_{ek} stronger in the downstream plume. Both the horizontal
30 and vertical circulations were much weaker over the plateau since it acts as a natural barrier to
31 the strong ACC fronts coming from the west. Unfortunately, no seasonal cycle was included
32 in the model forcing. Therefore the temporal root mean square of the vertical velocity

1 reported in Figure 12(b) of Rosso et al. (2014) was used for the plateau and plume sites ($w_{ek} =$
2 0.5 and 1 m d⁻¹, respectively) and a conservative value of $w_{ek} = 0.13$ m d⁻¹ for the open
3 Southern Ocean (used by de Baar et al. (1995); originally reported in Gordon et al., 1977) was
4 chosen for our reference station. Although w_{ek} was lower on the plateau compared to the
5 plume, the higher dFe concentration at 200 m resulted in comparable estimates of upwelled
6 Fe (Table 1).

7 Entrainment of Fe by episodic (intra-seasonal) deepening of the mixed layer has rarely been
8 taken into account in field studies (Frants et al., 2013) due to the absence of data
9 characterising the short term variability of the mixed layer depth, yet a recent compilation of
10 observations (Nishioka et al., 2011; Tagliabue et al., 2014) and modelling studies (Mongin et
11 al., 2008) suggests that entrainment could be a major vertical supply mechanism fuelling
12 surface biomass (Carranza et al. 2015). We used more than 6000 vertical profiles of salinity
13 and temperature collected in the KEOPS-2 regions of interest to estimate the seasonality of
14 the mixed layer depth and its variability (Supplementary Figure 3). We derived the vertical
15 supply of Fe by entrainment via hypotheses regarding the relation between the size of mixed
16 layer depth excursions and their frequency (Supplementary Methods). Entrainment data based
17 on transient deepening of the mixed layer was not available for station R-2; therefore we
18 calculated this by multiplying the dFe concentration in winter water (which reflects the dFe
19 concentration of the winter mixed layer) by the winter mixed layer depth (MLD) and assume
20 this entrainment event happens once per year. ‘Detrainment’ at R-2 was accounted for by
21 multiplying this new entrainment flux by the summer-to-winter MLD ratio.

22 For the vertical fluxes, in spring on KEOPS-2, entrainment was the dominant vertical Fe flux
23 term on the plateau, delivering ~70% of the total vertical supply and tripling the total vertical
24 flux in comparison to budgets that neglect this process. At the plume and reference sites,
25 entrainment was comparable to the upwelling flux. Vertical diffusion accounted for 4-8% of
26 the total vertical supply on the plateau. In contrast, the contribution from dFe entrainment was
27 much reduced in late summer on KEOPS-1 (42 and 8.8 nmol m⁻² d⁻¹ for plateau and plume,
28 respectively) due to the deepening and weakening of the ferricline (Figure 4b). The relative
29 magnitude of the total vertical Fe supply terms at the three study sites was: plateau > plume >
30 reference (Table 1, row ‘d’).

31 For the lateral fluxes, the horizontal supply at reference station R-2 was assumed to be zero
32 since HNLC waters upstream and downstream of this station contained similar dFe and pFe

1 concentrations, and as phytoplankton growth and biomass was low at this site, there would be
2 little biogenic Fe exported below the mixed layer. On plateau Fe supply at station A3 was
3 taken from the steady-state box model of Chever et al. (2010) which used the horizontal dFe
4 gradient and current velocities from Park et al. (2008a) to calculate the lateral flux of 180
5 $\text{nmol m}^{-2} \text{d}^{-1}$ in the 0-150 m depth band above the plateau; noting this model used KEOPS-1
6 data. Lateral transport into the plume E stations was assumed to originate from Fe-fertilised
7 plateau waters that were advected offshore (d'Ovidio et al., 2015). This value was estimated
8 by assuming that horizontal stirring occurs in a Lagrangian framework, and by using
9 altimetry-derived geostrophic velocities to determine transports across the plateau boundary.
10 We also used a depth band of 0–150 m, considered as the winter mixed layer in the plume
11 over the season. These estimates were combined with direct measurements of the dFe content
12 of three different types of on-plateau stations to calculate the lateral flux over a 3-month
13 supply period prior to the spring bloom; namely: (i) two coastal stations near to Kerguelen
14 Island occupied on KEOPS-2 (stations TEW-1 and TEW-2), (ii) one coastal station close to
15 Heard Island occupied during KEOPS-1 (station C1), and (iii) the central plateau station A3
16 considered here. This resulted in 5.4×10^7 mol Fe per day being injected into a plume size
17 (defined at a threshold of $>0.3 \mu\text{g Chl-a L}^{-1}$ and identified from satellite images) of 2.5×10^{11}
18 m^2 over 90 days in spring (full details of the calculations are contained in d'Ovidio et al.,
19 2015). This equated to a lateral flux into the plume of $2400 \text{ nmol m}^{-2} \text{d}^{-1}$ in the October-
20 November period.

21 By combining our in-situ Fe measurements with estimated ages of the water bodies in the
22 plume, we calculate a first order exponential scavenging removal constant between 0.041 to
23 0.058 d^{-1} , which equated to a residence time of 17 to 24 days, consistent with estimates based
24 on the Fe inventory and Fe export in free-floating traps (15-79 days; Laurenceau-Cornec et al.
25 2015). Since the total of the vertical and lateral fluxes in the plume were more than double
26 those on the plateau, this may imply that the source waters supplying the plume from the
27 northern Kerguelen Island shelves (which had a uniquely narrow T-S class in surface waters;
28 Grenier et al., 2015) were richer in Fe than the plateau further south at A3. This is supported
29 by observations of dFe in the surface ocean at stations TEW-1 and TEW-2 ($1.2\text{-}1.8 \text{ nmol L}^{-1}$)
30 which were close to Hillsborough Bay in waters only 86 m deep (Qu  rou   et al., 2015).

31 Considering only internal processes (diffusion, upwelling, entrainment, lateral transport) in
32 supplying Fe to the surface mixed layer, the vertical terms dominated at the reference station,

1 vertical terms were 6-fold greater than lateral terms on the plateau, whereas lateral advection
2 was the dominant term in the plume (4-5-fold greater than the vertical terms). Since the
3 particulate Fe stocks were abundant in surface waters (above the winter temperature minimum
4 layer) and significantly higher than the dissolved pools (most notably on the plateau), it is
5 likely that a fraction of the suspended lithogenic pFe from Heard Island or the Kerguelen
6 plateau sediments also contributed to the internal dFe supply and fuelled biological responses.
7 This is discussed in more detail later.

8 **3.2.3 External iron supply**

9 Data on atmospheric Fe fluxes through dust deposition and the solubility of Fe in the dust for
10 all three study sites were taken from the nearby land-based sampling site “Jacky”
11 (49°18'42.3”S, 70°07'47.6”E; altitude 250 m) on the Kerguelen Islands, as reported in
12 Heimbürger et al. (2012, 2013a). Mean total Fe fluxes taken over the period 24/11/2008 to
13 07/09/2010 were $500 \pm 390 \text{ nmol m}^{-2} \text{ d}^{-1}$ (Heimbürger et al., 2013a), which was comparable
14 to the Crozet region upstream ($895 \text{ nmol m}^{-2} \text{ d}^{-1}$; Planquette et al., 2007) and the Southern
15 Ocean sector south of Australia ($288\text{-}488 \text{ nmol m}^{-2} \text{ d}^{-1}$; Bowie et al., 2009), but greater than
16 that estimated during the KEOPS-1 study by Wagener et al. (2008) ($14\text{-}46 \text{ nmol m}^{-2} \text{ d}^{-1}$). The
17 remoteness of the Kerguelen region means it receives low quantities of atmospheric material
18 (Heimbürger et al., 2012; Wagener et al., 2008) the majority of which is crustal in origin, such
19 as desert dust from South America, South Africa or Australia (Prospero et al., 2002;
20 Mahowald, 2007; Bhattachan et al., 2012), although local anthropogenic activities, rock
21 outcrops and exposed soil may also impact dust fluxes.

22 Atmospheric fluxes were dominated by wet deposition (Heimbürger et al., 2012). Heimbürger
23 et al. (2013b) calculated the mean ‘soluble’ Fe deposition flux (defined as $<0.2 \mu\text{m}$) using a
24 median solubility of $82 \pm 18\%$ in rainwater on Kerguelen Islands. These high solubilities were
25 attributed to remoteness of the sampling location from dust sources resulting in strong cloud
26 chemical processing during transport. However, the solubility of Fe dissolved in seawater at
27 higher pH will be much lower (Schroth et al., 2009; Sedwick et al., 2007). Hence a
28 conservative value of 10% of Fe that is released into seawater was chosen (Baker et al., 2006;
29 Mackie et al., 2006) for our budgets here, resulting in a soluble Fe atmospheric deposition
30 flux to the Kerguelen region of $50 \text{ nmol m}^{-2} \text{ d}^{-1}$ (Table 1, row ‘f’). This value was lower than
31 the internal vertical supply on the plateau (~20-fold) and plume (~10-fold), insignificant
32 compared to the lateral supply to the plume, but comparable to the lateral supply on the

1 plateau. Although volcanic ash has not been considered here for atmospheric Fe supply, this
2 term may have played an important role for primary productivity on the Kerguelen plateau
3 during the middle Miocene climate transition (Abrajevitch et al., 2014).

4 **3.2.4 Iron export**

5 Downward Fe and C fluxes were measured directly in free-floating sediment P-traps at the
6 plateau (A3-2) and plume (E-1, E-3, E-5) stations, and estimated using the ^{234}Th fluxes and
7 Fe/Th ratios at the reference site (R-2) (Planchon et al., 2014). The sinking of pFe was by far
8 the greatest loss term in our budgets, with $5746 \text{ nmol m}^{-2} \text{ d}^{-1}$ of total Fe exported from the
9 mixed layer on the plateau, between 895 and $4579 \text{ nmol m}^{-2} \text{ d}^{-1}$ exported at the plume stations
10 and $1302 \text{ nmol m}^{-2} \text{ d}^{-1}$ exported at the reference station. The flux of sinking pFe decreased
11 from station E-1 to E3 to E-5 concurrent with the seasonal progression of the bloom, and
12 indicating the mixed layer assemblages were efficiently recycling Fe under strong grazing
13 pressure (Laurenceau-Cornec et al., 2015). The downward total pFe fluxes were greater than
14 the sum of the vertical, lateral and atmospheric dFe supply on the plateau, but generally less
15 in the plume.

16 Aluminium was used as a normaliser to estimate the fraction of lithogenic Fe in the exported
17 material. The percentage lithogenic fraction of total pFe exported at the E stations remained
18 much the same at each deployment (34-39 %), whereas the lithogenic fraction was a much
19 larger component at A3-2 (51 %), reflecting the close proximity to sources of particulate
20 material rich in Fe. The Fe/Al ratio of exported material was higher at E stations (1.0-1.1) and
21 on the plateau A3-2 (0.87) compared to the Fe/Al ratio of lithogenically-dominated particles
22 (0.2; Wedepohl, 1995), confirming a significant amount of exported Fe was biogenic in
23 origin. Interestingly, the Fe/Al export ratios were similar to those associated with suspended
24 particles at E stations (0.9-1.2) but lower than the Fe/Al of suspended particles at A3-2 (1.2).
25 This suggests that the biota associated with the plateau bloom at A3 were capable of
26 efficiently recycling and retaining biogenic particulate Fe in the mixed layer (through rapid
27 turnover to prevent aggregation and sinking) relative to lithogenic particulate Fe, which had a
28 shorter residence time and was preferentially exported to depth. This may be due to greater
29 ballasting of the lithogenic particles (Ellwood et al., 2014), and is consistent with other export
30 studies which have shown that biologically-processed particles have longer residence times
31 than lithogenic particles in the mixed layer (Lamborg et al., 2008a). Since P may be lost from
32 exported particles much faster than Fe due to bacterial remineralisation and zooplankton

1 consumption (Schneider et al., 2003; Lamborg et al., 2008b), it was not appropriate to apply a
2 biogenic normaliser to the P-trap data as this may underestimate the biogenic Fe component
3 of particles captured in the traps.

4 Iron export fluxes were greater during the spring study of KEOPS-2 compared to the late
5 summer study of KEOPS-1 (Table 2). This difference between the KEOPS studies was also
6 observed in Fe uptake rates (Fourquez et al., 2015). Such observations may be simply related
7 to the seasonal supply; in other words, greater Fe supply in spring resulted in greater Fe
8 uptake and export. Determined pFe sinking fluxes were also greater than the CROZEX study
9 (Planquette et al., 2011), the SAZ-Sense expedition south of Tasmania (Bowie et al., 2009)
10 and those observed during the FeCycle-I expedition east of New Zealand (Frew et al., 2006),
11 of similar magnitude to those reported by Bowie et al. (2001) during the SOIREE iron
12 fertilisation experiment ($5.2 \mu\text{mol m}^{-2} \text{d}^{-1}$), but much lower than Ellwood et al. (2014)
13 reported for FeCycle-II.

14 The export of particulate organic carbon (POC) into our P-traps followed the same trend to
15 that of pFe at the E stations, decreasing from $7.0 \pm 2.3 \text{ mmol m}^{-2} \text{d}^{-1}$ at E-1 to $2.0 \pm 1.0 \text{ mmol m}^{-2}$
16 d^{-1} at E-5 (Table 1). Despite the higher pFe vertical fluxes at A3-2, POC export was lower
17 than the E stations. The C export fluxes at 200 m at A3-2 using our P-traps (Laurenceau-
18 Cornec et al., 2015) were similar to results estimated from ^{234}Th deficits by Planchon et al
19 (2014; 2.3 ± 0.7 and $3.8 \pm 0.8 \text{ mmol C m}^{-2} \text{d}^{-1}$, respectively). Comparison of these POC fluxes
20 to results (for the A3 plateau site only) obtained during KEOPS-1 illustrates highly dynamic
21 variations, reflecting the rapid decline of biomass during autumn (Blain et al., 2007).
22 Specifically, P-trap measurements of POC fluxes at 200 m during KEOPS-1 decreased from
23 3.7 ± 0.3 to $1.3 \pm 0.3 \text{ mmol C m}^{-2} \text{d}^{-1}$ over two visits to A3 in February 2005 (Trull et al., 2008),
24 whereas estimates based on ^{234}Th at this time, reflecting the previous ~ 30 days of export,
25 suggested much higher values ($25 \pm 7 \text{ mmol C m}^{-2} \text{d}^{-1}$; Savoye et al. 2008). These variations
26 illustrate the difficulty of constraining budgets in temporally evolving systems, providing a
27 cautionary note to our efforts. Additional discussion of temporal and spatial export flux
28 variations during KEOPS-2 is provided in Laurenceau-Cornec et al. (2015) and Planchon et
29 al. (2014).

1 **3.2.5 Biological iron recycling**

2 Intracellular Fe uptake by phytoplankton and bacteria $>0.2 \mu\text{m}$ (Fourquez et al., 2015) was
3 measured at stations A3-2 and E-5 when the bloom was rapidly growing (Cavagna et al.,
4 2014). Iron uptake fluxes were similar on both the plateau (A3-2) and in the plume (E-5),
5 ranging between 1120 and 1745 $\text{nmol m}^{-2} \text{d}^{-1}$. If we assume that the Fe uptake rate of 28.1
6 $\text{pmol L}^{-1} \text{d}^{-1}$ measured at E-5 (Fourquez et al., 2015) was conservative at E stations, 0.17 nmol
7 L^{-1} of Fe could have been consumed in surface waters between the occupations of stations E-
8 4E and E-5. This is consistent with the observed decrease in surface dFe concentrations from
9 0.19 to 0.06 nmol L^{-1} at E-4E and E-5, respectively (Fabien Qu  rou  , pers. comm.). The net
10 and gross demand calculated at A3 during KEOPS-1 (204 and 408 $\text{nmol m}^{-2} \text{d}^{-1}$, respectively;
11 Sarthou et al., 2008) is approximately 3-5 times smaller than the intracellular Fe uptake at A3-
12 2 during KEOPS-2 for a similar C biomass (mean value of 12.7 and 10.3 $\mu\text{mol L}^{-1}$ POC in
13 surface at KEOPS-1 and KEOPS-2, respectively; Cavagna et al., 2014), perhaps indicating
14 luxury uptake as well as important differences in community composition and activity
15 (primary production). These studies enable opportunity to compare KEOPS-2 to KEOPS-1
16 data and generate a general picture of the seasonal progress from early spring to late summer,
17 assuming that inter-annual and spatial variability is low, which may not be the case (Grenier
18 et al., 2015).

19 The bacterial and mesozooplankton contributions to Fe regeneration were calculated
20 separately (Table 3). Volumetric values varied between 0.06 and 0.59 $\text{pmol Fe L}^{-1} \text{d}^{-1}$, and
21 between 0.02 and 0.08 $\text{pmol Fe L}^{-1} \text{d}^{-1}$, for bacterial and mesozooplankton Fe regeneration,
22 respectively. The mesozooplankton rates were much lower than for KEOPS-1 because there
23 were much fewer individuals (0.26-0.56 per L, compared to about 1-6 individuals per L for
24 KEOPS-1; see Figure 2 in Carlotti et al., 2008). Total Fe regeneration fluxes ranged from 10
25 (R-2) to 71 (A3-2) $\text{nmol m}^{-2} \text{d}^{-1}$.

26 A similar Fe regeneration calculation was also performed based on the C budget by using the
27 percentage of gross community production (GCP) that is remineralized for KEOPS-2 and
28 results from Fe uptake experiments described above. This yielded higher Fe regeneration
29 estimates in the range 1-11 $\text{pmol L}^{-1} \text{d}^{-1}$. Specifically, for station A3-2, 23 % of GCP was
30 remineralised and therefore the Fe regeneration flux in the mixed layer was 1119 $\text{nmol m}^{-2} \text{d}^{-1}$
31 ¹. Similarly, for station E-5, 34 % of GCP was remineralised resulting in a Fe regeneration
32 flux of 504 $\text{nmol m}^{-2} \text{d}^{-1}$. Since the Fe regeneration fluxes based on the C budget are much

1 greater (~16 times) than those calculated using the first approach, this suggests that the
2 remineralisation efficiency for Fe regeneration appears to be less than that of C.

3 Iron regeneration fluxes can be compared with those from the KEOPS-1 study using the same
4 first approach above. For station A3 on KEOPS-1, this resulted in a Fe regeneration flux of 1
5 $\text{pmol L}^{-1} \text{d}^{-1}$ in surface waters. Malits et al. (2014) also calculated the release of bacterial
6 bound Fe by viral lysis ($0.42 \text{ pmol L}^{-1} \text{d}^{-1}$), which was the dominant loss term during KEOPS-
7 1 (Brussaard et al., 2008). This value compared to $1.5 \text{ pmol L}^{-1} \text{d}^{-1}$ determined in zooplankton
8 grazing experiments (Sarhou et al., 2008), suggesting that grazing and microbial Fe cycling
9 were in a similar range, and the total Fe regeneration was between 2-3 $\text{pmol L}^{-1} \text{d}^{-1}$ for
10 KEOPS-1.

11 Importantly, Fe regeneration was much lower during the early compared to late bloom stage
12 and was dominated by bacterial regeneration in spring (60-90% of total Fe regeneration).
13 Strezepek et al (2005) estimated Fe regeneration rates (during FeCycle-II) for herbivores
14 ($16.5\text{-}18.4 \text{ pmol L}^{-1} \text{d}^{-1}$), bacterivores ($15\text{-}25.5 \text{ pmol L}^{-1} \text{d}^{-1}$) and viruses ($0.4\text{-}28 \text{ pmol L}^{-1} \text{d}^{-1}$),
15 which is equivalent to a total Fe regeneration rate of $1435\text{-}3236 \text{ nmol m}^{-2} \text{d}^{-1}$ for a 45 m mixed
16 layer. Bowie et al. (2009) estimated Fe regeneration to be $261\text{-}1206 \text{ nmol m}^{-2} \text{d}^{-1}$ for the SAZ-
17 Sense study. So our determined KEOPS-2 mixed layer Fe regeneration rates (71 and 31 nmol
18 $\text{m}^{-2} \text{d}^{-1}$ at A3-2 and E-5, respectively) were on the lower end of the range reported in other
19 sectors of the Southern Ocean, and clearly insufficient to meet demand (measured as Fe
20 uptake) at all stations, indicating a reliance on 'new' Fe supply. This is discussed in more
21 detail below.

22

23 **3.3 Sequestration efficiencies: iron-to-carbon ratios**

24 The mixed layer phytoplankton intracellular Fe/C uptake ratios were calculated directly from
25 deckboard incubations for stations A3-2 ($0.007 \text{ mmol mol}^{-1}$) and E-5 ($0.021 \text{ mmol mol}^{-1}$)
26 (Table 1). These values are similar to those reported for other natural and artificial iron
27 fertilisation studies in the Southern Ocean, including for Fe-limited conditions during SOFeX
28 ($0.01 \text{ mmol mol}^{-1}$; Twining et al., 2004), those inside the KEOPS-1 plateau bloom (0.005
29 $\text{mmol Fe mol C}^{-1}$; Sarhou et al., 2008), but lower than those reported for SAZ-Sense (0.06-
30 $0.07 \text{ mmol mol}^{-1}$; Bowie et al., 2009).

1 Suspended mixed layer Fe/C ratios (Table 1) were significantly higher than phytoplankton
2 intracellular uptake ratios. This finding is likely the result of the contribution of lithogenic and
3 detrital Fe to suspended material Fe/C ratios, and is consistent with the removal of C at a
4 faster rate than that of Fe, and for Fe to be added through new sources after phytoplankton
5 uptake. Differences may also arise because of luxury uptake, the timescale of integration in
6 deckboard experiments compared to Fe/C ratios in ocean suspended and sinking particles
7 (which are broadly similar – see below), and/or that our system was not in steady-state. Also,
8 since a Ti-citrate-EDTA wash was used to remove extracellular surface Fe during the
9 incubation experiments, but not on particles collected in the ISPs and P-traps, our suspended
10 and sinking pFe concentrations include Fe present within cells, adsorbed to cell walls, detrital
11 Fe and lithogenic Fe. This would tend to increase Fe/C in suspended particles. Differences
12 between intracellular and suspended mixed layer Fe/C ratios may also derive from the C term,
13 since the ISP sampling includes detrital material as well as living cells. We also note that
14 suspended pFe data is the sum of 1-53um and >53um size fractions collected by ISPs and thus
15 may also include some sinking particles. This may affect the suspended Fe/C ratios.

16 In addition to the ratio of “total“ particulate (biogenic+lithogenic) Fe over POC (Fe/C) in
17 suspended particles discussed above, we also calculated the ratio of biogenic Fe over POC
18 (i.e., Fe_{bio}/C) following methods discussed in section 3.2.1. Profiles are shown in Figure 5.

19 Suspended Fe/C ratios were remarkably similar at all E stations and station R-2, but higher on
20 the plateau at A3 stations (Table 1). We also observed generally surface-to-deep increases in
21 Fe/C ratios in suspended particles at all stations (Figure 5), consistent with earlier findings
22 (Frew et al. 2006). The vertical profiles of Fe_{bio}/C showed similar structure at the three study
23 sites, with a general decreasing trend from the surface to sea floor (opposite to that of Fe/C),
24 noting that a constant Fe/P was used to estimate the Fe_{bio} component. These findings indicate
25 that Fe is preferentially retained within, and adsorbed to, sinking particles (i.e., scavenging
26 drives the “total” Fe/C ratio), but biogenic Fe is recycled at a faster rate compared to C,
27 similar to macronutrients N and P. A preferential loss of C relative to Fe from sinking
28 material implies that an external input of Fe is required to sustain a downward flux of carbon.

29 At station R-2, the Fe/C ratio peaked at 500 m, most likely due to lithogenic particulate Fe
30 input (and not C) from the Leclaire Rise (see above) (note this peak was not seen in the
31 Fe_{bio}/C ratios). At E stations, the Fe/C ratio showed maximum values in mesopelagic
32 intermediate waters in the 600-1000 m depth range. We also believe this was due to the lateral

1 transport of lithogenic particulate Fe (and not C) from the plateau (seafloor at ~600 m) into
2 the plume. This is supported by the absence of this feature in the Fe_{bio}/C ratios for E stations.
3 Fe/C ratios in deep waters were much higher at A3 stations (26-38 $mmol\ mol^{-1}$) compared to
4 R-2 (4 $mmol\ mol^{-1}$) and E stations (5-7 $mmol\ mol^{-1}$), indicating enrichment of lithogenic
5 particulate Fe above the plateau. Some fraction of this lithogenic Fe will be accessible to the
6 biota and then be incorporated into the biogenic Fe pool. This is confirmed by modification of
7 the Fe/Al ratio (van der Merwe et al., 2015). Inclusion of the biologically available fraction of
8 the lithogenic Fe flux is therefore required to calculate fully the yield of carbon exported per
9 unit Fe injected, consistent with Planquette et al. (2011) and Pollard et al. (2009).

10 Interestingly, although Fe/C ratios varied greatly between stations (0.2-37 $mmol\ mol^{-1}$), the
11 Fe_{bio}/C ratio fell within a narrow band (0.01-0.08 $mmol\ mol^{-1}$ for all stations and depths),
12 which encompasses the elemental ratios of Fe-replete (0.04 $mmol\ mol^{-1}$) and Fe-limited (0.01
13 $mmol\ mol^{-1}$) large diatoms (Sunda and Huntsman, 1995; de Baar et al., 2008). This highlights
14 the tight coupling between Fe_{bio} and POC in the absence of new sources of Fe, and allow us to
15 estimate the relative remineralisation efficiencies for Fe versus C. The Fe_{bio}/C data contrast
16 with the findings of Planquette et al. (2011) for the CROZEX study who observed variable
17 Fe_{bio}/C ratios to the north of Crozet (Fe-fertilised region) which were on average much higher
18 than those found to the south (Fe-limited region). The fraction of Fe_{bio} relative to lithogenic
19 Fe in particles collected below the mixed layer also depends on the stage of the bloom, the
20 nature and magnitude of supply of new lithogenic particles, and the rate of conversion from
21 lithogenic-to-biogenic Fe (Lam et al., 2006; Frew et al., 2006; Lam and Bishop, 2008). These
22 factors are highly variable in the Kerguelen region and this explains the wide range of Fe_{bio} -
23 to-“total” Fe values in particles observed during KEOPS-2.

24 The Fe/C export ratio of sinking particles in our traps were similar to suspended mixed layer
25 ratios for the E stations, but slightly higher at A3-2 (Figure 5), possibly due to the sinking of
26 recently supplied lithogenics over the plateau. Both pFe and POC export fluxes decreased
27 during bloom development at E stations, indicating the mixed layer became more retentive for
28 both Fe and C. This is consistent with the picture that emerges from the E time series from
29 primary and export production estimates which show that production was moderate and
30 matched by the moderate export during our visits (Planchon et al., 2014; Trull et al., 2015;
31 Cavagna et al., 2014).

1 Since POC export fluxes during spring (KEOPS-2) were similar to late summer (KEOPS-1),
2 but pFe export fluxes were higher in spring compared to summer (Table 2), this resulted in a
3 generally higher carbon sequestration efficiency (lower Fe/C) during late summer, consistent
4 with a rapidly exporting ecosystem during bloom decline. The exported particles may have
5 been dominated by more lithogenics and much more processed in KEOPS-2 compared to
6 KEOPS-1, where the system had already ran out of Fe. It was also expected that growing
7 communities during KEOPS-2 would retain dFe through luxury uptake, which may also result
8 in observed generally higher Fe/C ratios in sinking particles during the spring bloom
9 (KEOPS-2, FeCycle-II) compared to austral summer conditions (KEOPS-1, CROZEX,
10 FeCycle-I; Blue Water Zone; Morris and Charette, 2013) (Table 2 and Figure 6).

11 Morris and Charette (2013) presented a detailed synthesis of ^{234}Th -derived POC export and
12 dFe budgets in studies where natural iron fertilisation fuels the substantial phytoplankton
13 blooms observed in the Southern Ocean. Where data is available to calculate the seasonal
14 Fe/C ratios, an order of magnitude variation (0.006-0.06) is observed between different
15 Southern Ocean regions. It is likely that Fe/C ratio variations (Table 2) reflect both
16 experimental methodologies, different calculation approaches, observational limitations and
17 system complexities. Le Moigne et al. (2014) have also recently shown that variability in the
18 carbon sequestration efficiency is related to the mode of Fe delivery.

19

20 **3.4 Iron supply versus demand**

21 Using calculated flux estimates, a comparison of Fe supply and demand at the three sites
22 around the Kerguelen archipelago in spring was possible (Figure 7). In our short-term iron
23 biogeochemical budgets, the total dFe supply from ‘new’ sources (calculated as the sum of
24 diffusion, upwelling, vertical and lateral advection, and atmospheric dust) to surface waters of
25 the plume was more than twice that above the plateau and >20 times greater than at the
26 reference station (Table 1). The Fe demand (measured by cellular Fe uptake) in the plume was
27 similar (1.5 times greater) to the plateau but >40 times greater than at the reference station.
28 ‘New’ Fe supply was 14-94 times greater than ‘recycled’ Fe supply (‘iron remineralisation’;
29 row ‘i’ in Table 1) from bacterial regeneration and zooplankton grazing. This contrasts with
30 the findings of Bowie et al. (2009) for SAZ-Sense who reported recycled fluxes that were

1 broadly comparable with new Fe supply in the SAZ in summer at study sites further from
2 natural iron fertilisation.

3 Since Fe supply from 'new' sources was greater than the Fe demand (uptake minus
4 remineralisation as a 'recycled' Fe source) at all stations (R-2, A3-2 and E-5), this resulted in
5 a positive value for row 'k' in Table 1 (i.e., there was no additional Fe required to balance the
6 dissolved budget). This finding is consistent with other observations at both the plateau and
7 plume sites which were Fe replete in early spring, but somewhat surprising for the HNLC
8 reference site R-2. This may partly be a result of an over-estimate of the atmospheric supply
9 used in calculations presented here from literature data. Another explanation is that the
10 parameters used in our 'short-term' iron budget calculations are decoupled in time (e.g., there
11 will be an offset between the mechanisms for organism acquisition of Fe and the processes
12 resulting in Fe-laden particles leaving the upper ocean), and the short-term Fe budget is based
13 on an 'instantaneous picture' of different fluxes that were not in steady-state.

14 Interestingly, at station A3-2, the sink processes (Fe export and uptake) are so large and the
15 regenerated Fe flux so small, that the total (dissolved + particulate) Fe losses are far greater
16 than the net dFe supply (Figure 7a). In other words, to a first order the budget is not balanced
17 with known sources of Fe insufficient to account for the downward flux, even if we only
18 accounted for the non-lithogenic particulate Fe export flux (row 'l' in Table 1). Assuming all
19 flux calculations to be correct within the estimated error bounds in Table 1, this implies there
20 is a missing flux term in the budget at A3 and this is likely lithogenic pFe from the Kerguelen
21 plateau and/or Heard Island (and this may be converted to biogenic Fe). Currently, we do not
22 invoke a lithogenic pFe to dFe transfer in the budget, which could increase the Fe supply on
23 the plateau significantly, although at present we do not know what fraction of particulate
24 material is converted into the dissolved form. This will vary largely with the mineralogy
25 (Schroth et al., 2009), provenance of the particles, and seawater characteristics (e.g., organic
26 complexation; Shaked and Lis, 2012). Indeed, Thuróczy et al. (2012) previously measured
27 organic complexation in Antarctic waters and discussed the role of ligands in transporting and
28 dissolving pFe into dFe, using theoretical data provided by Borer et al. (2005).

29 By applying a solubility of 2.5 % used for KEOPS-1 at A3 to enable Fe supply to meet
30 demand (Blain et al., 2007), this would provide an extra $10\text{-}34 \mu\text{mol m}^{-2}$ of dFe to the mixed
31 layer over the plateau in KEOPS-2, approximately doubling the dFe standing stock. These
32 values are comparable to our observations and suggest that particulate material plays a major

1 role in the supply of dFe (van der Merwe et al., 2015). Further, if we assume pFe from glacial
2 melt is delivered over a 3 month period, this would provide an additional $111\text{-}387\text{ nmol m}^{-2}\text{ d}^{-1}$
3 to the mixed layer at A3, values of similar magnitude to the individual vertical and lateral
4 supply terms. Whilst a dissolution estimate of 2.5 % may be considered to be at the upper
5 extent of the range, Schroth et al. (2009) have reported that 2-3 % of Fe is soluble in glacial
6 flour which can remain suspended in surface water for several months after delivery from
7 Kerguelen or Heard Islands.

8 The release of Fe to biota via conversion of lithogenic to biogenic Fe has been previously
9 suggested (Lam et al., 2006; Frew et al., 2006; Borer et al., 2009; Planquette et al., 2011) and
10 the present work strongly supports this hypothesis, with our data (Figure 5) indicating that
11 biogenic Fe has a longer residence time in the upper ocean than lithogenic Fe which is not
12 accessed by biota. The role of pFe in supplying bioavailable Fe is also supported by the
13 similarity of the pFe and dFe profile shapes in Figure 3, which infer that pFe may be
14 contributing to the control of dFe, either by supplying it or because biogenic particles are
15 controlling both.

16 Finally, our estimation of Fe supply and regeneration allowed us to estimate an *fe* ratio,
17 defined by Boyd et al. (2005) as $fe = \text{uptake of new} / \text{uptake of new} + \text{regenerated Fe}$. For the
18 plume region, *fe* was 1.4 (Table 1). This was higher than the *fe* ratio calculated for KEOPS-1
19 (0.49; Sarthou et al. 2008), which at that time was comparable to the average *f*-ratio for
20 nitrogen of 0.41 (corresponding to NO_3^- uptake / (NO_3^- uptake + NH_4^+ uptake); Mosseri et al.,
21 2008), indicating that both NH_4^+ and regenerated Fe could support export production.
22 Conversely, the KEOPS-2 *f*-ratio was higher (up to 0.9; Cavagna et al., 2014), indicating that
23 primary production was mainly sustained by nitrate uptake. The *fe* ratios for both KEOPS
24 studies were much higher than the *fe* ratio estimated during FeCycle-I (0.17, Boyd et al.,
25 2005) and SAZ-Sense (0.06-0.16; Bowie et al., 2009). This confirms that in the Kerguelen
26 region, there are sufficient ‘new’ sources of Fe delivered on a seasonal timescale
27 (predominantly via intra-seasonal entrainment, winter mixing, lateral transport and particulate
28 Fe dissolution) available to sustain the massive bloom observed in spring.

30 **4 Conclusions**

31 The complex regional circulation, multiple iron sources, and transport pathways above and
32 downstream of the naturally fertilised Kerguelen plateau region results in a mosaic of

1 phytoplankton blooms. The budgets presented here result from direct measurements of the Fe
2 inventories and fluxes between different pools. The system was not in steady-state during the
3 period of the KEOPS-2 observations, and the exchange of Fe between the dissolved, biogenic
4 and lithogenic pools was highly dynamic in time and space. Our analysis highlights the
5 important role of pFe, the inherent heterogeneity and biogeochemical differences associated
6 with particulates within and exported below the mixed layer, and the lithogenic to biogenic
7 conversion pathways.

8 This study also highlights the significance not only of the mode of Fe fertilisation on the
9 plateau (predominantly vertical) versus the plume (predominantly lateral), but also of the
10 relative magnitude. Importantly, since the Fe supply from ‘new’ sources to the plume was
11 more than double that above the plateau, this implies the waters that supply the plume are not
12 the same as those at station A3 on the southern plateau, and the plume must be supplied with
13 water from the northern part of the plateau or Kerguelen coastal waters which are richer in
14 dFe (Qu  rou   et al., 2015; Trull et al., 2015). This source of Fe, which will contain a large
15 fraction of particulate material (van der Merwe et al., 2015) that is transported off the
16 Kerguelen plateau, is therefore an important but previously unquantified contribution to the
17 downward flux of Fe exiting the upper ocean in the plume. Moreover, the KEOPS-2 results
18 are tightly linked to the mode of Fe supply that is different from dust deposition or purposeful
19 additions, and to the concomitant supply of major nutrients, and this has consequences for the
20 carbon sequestration efficiency of the system. When Fe supply is predominantly vertical (as it
21 is at station A3), then the C sequestration efficiency is lower (i.e., higher Fe/C) as C would be
22 re-supplied to the mixed layer as well as Fe. This coupling has important implications for
23 geoengineering schemes that propose to increase the supply of Fe to surface waters by
24 pumping waters from below.

25 Future efforts should focus on the quantification of the full seasonal cycle of Fe delivery,
26 which will be fundamental to closing the iron budget around the Kerguelen archipelago over
27 annual timescales. This will allow assessment of the important longer-term climatic and
28 ecosystem implications with changes in the nature and strength of Fe supply with physical
29 (weakening overturning circulation, warming, increased stratification), and chemical (ocean
30 acidification, deoxygenation) environmental forcings, together with increases in glacial melt,
31 rainfall and dust deposition on a warming planet.

32

1 **Author contributions**

2 A. R. B. designed the iron budgets, performed the calculations and prepared the manuscript
3 with contributions from all co-authors. P. vd M., F. Q., G. S., F. C. and A. T. collaborated on
4 trace metal sampling, analyses and interpretation, M. F. and I. O. were responsible for
5 biological cycling, T. T. for carbon dynamics and the P-trap deployments, F. P. for Th-based
6 export, and J.-B. S. for vertical flux estimates. S. B. designed the overall KEOPS-2 study and
7 helped with budget calculations.

8

9 **Acknowledgements**

10 We thank the captain B. Lassiette, officers and crew of M.D. *Marion Dufresne*, Pierre
11 Sangiardi (Institut Paul Emile Victor) and the Institut National des Sciences de l'Univers for
12 voyage logistics and their support of the science, and voyage leader Bernard Quéguiner
13 (Institut Méditerranéen d'Océanologie) and chief scientist Stéphane Blain (LOMIC,
14 Université Pierre et Marie) for leading the KEOPS-2 expedition. We acknowledge Thomas
15 Rodemann (UTAS) for CHN analysis in the Central Science Laboratory, together with
16 members of the ISP and P-trap teams for support at sea. Michael Ellwood (Australian
17 National University) kindly loaned the TMR for the project. Access to ICP-MS was provided
18 through Australian Research Council LIEF funds (LE0989539). The altimeter and
19 colour/temperature products for the Kerguelen area were produced by Ssalto/Duacs and CLS
20 with support from CNES, and kindly prepared by Emmanuel Laurenceau-Cornec (UTAS) and
21 Francesco d'Ovidio (LOCEAN – IPSL, Université Pierre et Marie Curie). We thank Isabella
22 Rosso (Australian National University) for useful discussion.

23 This KEOPS-2 project was supported by the French Research program of INSU-CNRS
24 LEFE–CYBER ('Les enveloppes fluides et l'environnement' – 'Cycles biogéochimiques,
25 environnement et ressources'), the French ANR ('Agence Nationale de la Recherche', SIMI-6
26 program, ANR-2010-BLAN-614 KEOPS2 and, ANR-10-JCJC-606 ICOP), the French CNES
27 program ('Centre National d'Etudes Spatiales') and the French Polar Institute IPEV (Institut
28 Polaire Paul–Emile Victor). The Australian participation in the project was supported by the
29 Antarctic Climate and Ecosystems Cooperative Research Centre and a University of
30 Tasmania 'Rising Stars' award to the lead author.

1 We thank two anonymous reviewers for their very constructive comments which improved
2 our manuscript.
3

1 **References**

- 2 Abrajevitch, A., Roberts, A. P., and Kodama, K.: Volcanic iron fertilization of primary
3 productivity at Kerguelen Plateau, Southern Ocean, through the Middle Miocene Climate
4 Transition, *Palaeogeogr. Palaeoclimatol. Palaeoecol.*, 410, 1–13,
5 doi:10.1016/j.palaeo.2014.05.028, 2014.
- 6 Assmy, P., et al.: Thick-shelled, grazer-protected diatoms decouple ocean carbon and silicon
7 cycles in the iron-limited Antarctic Circumpolar Current, *Proc. Natl. Acad. Sci. USA* 110,
8 20633–20638, doi:10.1073/pnas.1309345110, 2013.
- 9 Baker, A. R., Jickells, T. D., Witt, M., and Linge, K. L.: Trends in the solubility of iron,
10 aluminium, manganese and phosphorus in aerosol collected over the Atlantic Ocean, *Mar.*
11 *Chem.*, 98(1), 43–58, doi:10.1016/j.marchem.2005.06.004, 2006.
- 12 Bhattachan, A., D’Odorico, P., Baddock, M. C., Zobeck, T. M., Okin, G. S., and Cassar, N.:
13 The Southern Kalahari: A potential new dust source in the Southern Hemisphere?, *Environ.*
14 *Res. Lett.*, 7, 1–7, doi:10.1088/1748-9326/7/2/024001, 2012.
- 15 Bishop, J. K. B., Lam, P. J., and Wood T. J.: Getting good particles: Accurate sampling of
16 particles by large volume in-situ filtration, *Limnol. Oceanogr.: Methods*, 10, 681-710,
17 doi:10.4319/lom.2012.10.681, 2012.
- 18 Blain S. et al.: Effect of natural iron fertilization on carbon sequestration in the Southern
19 Ocean, *Nature*, 446, 1070-1074, doi:10.1038/nature05700, 2007.
- 20 Blain, S., Quéguiner, B., and Trull, T.: The natural iron fertilization experiment KEOPS
21 (Kerguelen Ocean and Plateau compared Study): An overview, *Deep Sea Res. II* 55, 559-565,
22 doi:10.1016/j.dsr2.2008.01.002, 2008a.
- 23 Blain, S., Sarthou, G., and Laan, P.: Distribution of dissolved iron during the natural iron-
24 fertilization experiment KEOPS (Kerguelen Plateau, Southern Ocean), *Deep Sea Res. II* 55,
25 594-605, doi: 10.1016/j.dsr2.2007.12.028, 2008b.
- 26 Blain, S., Capparos, J., Guéneuguès, A., Obernosterer, I., and Oriol, L.: Distributions and
27 stoichiometry of dissolved nitrogen and phosphorus in the iron-fertilized region near
28 Kerguelen (Southern Ocean), *Biogeosciences*, 12, 623-635, doi:10.5194/bg-12-623-2015,
29 2015.
- Borer, P. M., Sulzberger, B., Reichard, P., and Kraemer, S. M.: Effect of siderophores

1 on the light-induced dissolution of colloidal iron(III)(hydr)oxides, *Mar. Chem.*, 93, 179–193,
2 doi:10.1016/j.marchem.2004.08.006, 2005.

3 Borer, P., Sulzberger, B., Hug, S. J., Kraemer, S. M., and Kretzschmar, R.: Photoreductive
4 dissolution of iron(III) (hydr)oxides in the absence and presence of organic ligands:
5 experimental studies and kinetic modelling, *Environ. Sci. Technol.*, 43 (6), 1864–1870,
6 doi:10.1021/es801352k, 2009.

7 Bowie A. R. and Lohan M. C.: Analysis of Iron in Seawater. Chapter 12 in: “Practical
8 Guidelines for the Analysis of Seawater”, Wurl O. (Ed.), Taylor and Francis, Boca Raton
9 (USA), Chapter 12, pp. 235-257, ISBN 978-1-4200-7306-5,
10 doi:10.1201/9781420073072.ch12, 2009.

11 Bowie A. R., Maldonado M. T., Frew R. D., Croot P. L., Achterberg E. P., Mantoura R. F. C.,
12 Worsfold P. J., Law C. S., and Boyd P. W.: The fate of added iron during a mesoscale
13 fertilisation experiment in the Southern Ocean. *Deep Sea Res. II*, 48, 2703-2743, doi:
14 10.1016/S0967-0645(01)00015-7, 2001.

15 Bowie A. R., Lannuzel D., Remenyi T.A., Wagener T., Lam P.J., Boyd P.W., Guieu C.,
16 Townsend A.T., and Trull T.W.: Biogeochemical iron budgets of the Southern Ocean south of
17 Australia: Decoupling of iron and nutrient cycles in the subantarctic zone by the summertime
18 supply, *Glob. Biogeochem. Cycles*, 23, GB4034, doi:10.1029/2009GB003500, 2009.

19 Bowie A. R., Townsend A. T., Lannuzel D., Remenyi T., van der Merwe P.: Modern
20 sampling and analytical methods for the determination of trace elements in marine particulate
21 material using magnetic sector ICP-MS, *Anal. Chim. Acta*, 676 (1-2) 15-27,
22 doi:10.1016/j.aca.2010.07.037, 2010

23 Boyd, P. W. and Ellwood, M. J.: The biogeochemical cycle of iron in the ocean, *Nat. Geosci.*,
24 3, 675–682, doi:10.1038/ngeo964, 2010.

25 Boyd P., et al.: A mesoscale phytoplankton bloom in the polar Southern Ocean stimulated by
26 iron fertilization, *Nature*, 407, 695–702, doi:10.1038/35037500, 2000.

27 Boyd, P.W. et al.: FeCycle: Attempting an iron biogeochemical budget from a mesoscale SF6
28 tracer experiment in unperturbed low iron waters, *Glob. Biogeochem. Cycles*, 19, GB4S20,
29 doi:10.1029/2005GB002494, 2005.

1 Boyd, P. W., et al.: Mesoscale Iron Enrichment Experiments 1993-2005: Synthesis and Future
2 Directions, *Science*, 315, 612-617, doi:10.1126/science.1131669, 2007.

3 Breitbarth, E., et al.: Iron biogeochemistry across marine systems – progress from the past
4 decade, *Biogeosciences*, 7(3), p. 1075-1097, doi:10.5194/bg-7-1075-2010, 2010.

5 Brussaard, C. P. D., Timmermans, K. R. , Uitz, J., and Veldhuis, M. J. W.: Virioplankton
6 dynamics and virally induced phytoplankton lysis versus microzooplankton grazing southeast
7 of the Kerguelen (Southern Ocean), *Deep-Sea Research II* 55, 752–765,
8 doi:10.1016/j.dsr2.2007.12.034, 2008.

9 Carlotti, F., Thibault-Botha, D., Nowaczyk, A. and Lefèvre, D.: Zooplankton community
10 structure, biomass and role in carbon fluxes during the second half of a phytoplankton bloom
11 in the eastern sector of the Kerguelen shelf (January-February 2005), *Deep Sea Res. II*, 55,
12 720-733, doi: 10.1016/j.dsr2.2007.12.010, 2008.

13 Carlotti, F., Jouandet, M.-P., Nowaczyk, A., Harmelin-Vivien, M., Lefèvre, D., Guillou, G.,
14 Zhu, Y., and Zhou, M.: Mesozooplankton structure and functioning during the onset of the
15 Kerguelen phytoplankton bloom during the Keops2 survey, *Biogeosciences Discuss.*, 12,
16 2381-2427, doi:10.5194/bgd-12-2381-2015, 2015.Carranza, M. M., and Gille, S. T.: Southern
17 Ocean wind-driven entrainment enhances satellite chlorophyll-a through the summer, *J.*
18 *Geophys. Res. Oceans*, 120, 304–323, doi:10.1002/2014JC010203, 2015.

19 Cavagna, A. J., Fripiat, F., Elskens, M., Dehairs, F., Mangion, P., Chirurgien, L., Closset, I.,
20 Lasbleiz, M., Flores–Leiva, L., Cardinal, D., Leblanc, K., Fernandez, C., Lefèvre, D., Oriol,
21 L., Blain, S., and Quéguiner, B.: Biological productivity regime and associated N cycling in
22 the vicinity of Kerguelen Island area, Southern Ocean, *Biogeosciences Discuss.*, 11, 18073-
23 18104, doi:10.5194/bgd-11-18073-2014, 2014.Chever, F., Sarthou, G., Bucciarelli, E., Blain
24 S., and Bowie A. R.: An iron budget during the natural iron fertilization experiment KEOPS
25 (Kerguelen Island, Southern Ocean), *Biogeosciences*, 7, 455–468, doi:10.5194/bg-7-455-
26 2010, 2010.

27 Christaki, U., Lefèvre, D., Georges, C., Colombet, J., Catala, P., Courties, C., Sime-Ngando,
28 T., Blain, S., and Obernosterer, I.: Microbial food web dynamics during spring phytoplankton
29 blooms in the naturally iron-fertilized Kerguelen area (Southern Ocean), *Biogeosciences*, 11,
30 6739-6753, doi:10.5194/bg-11-6739-2014, 2014.Cutter, G. A. and Bruland K. W.: Rapid and

1 noncontaminating sampling system for trace elements in global ocean surveys, *Limnol.*
2 *Oceanogr: Methods*, 10, 425-436, doi:10.4319/lom.2012.10.425, 2012.

3 de Baar, H. J. W., de Jong, J. T. M., Bakker, D. C. E., Löscher, B. M., Veth, C., Bathmann,
4 U., and Smetacek, V.: Importance of iron for plankton blooms and carbon dioxide drawdown
5 in the Southern Ocean, *Nature*, 373, 412-415, doi:10.1038/373412a0, 1995.

6 de Baar, H. J. W. et al.: Synthesis of iron fertilization experiments: From the iron age in the
7 age of enlightenment, *J. Geophys. Res.*, 110, C09S16, doi:10.1029/2004JC002601, 2005.

8 de Baar, H. J. W. et al.: Efficiency of carbon removal per added iron in ocean iron
9 fertilization, *Mar. Ecol. Prog. Ser.*, 364, 269-282, doi:10.3354/meps07548, 2008.

10 de Jong J.T.M. et al.: Dissolved iron at sub-nanomolar levels in the Southern Ocean as
11 determined by ship-board analysis, *Anal. Chim. Acta*, 377, 113-124, doi: 10.1016/S0003-
12 2670(98)00427-9, 2008.

13 de Jong, J., Schoemann, V., Lannuzel, D., Croot, P., de Baar, H., and Tison, J.-L.: Natural
14 iron fertilization of the Atlantic sector of the Southern Ocean by continental shelf sources of
15 the Antarctic Peninsula, *J. Geophys. Res.*, 117, G01029, doi:10.1029/2011JG001679, 2012.

16 d'Ovidio, F., Della Penna, A., Trull, T. W., Nencioli, F., Pujol, I., Rio, M. H., Park, Y.-H.,
17 Cotté, C., Zhou, M., and Blain, S.: The biogeochemical structuring role of horizontal stirring:
18 Lagrangian perspectives on iron delivery downstream of the Kerguelen plateau,
19 *Biogeosciences Discuss.*, 12, 779-814, doi:10.5194/bgd-12-779-2015, 2015.Ellwood, M. J.,
20 Nodder, S. D., Boyd, P. W., King, A. L., Hutchins, D. A., and Wilhelm, S. W.: Pelagic iron
21 cycling during the subtropical spring bloom, east of New Zealand, *Mar. Chem.*, 160, 18-33,
22 doi: 10.1016/j.marchem.2014.01.00, 2014.

23 Fourquez, M., Obernosterer, I., Davies, D. M., Trull, T. W., and Blain, S.: Microbial iron
24 uptake in the naturally fertilized waters in the vicinity of the Kerguelen Islands:
25 phytoplankton–bacteria interactions, *Biogeosciences*, 12, 1893-1906, doi:10.5194/bg-12-
26 1893-2015, 2015.Frants, M. et al.: Analysis of horizontal and vertical processes contributing
27 to natural iron supply in the mixed layer in southern Drake Passage, *Deep Sea Res. II*, 90, 68–
28 76, doi:10.1016/j.dsr2.2012.06.001, 2013.

29 Frew, R. D., Hutchins D. A., Nodder S., Sanudo-Wilhelmy S., Tovar-Sanchez A., Leblanc K.,
30 Hare C. E., and Boyd P. W.: Particulate iron dynamics during FeCycle in subantarctic waters

1 southeast of New Zealand, *Glob. Biogeochem. Cycles*, 20, GB1S93,
2 doi:10.1029/2005GB002558, 2006.

3 Gerringa, L. J. A., Blain, S., Laan, P., Sarthou, G., Veldhuis, M. J. W., Brussaard, C. P. D.,
4 Viollier, E., Timmermans, K. R.: Fe-binding dissolved organic ligands near the Kerguelen
5 Archipelago in the Southern Ocean (Indian sector), *Deep Sea Res. II*, 55, 606-621,
6 doi:10.1016/j.dsr2.2007.12.007, 2008.

7 Gordon, A. L., Taylor, H. W., and Georgi, D. T.: Antarctic oceanography zonation. In:
8 Proceedings of SCOR/SCAR Polar Oceans Conference, Montreal, Canada, May 5–11, 1974.
9 Dunbar, M.J. (Ed.), Arctic Institution of North America. McGill University, Montreal, 1977.

10 Grenier, M., Della Penna, A., and Trull, T. W.: Autonomous profiling float observations of
11 the high-biomass plume downstream of the Kerguelen Plateau in the Southern Ocean,
12 *Biogeosciences*, 12, 2707-2735, doi:10.5194/bg-12-2707-2015, 2015. Gunn, B. M., Coyyll,
13 R., Watkins, N. D., Abranson, C. E., and Nougier, J.: Geochemistry of an oceanite–
14 ankaramite–basalt suite from East Island, Crozet Archipelago, *Contrib. Mineral. Petrol.*,
15 28(4), 319–339, doi:10.1007/BF00388954, 1970.

16 Heimburger, A., Losno, R., Triquet, S., Dulac, F., and Mahowald, N.: Direct measurements of
17 atmospheric iron, cobalt, and aluminum-derived dust deposition at Kerguelen Islands, *Glob.*
18 *Biogeochem. Cycles*, 26, GB4016, doi:10.1029/2012GB004301, 2012.

19 Heimburger, A., Losno, R., Triquet, S. and Bon Nguyen, E.: Atmospheric deposition fluxes of
20 26 elements over the Southern Indian Ocean: time series on Kerguelen and Crozet Islands,
21 *Glob. Biogeochem. Cycles*, 27-2, 440-449, doi:10.1002/gbc.20043, 2013a.

22 Heimburger, A., Losno, R., and Triquet, S.: Solubility of iron and other trace elements over
23 the Southern Indian Ocean, *Biogeosciences*, 10, 6617-6628, doi:10.5194/bg-10-6617-2013,
24 2013b.

25 Homoky, W. B., John, S. G., Conway, T. M. and Mills, R. A.: Distinct iron isotopic
26 signatures and supply from marine sediment dissolution, *Nat. Comm.*, 4, 2143,
27 doi:10.1038/ncomms3143, 2013.

28 Hudson, R. J. M. and Morel, F. M. M.: Distinguishing between extra- and intracellular iron in
29 marine phytoplankton, *Limnol. Oceanogr.* 34: 1113-1120, doi:10.4319/lo.1989.34.6.1113,
30 1989.

1 Johnson, K. et al.: Developing standards for dissolved iron in seawater, *Eos Trans. AGU*,
2 88(11), 131–132, doi:10.1029/2007EO110003, 2007.

3 Kieffer, B., Arndt, N. T. and Weis, D.: A Bimodal Alkalic Shield Volcano on Skiff Bank: its
4 Place in the Evolution of the Kerguelen Plateau, *J. Petrology*, 43(7), 1259-1286,
5 doi:10.1093/petrology/43.7.1259, 2002.

6 King, P. et al.: Analysis of total and organic carbon and total nitrogen in settling oceanic
7 particles and a marine sediment: an interlaboratory comparison, *Mar. Chem.*, 60, 203-216,
8 doi: 10.1016/S0304-4203(97)00106-0, 1998.

9 Lam, P. J. and Bishop, J. K. B.: The continental margin is a key source of iron to the HNLC
10 North Pacific Ocean, *Geophys. Res. Lett.*, 35, L07608, doi:10.1029/2008GL033294, 2008.

11 Lam, P. J., Bishop, J. K. B., Henning, C. C., Marcus, M. A., Waychunas, G. A., and Fung, I.
12 Y.: Wintertime phytoplankton bloom in the subarctic Pacific supported by continental margin
13 iron, *Glob. Biogeochem. Cycles*, 20, GB1006, doi:10.1029/2005GB002557, 2006.

14 Lamborg, C. H., Buesseler, K. O., and Lam, P. J.: Sinking fluxes of minor and trace elements
15 in the North Pacific Ocean measured during the VERTIGO program, *Deep Sea Res. II*, 55
16 (14–15), 1564–1577, doi:10.1016/j.dsr2.2008.04.012, 2008a.

17 Lamborg, C. H., Buesseler, K. O., Valdes, J., Bertrand, C. H., Bidigare, R., Manganini, S.,
18 Pike, S., Steinberg, D., Trull, T., Wilson, S.: The flux of bio- and lithogenic material
19 associated with sinking particles in the mesopelagic “Twilight Zone” of the northwest and
20 north central Pacific Ocean, *Deep Sea Res. II*, doi:10.1016/j.dsr1012.2008.1004.1011, 2008b.

21 Lasbleiz, M., Leblanc, K., Blain, S., Ras, J., Cornet-Barthaux, V., Hélias Nunige, S., and
22 Quéguiner, B.: Pigments, elemental composition (C, N, P, and Si), and stoichiometry of
23 particulate matter in the naturally iron fertilized region of Kerguelen in the Southern Ocean,
24 *Biogeosciences*, 11, 5931-5955, doi:10.5194/bg-11-5931-2014, 2014.Laurenceau-Cornec, E.
25 C., Trull, T. W., Davies, D. M., Bray, S. G., Doran, J., Planchon, F., Carlotti, F., Jouandet,
26 M.-P., Cavagna, A.-J., Waite, A. M., and Blain, S.: The relative importance of phytoplankton
27 aggregates and zooplankton fecal pellets to carbon export: insights from free-drifting
28 sediment trap deployments in naturally iron-fertilised waters near the Kerguelen Plateau,
29 *Biogeosciences*, 12, 1007-1027, doi:10.5194/bg-12-1007-2015, 2015.Le Moigne F. A. C,
30 Moore C. M., Sanders R. J., Villa-Alfageme M., Steigenberger S., and Achterberg E. P.:

1 Sequestration efficiency in the iron limited North Atlantic: Implications for iron supply mode
2 to fertilized blooms, *Geophys. Res. Lett.*, 41, 4619–4627, doi:10.1002/2014GL060308, 2014.

3 Mackie, D. S., Peat, J. M., McTainsh, G. H., Boyd, P. W., and Hunter, K. A.: Soil abrasion
4 and eolian dust production: Implications for iron partitioning and solubility, *Geochem.*
5 *Geophys. Geosyst.*, 7, Q12Q03, doi:10.1029/2006GC001404, 2006.

6 Mackie, D. S., Boyd, P. W., McTainsh, G. H., Tindale, N. W., Westberry, T. K., and Hunter,
7 K. A.: Biogeochemistry of iron in Australian dust: From eolian uplift to marine uptake,
8 *Geochem. Geophys. Geosyst.*, 9, Q03Q08, doi:10.1029/2007GC001813, 2008.

9 Mahowald, N. M.: Anthropocene changes in desert area: Sensitivity to climate model
10 predictions, *Geophys. Res. Lett.*, 34, L18817, doi:10.1029/2007GL030472, 2007.

11 Malits, A., Christaki, U., Obernosterer, I., and Weinbauer, M. G.: Enhanced viral production
12 and virus-mediated mortality of bacterioplankton in a natural iron-fertilized bloom event
13 above the Kerguelen Plateau, *Biogeosciences*, 11, 6841-6853, doi:10.5194/bg-11-6841-2014,
14 2014.Marsay, C. M., Sedwick, P. N., Dinninman, M. S., Barrett, P. M., Mack, S. L. and
15 McGillicuddy Jr, D. J.: Estimating the benthic efflux of dissolved iron on the Ross Sea
16 continental shelf, *Geophys. Res. Lett.*, 41, doi:10.1002/2014GL061684, 2014.

17 Martin, J. H.: Glacial-interglacial CO₂ change: The iron hypothesis, *Paleoceanography*, 5(1),
18 1–13, doi:10.1029/PA005i001p00001, 1990.

19 Measures, C. I., Landing, W. M., Brown, M. T., and Buck, C. S.: High-resolution Al and Fe
20 data from the Atlantic Ocean CLIVAR-CO₂ Repeat Hydrography A16N transect: extensive
21 linkages between atmospheric dust and upper ocean geochemistry, *Glob. Biogeochem.*
22 *Cycles*, 22, GB1005, doi:10.1029/2007GB003042, 2008.

23 Mongin, M., Molina, E. and Trull, T. W.: Seasonality and scale of the Kerguelen plateau
24 phytoplankton bloom: A remote sensing and modeling analysis of the influence of natural
25 iron fertilization in the Southern Ocean, *Deep Sea Res. II*, 55(5-7): 880,
26 doi:10.1016/j.dsr2.2007.12.039, 2008.

27 Moore, C. M., Hickman, A. E., Poulton, A. J., Seeyave, S. and Lucas, M. I.: Iron-light
28 interactions during the CROZet natural iron bloom and EXport experiment (CROZEX) II:
29 taxonomic responses and elemental stoichiometry, *Deep Sea Res. II*, 54 (18-20) 2066-2084,
30 doi:10.1016/j.dsr2.2007.06.015, 2008.

1 Moore, J. K. and Doney, S. C.: Iron availability limits the ocean nitrogen inventory stabilizing
2 feedbacks between marine denitrification and nitrogen fixation. *Glob. Biogeochem. Cycle* 21,
3 GB2001, doi:10.1029/2006GB002762, 2007.

4 Morris P. J. and Charette M. A.: A synthesis of upper ocean carbon and dissolved iron
5 budgets for Southern Ocean natural iron fertilisation studies, *Deep Sea Res. II*, 90, 147–157,
6 doi:10.1016/j.dsr2.2013.02.001, 2013.

7 Mosseri, J., Quéguiner, B., Armand, L. and Cornet-Barthaux, V.: Impact of iron on silicon
8 utilization by diatoms in the Southern Ocean: A case study of Si/N cycle decoupling in a
9 naturally iron-enriched area, *Deep Sea Res. II*, 55, 801-819, doi: 10.1016/j.dsr2.2007.12.003,
10 2008.

11 Nishioka, J., Ono, T., Saito, H., Sakaoka, K., and Yoshimura, T.: Oceanic iron supply
12 mechanisms which support the spring diatom bloom in the Oyashio region, western subarctic
13 Pacific, *J. Geophys. Res.*, 116, C02021, doi:10.1029/2010JC006321, 2011.

14 Obata, H., Karatani, H. and Nakayama, E.: Automated determination of iron in seawater by
15 chelating resin concentration and chemiluminescence detection, *Anal. Chem.*, 5, 1524-1528,
16 doi: 10.1021/ac00059a007, 1993.

17 Osborn, T.R.: Estimates of the local rate of vertical diffusion from dissipation measurements,
18 *Journal of Physical Oceanography* 10, 83–89, doi:10.1175/1520-
19 0485(1980)010<0083:EOTLRO>2.0.CO;2, 1980.

20 Park, Y.-H., Fuda, J.-L., Durand, I. and Naveira Garabato, A.C.: Internal tides and vertical
21 mixing over the Kerguelen Plateau, *Deep Sea Res. II*, 55(5-7), 582-593,
22 doi:10.1016/j.dsr2.2007.12.027, 2008a.

23 Park, Y.-H., Roquet, F., Durand, I. and Fuda, J.-L.: Large-scale circulation over and around
24 the Northern Kerguelen Plateau, *Deep Sea Res. II*, 55(5-7), 566-581,
25 doi:10.1016/j.dsr2.2007.12.030, 2008b.

26 Park, Y.-H., Durand, I., Kestenare, E., Rougier, G., Zhou, M., d'Ovidio, F., Cotté, C., and Lee,
27 J.-H.: Polar Front around the Kerguelen Islands: An up-to-date determination and associated
28 circulation of surface/subsurface waters, *J. Geophys. Res. Oceans*, 119,
29 doi:10.1002/2014JC010061, 2014a.

1 Park, Y.-H., Lee, J.-H., Durand, I., and Hong, C.-S.: Validation of Thorpe-scale-derived
2 vertical diffusivities against microstructure measurements in the Kerguelen region,
3 *Biogeosciences*, 11, 6927-6937, doi:10.5194/bg-11-6927-2014, 2014. Planchon, F., Ballas, D.,
4 Cavagna, A.-J., Bowie, A. R., Davies, D., Trull, T., Laurenceau, E., Van Der Merwe, P., and
5 Dehairs, F.: Carbon export in the naturally iron-fertilized Kerguelen area of the Southern
6 Ocean based on the ^{234}Th approach, *Biogeosciences Discuss.*, 11, 15991-16032,
7 doi:10.5194/bgd-11-15991-2014, 2014.

8 Planquette, H. and Sherrell, R. M.: Sampling for particulate trace element determination
9 using water sampling bottles: methodology and comparison to in situ pumps, *Limnol.*
10 *Oceanogr. Methods*, 10, 367–388, doi:10.4319/lom.2012.10.367, 2012.

11 Planquette H. et al.: Dissolved iron in the vicinity of the Crozet Islands, Southern Ocean,
12 *Deep Sea Res. II*, 54(18-20), 1999-2019, doi:10.1016/j.dsr2.2007.06.019, 2007.

13 Planquette H., Fones G. R., Statham P. J., and Morris P. J.: Origin of iron and aluminium in
14 large particles (>53 μm) in the Crozet region, Southern Ocean, *Mar. Chem.*, 115, 31–42, doi:
15 10.1016/j.marchem.2009.06.002, 2009.

16 Planquette, H., Sanders, R. R., Statham, P. J., Morris, P. J., and Fones, G. R.: Fluxes of
17 particulate iron from the upper ocean around the Crozet Islands: A naturally iron-fertilized
18 environment in the Southern Ocean, *Glob. Biogeochem. Cycles*, 25, GB2011,
19 doi:10.1029/2010GB003789, 2011.

20 Planquette, H., Sherrell R. M., Stammerjohn, S., and Field M. P.: Particulate iron delivery to
21 the water column of the Amundsen Sea, Antarctica, *Mar. Chem.*, 153, 15–30,
22 doi:10.1016/j.marchem.2013.04.006, 2013.

23 Pollard, R. T. et al.: Southern Ocean deep-water carbon export enhanced by natural iron
24 fertilization, *Nature*, 457, 577–580, doi:10.1038/nature07716, 2009.

25 Price, N. M. and Morel, F. M. M.: Biological cycling of iron in the ocean. In: “Metal Ions in
26 Biological Systems”, Vol. 35, Iron Transport and Storage in Micro-organisms, Plants and
27 Animals. Marcel Dekker, New York, pp. 1-36, 1998.

28 Prospero, J. M., Ginoux, P., Torres, O., Nicholson, S. E., and Gill, T. E.: Environmental
29 characterization of global sources of atmospheric soil dust identified with the Nimbus 7 Total
30 Ozone Mapping Spectrometer (TOMS) absorbing aerosol product, *Rev. Geophys.*, 40 (1),
31 1002, doi:doi:10.1029/2000RG000095, 2002.

1 Qu erou , F., Sarthou, G., Planquette, H. F., Bucciarelli, E., Chever, F., van der Merwe, P.,
2 Lannuzel, D., Townsend, A. T., Cheize, M., Blain, S., d'Ovidio, F., and Bowie, A. R.: High
3 variability of dissolved iron concentrations in the vicinity of Kerguelen Island (Southern
4 Ocean), *Biogeosciences Discuss.*, 12, 231-270, doi:10.5194/bgd-12-231-2015, 2015. Roquet,
5 F., Park, Y.-H., Guinet, C., Bailleul, F., and Charrassin, J.-B.: Observations of the Fawn
6 Trough Current over the Kerguelen Plateau from instrumented elephant seals, *J. Mar. Sys.*,
7 doi:10.1016/j.jmarsys.2008.11.017, 2009.

8 Rosso, I., et al.: Vertical transport in the ocean due to sub-mesoscale structures: Impacts in the
9 Kerguelen region, *Ocean Model.*, doi:10.1016/j.ocemod.2014.05.001, 2014.

10 Sanial, V., van Beek, P., Lansard, B., Souhaut, M., Kestenare, E., d'Ovidio, F., Zhou, M., and
11 Blain, S.: Use of Ra isotopes to deduce rapid transfer of sediment-derived inputs off
12 Kerguelen, *Biogeosciences*, 12, 1415-1430, doi:10.5194/bg-12-1415-2015, 2015. Sarmiento,
13 J. L., Gruber, N.: Carbon Cycle. Chapter 8 in: "Ocean Biogeochemical Dynamics", Princeton
14 University Press, Princeton (USA), pp. 318-358, ISBN: 9780691017075, 2006.

15 Sarthou, G., Baker, A. R., Blain, S., Achterberg, E. P., Boye, M., Bowie, A. R., Croot, P.,
16 Laan, P., de Baar, H. J. W., Jickells, T. D. and Worsfold, P. J.: Atmospheric iron deposition
17 and sea-surface dissolved iron concentrations in the eastern Atlantic Ocean, *Deep Sea Res. I*,
18 50, 1339–1352, doi:10.1016/S0967-0637(03)00126-2, 2003.

19 Sarthou, G., Vincent, D., Christaki, U., Obernosterer, I., Timmermans, K.R. and Brussaard,
20 C.P.D.: The fate of biogenic iron during a phytoplankton bloom induced by natural
21 fertilisation: Impact of copepod grazing, *Deep Sea Res. II*, 55(5-7), 734,
22 doi:10.1016/j.dsr2.2007.12.033, 2008.

23 Savoye, N., Trull, T. W., Jacquet, S. H. M., Navez, J. and Dehairs, F.: ²³⁴Th-based export
24 fluxes during a natural iron fertilization experiment in the Southern Ocean (KEOPS), *Deep*
25 *Sea Res. II*, 55(5-7): 841, doi:10.1016/j.dsr2.2007.12.036, 2008.

26 Schlitzer, R.: Carbon export fluxes in the Southern Ocean: results from inverse modelling and
27 comparison with satellite-based estimates, *Deep Sea Res. II*, 49, 1623–1644,
28 doi:10.1016/S0967-0645(02)00004-8, 2002.

29 Schneider, B., Schlitzer, R., Fischer, G., and Nothig, E.-M.: Depth dependent elemental
30 compositions of particulate organic matter (POM) in the ocean, *Glob. Biogeochem. Cycles*,
31 17(2), doi:10.1029/2002GB001871, 2003.

- 1 Schroth, A. W., Crusius, J., Sholkovitz, E. R., and Bostick, B. C.: Iron solubility driven by
2 speciation in dust sources to the ocean, *Nat. Geosci.* 2, 337–340, doi: doi:10.1038/ngeo501,
3 2009.
- 4 SCOR Working Group: GEOTRACES – An international study of the global marine
5 biogeochemical cycles of trace elements and their isotopes, *Chem. Erde*, 67, 85–131,
6 doi:10.1016/j.chemer.2007.02.001, 2007.
- 7 Sedwick, P. N., Sholkovitz, E. R., and Church, T. M.: Impact of anthropogenic combustion
8 emissions on the fractional solubility of aerosol iron: Evidence from the Sargasso Sea,
9 *Geochem. Geophys. Geosyst.*, 8, Q10Q06, doi:10.1029/2007GC001586, 2007.
- 10 Shaked, Y. and Lis, H.: Disassembling Iron Availability to Phytoplankton. *Front. Microbiol.*
11 3:123, doi:10.3389/fmicb.2012.00123, 2012.
- 12 Sherrell, R. M. and Boyle, E. A.: The trace metal composition of suspended particles in the
13 oceanic water column near Bermuda, *Earth Planet. Sci. Lett.*, 111 (1), 155–174,
14 doi:10.1016/0012-821X(92)90176-V, 1992.
- 15 Shih, L. H., Koseff, J. R., Ivey, G. N., and Ferziger, J. H.: Parameterization of turbulent fluxes
16 and scales using homogeneous sheared stably stratified turbulence simulations, *Journal of*
17 *Fluid Mechanics*, 525, 193–214, doi:10.1017/S0022112004002587, 2005.
- 18 Sokolov, S. and Rintoul, S. R.: Circumpolar structure and distribution of the Antarctic
19 Circumpolar Current fronts: 1. Mean circumpolar paths, *J. Geophys. Res.*, 114, C11018,
20 doi:10.1029/2008JC005108, 2009.
- 21 Strzepek, R. F., Maldonado, M. T., Higgins, J. L., Hall, J., Safi, K., Wilhelm, S. W., and
22 Boyd, P.W.: Spinning the “Ferrous Wheel”: the importance of the microbial community in an
23 iron budget during the FeCycle experiment, *Glob. Biogeochem. Cycles*, 19, GB4S26,
24 doi:10.1029/2005GB002490, 2005
- 25 Sunda, W. G. and Huntsman, S. A.: Iron uptake and growth limitation in oceanic and coastal
26 phytoplankton, *Mar. Chem.*, 50: 189-206, doi:10.1016/0304-4203(95)00035-P, 1995.
- 27 Tagliabue, A., Bopp, L., and Aumont, O.: Evaluating the importance of atmospheric and
28 sedimentary iron sources to Southern Ocean biogeochemistry, *Geophys. Res. Lett.*, 36,
29 L13601, doi:10.1029/2009GL038914, 2009.

1 Tagliabue, A., Sallée, J.-B., Bowie, A. R., Lévy, M., Swart, S., and Boyd, P. W.: Surface-
2 water iron supplies in the Southern Ocean sustained by deep winter mixing, *Nat. Geosci.*, 7,
3 314–320, doi:10.1038/ngeo2101, 2014.

4 Tang D. G. and Morel F. M. M.: Distinguishing between cellular and Fe-oxide-associated
5 trace elements in phytoplankton, *Mar. Chem.*, 98, 18-30, doi:10.1016/j.marchem.2005.06.003,
6 2006.

7 Taylor, S. R. and McLennan, S. M.: The geochemical evolution of the continental crust. *Rev.*
8 *Geophys.*, 33(2), 241-265, doi:10.1029/95RG00262, 1995.

9 Thuróczy, C.-E., Alderkamp, A.-C., Laan, P., Gerringa, L. J. A., de Baar, H. J. W., Arrigo, K.
10 R.: Key role of organic complexation of iron in sustaining phytoplankton blooms in the Pine
11 Island and Amundsen Polynyas (Southern Ocean), *DSR II*, 71-76, 49-60,
12 doi:10.1016/j.dsr2.2012.03.009, 2012.

13 Tortell, P. D., Maldonado, M. T., and Price, N. M.: The role of heterotrophic bacteria in iron-
14 limited ocean ecosystems, *Nature*, 383, 330–332, doi:10.1038/383330a0, 1996.

15 Trull, T. W., Davies, D., and Casciotti, K.: Insights into nutrient assimilation and export in
16 naturally iron-fertilized waters of the Southern Ocean from nitrogen, carbon and oxygen
17 isotopes, *Deep Sea Res. II*, 55(5-7), 820-840, doi:10.1016/j.dsr2.2007.12.035, 2008.

18 Trull, T. W., Davies, D. M., Dehairs, F., Cavagna, A.-J., Lasbleiz, M., Laurenceau-Cornec, E.
19 C., d'Ovidio, F., Planchon, F., Leblanc, K., Quéguiner, B., and Blain, S.: Chemometric
20 perspectives on plankton community responses to natural iron fertilisation over and
21 downstream of the Kerguelen Plateau in the Southern Ocean, *Biogeosciences*, 12, 1029-1056,
22 doi:10.5194/bg-12-1029-2015, 2015. Twining, B. S., Baines, S. B., Fisher, N. S., and Landry
23 M. R.: Cellular iron contents of plankton during the Southern Ocean Iron Experiment
24 (SOFeX), *Deep Sea Res. I*, 51, 1827– 1850, doi:10.1016/j.dsr.2004.08.007, 2004.

25 van Beek, P., Bourquin, M., Reyss, J. L., Souhaut, M., Charette, M. A., and Jeandel, C.:
26 Radium isotopes to investigate the water mass pathways on the Kerguelen Plateau (Southern
27 Ocean), *Deep Sea Res. II*, 55, 622-637, doi:10.1016/j.dsr2.2007.12.025, 2008.

28 van der Merwe, P., Bowie, A. R., Quéroué, F., Armand, L., Blain, S., Chever, F., Davies, D.,
29 Dehairs, F., Planchon, F., Sarthou, G., Townsend, A. T., and Trull, T. W.: Sourcing the iron in
30 the naturally fertilised bloom around the Kerguelen Plateau: particulate trace metal dynamics,
31 *Biogeosciences*, 12, 739-755, doi:10.5194/bg-12-739-2015, 2015. Wadley, M. R., Jickells, T.

1 D., and Heywood, K. J.: The role of iron sources and transport for Southern Ocean
2 productivity, *Deep Sea Res. I*, 87, 82-94, doi:10.1016/j.dsr.2014.02.003, 2014.

3 Wagener, T., Guieu, C., Losno, R., Bonnet, S., and Mahowald, N.: Revisiting atmospheric
4 dust export to the southern hemisphere ocean: biogeochemical implication, *Glob.*
5 *Biogeochem. Cycles*, 22, GB2006, 1-13, doi:10.1029/2007GB002984, 2008.

6 Wedepohl, K. H.: The composition of the continental crust, *Geochim. Cosmochim. Acta*, 59,
7 1217–1232, doi:10.1016/0016-7037(95)00038-2, 1995.

8 Westberry, T. K., Behrenfeld, M. J., Milligan, A. J., and Doney, S. C.: Retrospective satellite
9 ocean color analysis of purposeful and natural ocean iron fertilization, *Deep Sea Res. I*, 73, 1-
10 16, doi:10.1016/j.dsr.2012.11.010, 2013.

11 Zhang, Y., Lacan, F., and Jeandel, C.: Dissolved rare earth elements tracing lithogenic inputs
12 over the Kerguelen Plateau (Southern Ocean), *Deep Sea Res. II*, 55, 638-652,
13 doi:10.1016/j.dsr2.2007.12.029, 2008.

14 Zhou, M., Zhu, Y., Dorland, R. D., and Measures, C. I.: Dynamics of the current system in the
15 southern Drake Passage, *Deep Sea Res. I*, 57, 1039-1048, doi:10.1016/j.dsr.2010.05.012,
16 2014.

17 Zhou, M., Zhu, Y., d'Ovidio, F., Park, Y.-H., Durand, I., Kestenare, E., Sanial, V., Van-Beek,
18 P., Quéguiner, B., Carlotti, F., and Blain, S.: Surface currents and upwelling in Kerguelen
19 Plateau regions, *Biogeosciences Discuss.*, 11, 6845-6876, doi:10.5194/bgd-11-6845-2014,
20 2014.

21

1 **Figure captions**

2 Figure 1. (a) The location of the KEOPS-2 study in the Indian sector of the Southern Ocean
3 showing bathymetry around the Kerguelen archipelago. Our biogeochemical iron budgets
4 focus on three process stations (open black circles): reference R-2 (50°2' S, 66°4' E), plateau
5 A3 (50°4' S, 72°0' E) and plume E (48°3' S, 72°1' E). Black dots mark the positions of the
6 other stations visited, including N-S and E-W survey transects at the start of the KEOPS-2
7 expedition. (b) A schematic of the mean regional circulation of surface/subsurface waters
8 around the Kerguelen archipelago, indicating circumpolar Southern Ocean fronts, locations of
9 stations conducted along N-S and E-W transects, and pathways and origins of different water
10 masses flowing on the plateau and offshore into the plume. The abbreviations are Antarctic
11 Surface Water (AASW), Polar Frontal Surface Water (PFSW), Subantarctic Surface Water
12 (SASW), and Subtropical Surface Water (STSW), subantarctic front (SAF), polar front (PF)
13 (reproduced with permission from Park et al. (2014a), courtesy of Isabelle Durand and
14 Young-Hyang Park, LOCEAN/DMPA, MNHN, Paris).

15 Figure 2. MODIS ocean-colour satellite images showing the development of the plateau and
16 plume blooms during the KEOPS-2 study. Surface chlorophyll ($\mu\text{g L}^{-1}$) biomass is shown for
17 the nearest clear sky day to the final sampling day at stations R-2 (panel a), A3-2 (panel b)
18 and E-5 (panel c). The polar front is shown as a black dashed line in panels b and c. Trull et
19 al. (2015) discuss the timing of the stations relative to bloom development.

20 Figure 3(a). Vertical profiles of dissolved iron (dFe) and particulate iron (pFe), potential
21 temperature, salinity and nitrate at reference station R-2. The seafloor depth at 2528 m is
22 shown. (b, c) Vertical profiles of dFe and pFe, potential temperature, salinity and nitrate at
23 plateau stations A3-1 (panel b) and A3-2 (panel c). The seafloor depth at ~530 m is shown.
24 Note different scales for dFe and pFe compared to R-2 and E stations. (d, e, f) Vertical
25 profiles of dFe and pFe, potential temperature, salinity and nitrate at plume stations E1 (panel
26 d), E3 (panel e) and E5 (panel f). The seafloor depth ranging from 1905 m (E3) to 2057 m
27 (E1) is shown.

28 Figure 4. (a) Comparison of dFe and pFe at reference stations for KEOPS-1 (station C11,
29 open blue diamonds) and KEOPS-2 (station R-2, closed red squares) studies. The water
30 depths were 3110 m at C11 and 2530 m at R-2. (b) Comparison of dFe and pFe at A3 plateau
31 stations for KEOPS-1 (open symbols) and KEOPS-2 (closed symbols) studies. Data are

1 shown for all visits to A3 on both KEOPS cruises. Note difference in scale for dFe and pFe
2 between (a) and (b).

3 Figure 5. Vertical profiles of Fe/C ratios in suspended (ISP) and sinking (P-trap) particles.
4 Solid symbols indicate “total” Fe/C (i.e., ratio of biogenic + lithogenic Fe over POC) and
5 joined open symbols indicate Fe_{bio}/C (i.e., ratio of biogenic Fe only over POC; calculated
6 using P as a normaliser). The asterisk markers (*) show the export “total” Fe/C ratio (P-traps).
7 Note the different scale on the x-axis for Fe/C at A3 stations.

8 Figure 6. A comparison of export fluxes of pFe versus POC in sinking particles for natural
9 iron fertilisation studies in the Southern Ocean. For details of the sampling methods, refer to
10 Table 2 and the original articles. The lines indicate Fe/C ratios for Fe limited (black dashed)
11 and Fe replete (black solid) phytoplankton (Twining et al., 2004), and the mean mixed layer
12 intracellular Fe/C ratios at stations A3-2 (orange dashed) and E5 (orange solid) on KEOPS-2
13 (taken from Table 1). FeCycle-II had complex biogeochemical dynamics due to a storm event
14 and subsequent deep water mixing (during sediment trap deployment at their station A3),
15 splitting the study into two phases (“eddy centre” and “eddy periphery”). To aid interpretation
16 of Fe/C export data in the context of iron fertilisation, only data from the pseudo Lagrangian
17 phase 1 (i.e., deployments A1 and A2 during bloom development and export) from that study
18 is included in this plot (Ellwood et al., 2014).

19 Figure 7. Biogeochemical iron budgets for the reference (R-2, panel a), plateau (A3-2, panel
20 b) and plume (E-5, panel c) stations. Iron pools are given in $\mu\text{mol m}^{-2}$ and iron fluxes in nmol
21 $\text{m}^{-2} \text{d}^{-1}$. Iron sources are shown as blue arrows, sinks as red arrows and the green arrows
22 indicate biological Fe cycling. The size of the arrows is roughly proportional to the magnitude
23 of the Fe fluxes, with major fluxes shown as bold underlined text..

24

1 Table 1. Summary of iron standing stocks and fluxes for the upper mixed layer at KEOPS-2 process station sites R-2 (reference), A3 (plateau)
 2 and E (plume). For full details of the calculations, see text. Error bounds are provided where available. Due to logistical constraints resulting
 3 in missing data at some stations, we will focus on R-2, A3-2 and E-5 in the discussion. Data for stations A3-1, E-1 and E-3 are given to
 4 provide a context for spatial and temporal changes in the pools and fluxes during KEOPS-2.

5

Region	Reference	Plateau		Plume		
Station	R-2	A3-1	A3-2	E-1	E-3	E-5
Location	50°21.53' S 66°42.44' E	50°37.88' S 72°04.99' E	50°37.47' S 72°03.35' E	48°27.44' S 72°11.26' E	48°42.13' S 71°58.01' E	48°24.69' S 71°53.99' E
Mixed layer depth (m) ¹	76	165	123	64	32	39
Bottom depth (m)	2528	533	530	2057	1905	1920
<i>Iron pools, integrated over the mixed layer ($\mu\text{mol m}^{-2}$, unless otherwise stated)</i>						
dFe	7 ± 1	54 ± 10	21 ± 4	n.d. ²	12 ± 0	2 ± 0
pFe	43 ± 0	1392 ± 195	401 ± 52	117 ± 1	n.d. ³	61 ± 1
Biogenic pFe	9	13	14	11	n.d.	9
Lithogenic pFe	12	892	265	33	n.d.	9
POC (mmol m^{-2})	124 ± 11	239 ± 33	274 ± 24	198 ± 10	n.d.	150 ± 12
<i>Iron fluxes ($\text{nmol m}^{-2} \text{d}^{-1}$, unless otherwise stated)</i>						
(a) Diffusion	2	42	93	n.d.	1	0.5
(b) Upwelling	35	200	250	n.d.	330	140
(c) Entrainment	57	769	769	n.d.	330	330
(d) Total vertical dFe supply [a+b+c]	94	1011	1112	n.d.	661	471
(e) Lateral advective dFe supply	0	180		2400±600		
Ratio of lateral-to-vertical supply [e/d]	0	0.2		4-5		

Atmospheric total Fe deposition	500 ± 390					
(f) Atmospheric soluble Fe deposition	50 ± 39					
Downward total pFe export flux	1302 ± 586 ⁴	n.d.	5746 ± 1198	4579 ± 1376	1890 ± 286	895 ± 358
(g) Downward non-lithogenic pFe export flux			2797 ± 583			541 ± 216
Downward POC export (mmol m ⁻² d ⁻¹)	1.8 ± 0.9 ⁵	n.d.	2.2 ± 0.7	7.0 ± 2.3	4.9 ± 1.5	2.0 ± 1.0
(h) Iron uptake ⁶	40 ± 6	2528 ± 704	1120 ± 389	n.d.	743 ± 194	1745 ± 350
(i) Iron remineralization ⁷	10 ± 2	19 ± 6	71 ± 12	27 ± 2	23 ± 2	31 ± 2
<i>Fe/C ratios (mmol mol⁻¹)</i>						
(j) Mixed layer Fe/C cellular uptake ratio ⁸	n.d.	n.d.	0.007 ± 0.004	n.d.	n.d.	0.021 ± 0.002
Suspended mixed layer particulate “total” Fe/C ratio ⁸	0.2 ± 0.1	3.3 ± 0.4	1.5 ± 0.2	0.5 ± 0.1	n.d.	0.4 ± 0.1
Sinking “total” Fe/C export ratio	n.d.	n.d.	2.6 ± 1.0	0.7 ± 0.5	0.4 ± 0.3	0.5 ± 0.1
<i>Iron supply vs demand (for reference R-2, plateau A3-2 and plume E-5 stations ONLY) (nmol m⁻² d⁻¹)</i>						
Total iron supply from ‘new’ sources [d+e+f] ⁹	144		1342			2921
(k) Additional iron requirement to balance the dissolved budget [d+e+f-h+i] ¹⁰	114		293			1207
(l) Biological uptake of ‘new’ iron [d+e+f-g] ¹¹	-1158		-1455			2380
fe ratio [l/h] ¹²						1.4
Fe ratio [g/h] ¹²						0.3
<i>Estimated vs observed production (mmol C m⁻² d⁻¹)</i>						
Potential new primary production [l/j] ¹³						132
Observed net primary production ¹⁴	11 ± 0	n.d.	158 ± 15	44 ± 4	57 ± 8	79 ± 9

1

1 n.d. = no data

2 ¹ The mixed layer depths were calculated on the density plane to allow for heave (internal tides driven by topography) and other localised
3 events

4 ² Due to logistical reasons there was no TMR cast for dFe at station E-1

5 ³ Due to ISP failure, there were no mixed layer samples for pFe at station E-3

6 ⁴ The P-trap was lost at R-2. We therefore estimated the pFe export flux using the ²³⁴Th flux in suspended particles at 200 m (449 ± 203 dpm
7 $\text{m}^{-2} \text{d}^{-1}$; from Table 1 in Planchon et al., 2014) and a mean Fe/Th ratio collected in the upper 200 m above the trap (2.9 ± 1.3 nmol dpm⁻¹). This
8 estimation method will reflect the integrated Fe export over the previous ~30 days, rather than an instantaneous flux at the time of sampling.
9 Since this was a reference site, with low phytoplankton abundance, the longer time period probably has a minimal effect upon interpretation of
10 the data

11 ⁵ Estimated using the ²³⁴Th flux and Fe/C ratio in suspended particles at 200 m

12 ⁶ For stations R-2, A3-1, E-1 and E-3, seawater for iron uptake experiments were conducted for small cells filtered through a 25 μm mesh.
13 This size-fraction represented between 77% and 91% of the total POC pool. At stations A3-2 and E-5, we also used unfiltered seawater for our
14 uptake experiments. Similar results were obtained for both the 0.2-25 μm and unfiltered fractions at station A3-2

15 ⁷ Includes bacterial and mesozooplankton contributions

16 ⁸ Mean of all samples collected in the mixed layer

17 ⁹ Assumes only the soluble iron atmospheric supply is available (see text)

18 ¹⁰ A negative value indicates an additional iron requirement

19 ¹¹ At stations R-2 and A3-2, the negative values most likely occurred due to differences in the timescales of observations and calculations of
20 fluxes (parameters were decoupled in time). The iron budget was based on an 'instantaneous picture' of different fluxes that were not strictly
21 measured at the same time (i.e., export fluxes operated on a different timeframe to the iron supply (vertical, lateral and atmospheric) and were
22 very large at R-2 and A3-2

23 ¹² f_e = uptake of new/uptake of new + regenerated iron and F_e = biogenic iron export/uptake of new + regenerated iron [Boyd et al., 2005].
24 Note the f_e and F_e ratios have considerable plasticity due to uncertainties in the lithogenic vs biogenic fraction of exported particulate iron,
25 and the missing iron source at A3-2

- 1 ¹³ Calculated using the biological uptake of 'new' iron (k) and molar Fe/C cellular uptake ratio (j)
- 2 ¹⁴ Net primary production (NPP) integrated within the euphotic zone down to 1% PAR, based on ¹³C incorporation (Cavagna et al., 2014)

1 Table 2. Fluxes of iron and carbon exported in sinking particles (trap deployed at 200 m) and
 2 ratio of Fe/C in sinking (traps) and suspended mixed layer (ISP) particles at stations A3-2 and
 3 E-stations. There was no successful trap deployment at station R-2. A comparison to previous
 4 studies is provided.

Site	PFe flux ($\mu\text{mol m}^{-2} \text{d}^{-1}$)		POC flux ($\text{mmol m}^{-2} \text{d}^{-1}$)		Fe/C (sinking) (mmol mol^{-1})		Fe/C (suspended) (mmol mol^{-1})
	mean	stdev	mean	stdev	mean	stdev	mean
KEOPS-2							
A3-2	5.75	1.20	2.23	0.68	2.57	0.97	1.51
E-1	4.58	1.38	7.02	2.28	0.65	0.52	0.49
E-3	1.89	0.29	4.87	1.54	0.39	0.29	0.39
E-5	0.90	0.36	2.00	1.00	0.45	0.13	0.33
KEOPS-1 ¹							
A3-initial	0.33	0.05	3.60	0.43	0.09		
A3-final	0.20	0.02	1.36	0.39	0.15		
C5	1.51	0.32	1.57	0.08	0.96		
CROZEX ²							
North	0.84		15.9		2.55		0.69
South	0.23		12.9		0.57		0.31
SAZ-Sense ³							
P1	0.17	0.09	3.34	1.81	0.05	0.04	0.04
P2	0.07	0.01	2.11	0.88	0.04	0.02	0.06
P3	0.21	0.05	0.86	0.38	0.25	0.13	0.03
FeCycle-I ⁴							
F1-80 m	0.22	0.03	n.d.		n.d.		0.04
F1-120 m	0.36	0.05	2.09	0.03	0.17		
F2-80 m	0.55	0.06	2.51	0.17	0.22		
F2-120 m	0.35	0.03	2.10	0.01	0.17		
FeCycle-II ⁵							
A1-100 m	5.0	0.7	11		0.45		0.78
A1-200 m	7.3	1.6	5.8		1.26		
A2-100 m	10	1.0	42		0.24		1.12
A2-200 m	10	9	6.8	1.8	1.47		
A3-100 m	17	2	12	2	1.42		0.63
A3-200 m	10	1	14		0.71		
A4-100 m	20	8	9.3	0.9	2.15		0.86
A4-200 m	15	6	6.1	1.8	2.46		
Other literature data							
Mixed plankton assemblages ⁶							0.01-0.05
Iron limited algae ⁷							0.01
Iron replete algae ⁷							0.02-0.05
Southern Ocean synthesis ⁸					0.01-0.06		

1

2 n.d. = no data

3 ¹ Data for particles >0.2 μm (Blain et al., 2007; Bowie et al., unpublished data)

4 ² Data for >53 μm particles only (Planquette et al., 2011). Downward Fe fluxes were
5 estimated from samples collected from in situ pumps using ²³⁴Th depletions and Fe/Th ratios
6 in sinking particles. Waters to the north of Crozet Island were “downstream” of the islands
7 and iron fertilised, whilst those to the south were “upstream” HNLC conditions. The Fe/C
8 from bioassay culturing experiments conducted during CROZEX was 0.25 mmol mol⁻¹
9 (Moore et al., 2008)

10 ³ Data for particles >1 μm (Bowie et al., 2009)

11 ⁴ Data for particles >0.4 μm (Frew et al., 2006). Only 1 mixed layer Fe/C ratio was reported.
12 The biogenic Fe/C mixed layer ratio was estimated to be 0.004-0.012 mmol mol⁻¹

13 ⁵ Data for particles >0.4 μm , except deployment A1 (>2 μm) (Ellwood et al., 2014). The
14 mixed layer Fe/C ratios were calculated from Table 4 using the sediment traps deployment
15 periods reported in Table 3 in the original publication

16 ⁶ Estimates of Fe/C for diatoms and whole plankton assemblages compiled by de Baar et al.
17 (2008), with optimal ratios for growth tending towards the upper end of the range

18 ⁷ Intracellular ratio reported for HNLC polar water south of New Zealand during SOFeX
19 (Twining et al., 2004)

20 ⁸ Ratio of dFe supply to POC export, synthesis by Morris and Charette (2013)

21

1 Table 3. Iron regeneration rates based on bacterivore and herbivore contributions.

2

Site	Bacterial ($\text{pmol L}^{-1} \text{d}^{-1}$)	Mesozooplankton ($\text{pmol L}^{-1} \text{d}^{-1}$)	Total Fe regeneration ($\text{pmol L}^{-1} \text{d}^{-1}$)	% bacterial contribution	Total integrated mixed layer Fe regeneration ($\text{nmol m}^{-2} \text{d}^{-1}$)
R-2	0.06 ± 0.01	0.04	0.10	61	10
A3-1	0.10 ± 0.03	0.02	0.12	87	19
A3-2	0.43 ± 0.07	0.03	0.46	93	71
E-1	0.33 ± 0.02	0.04	0.37	88	27
E-3	0.54 ± 0.04	0.06	0.60	90	23
E-5	0.59 ± 0.03	0.08	0.67	88	31

3

Figure 1

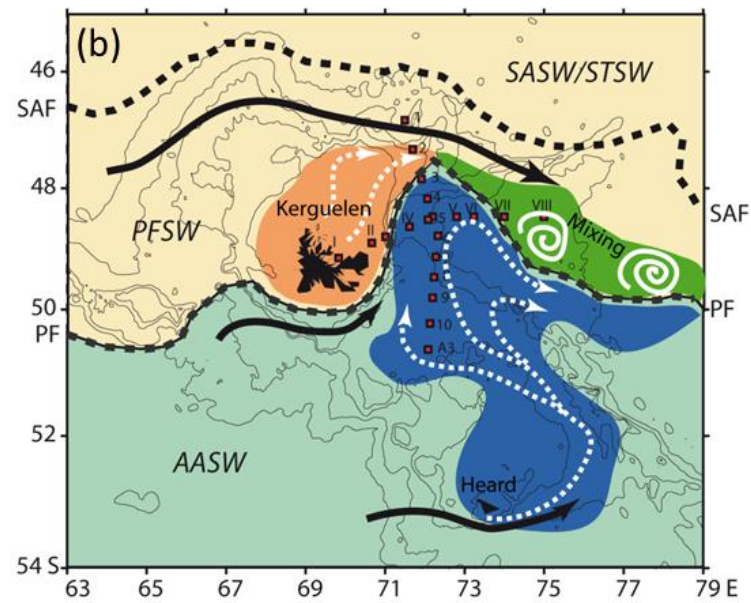
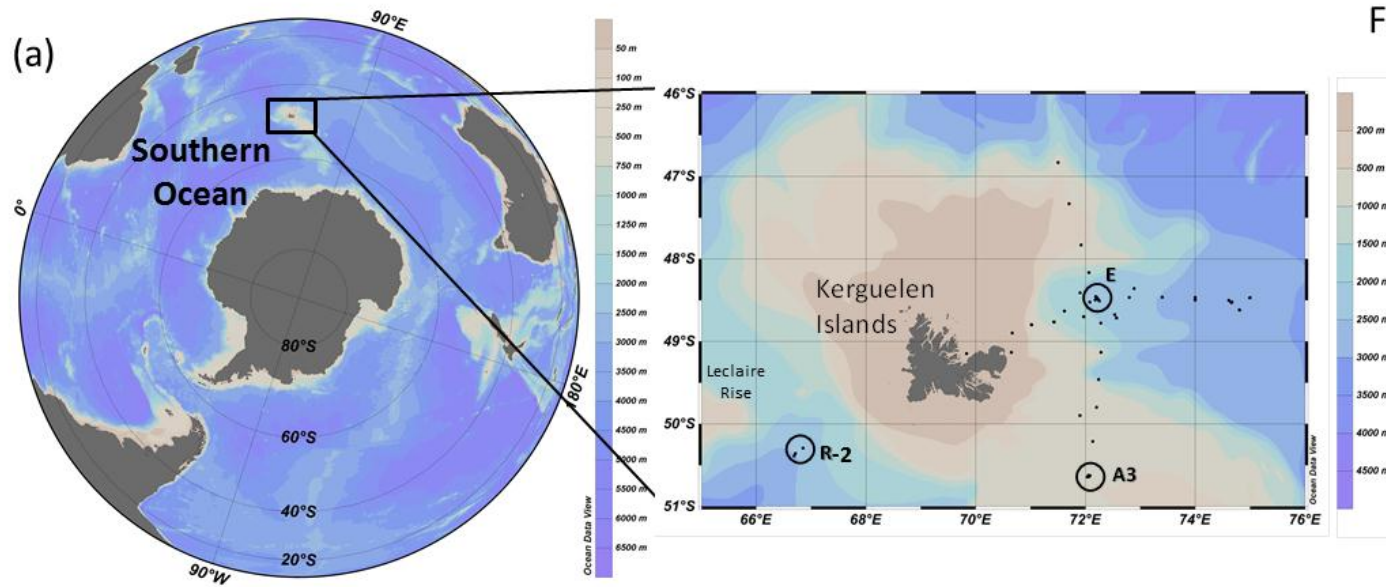
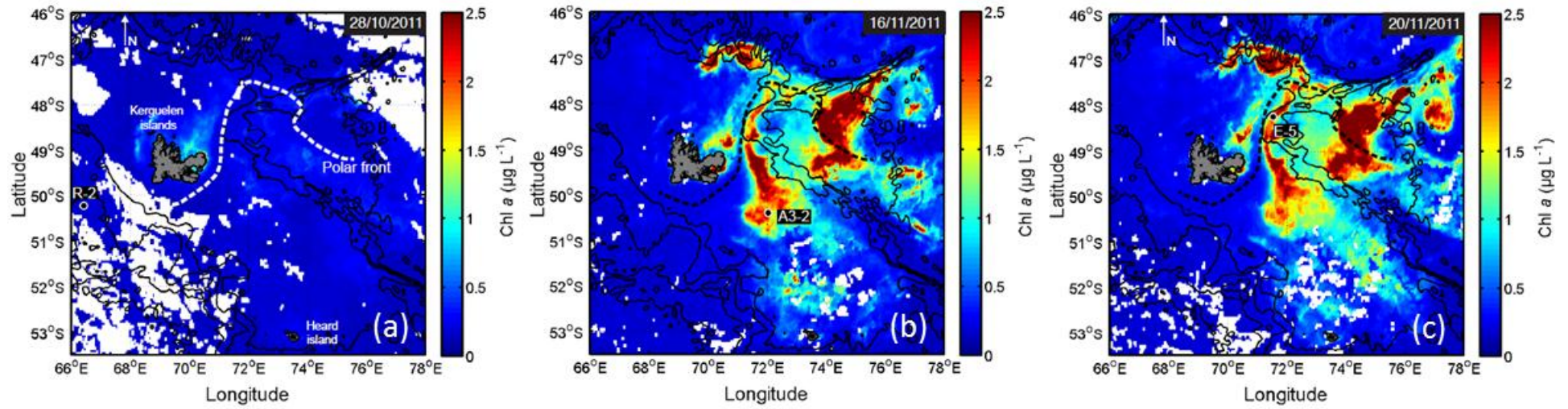


Figure 2



1
2

Figure 3a

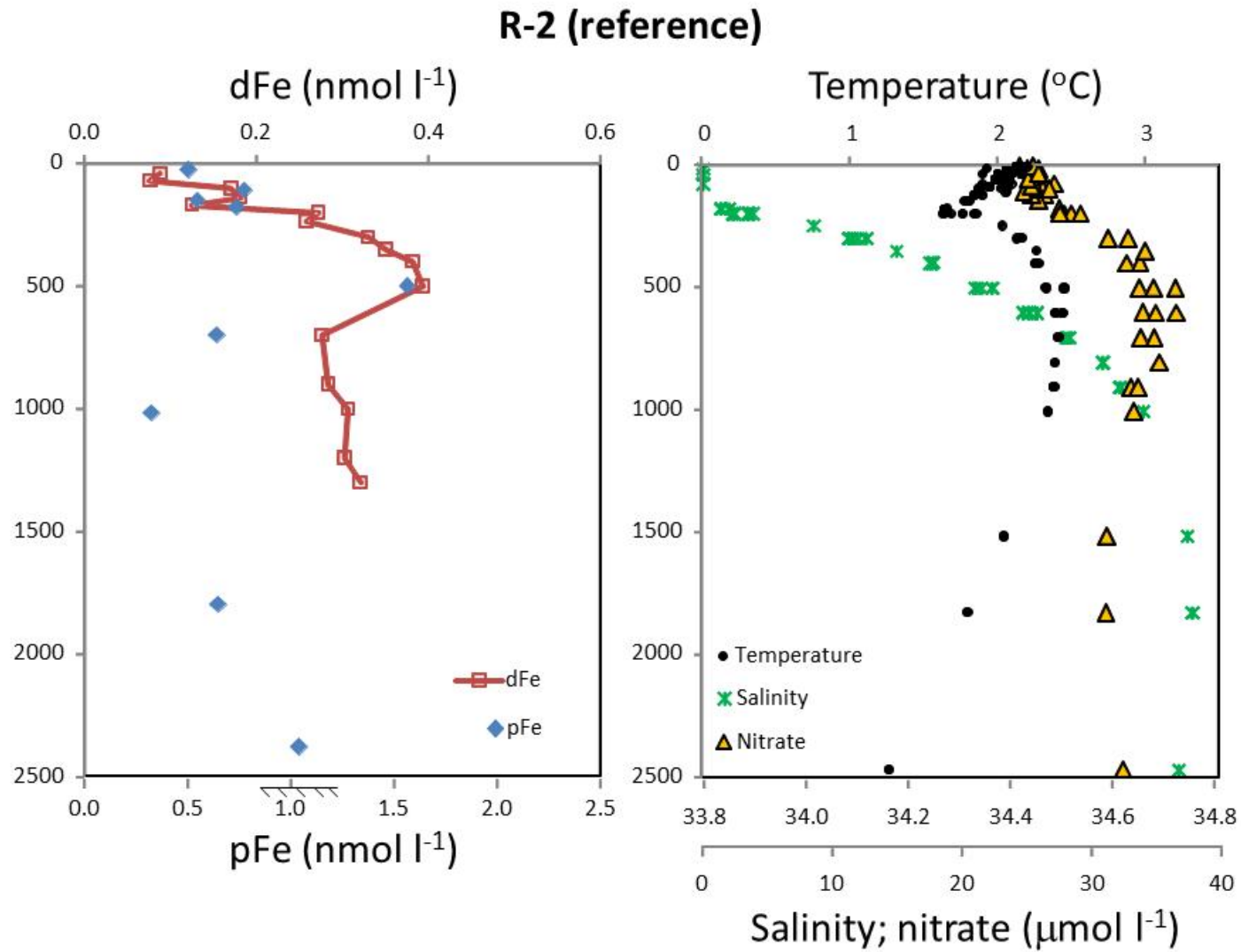


Figure 3b

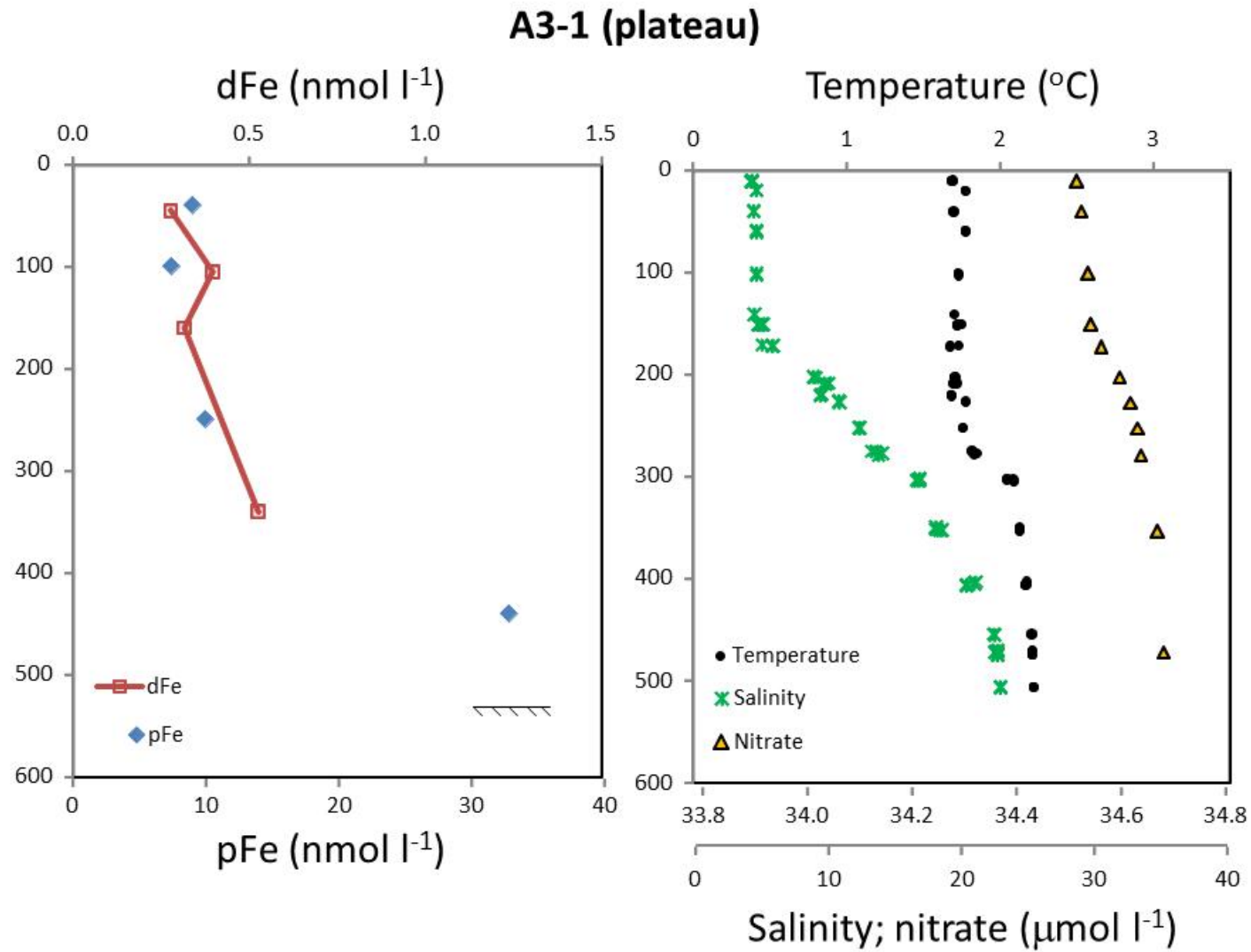


Figure 3c

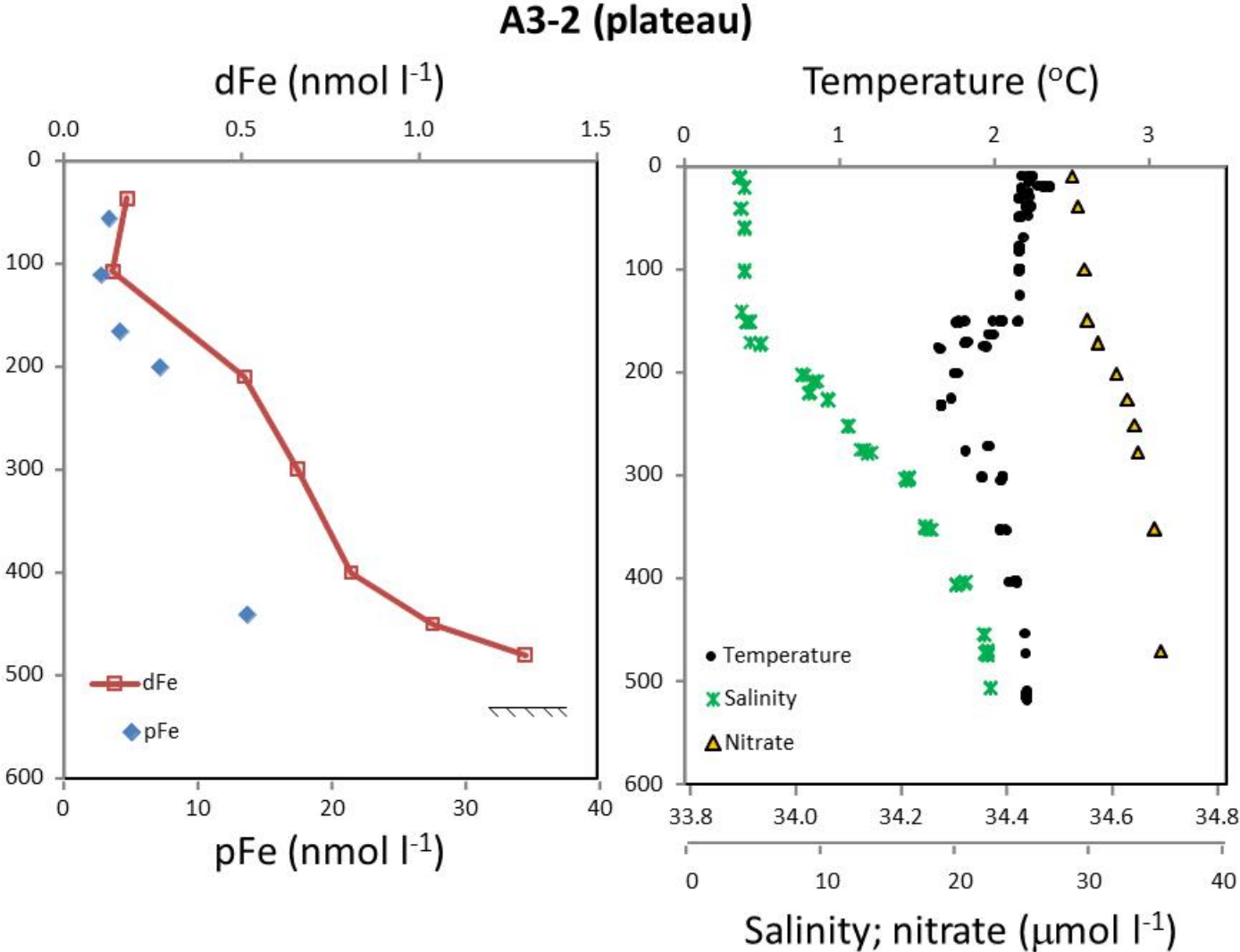


Figure 3d

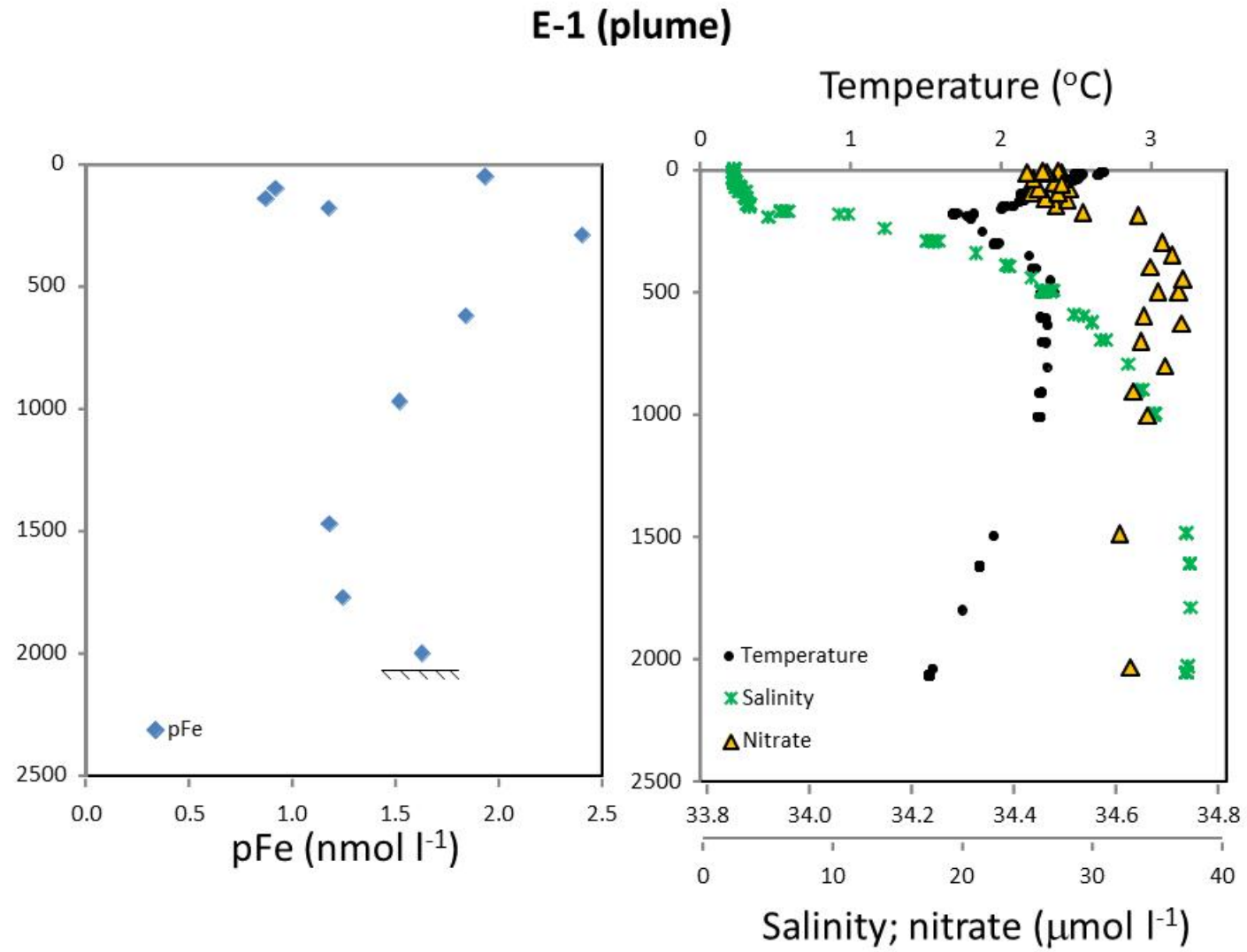


Figure 3e

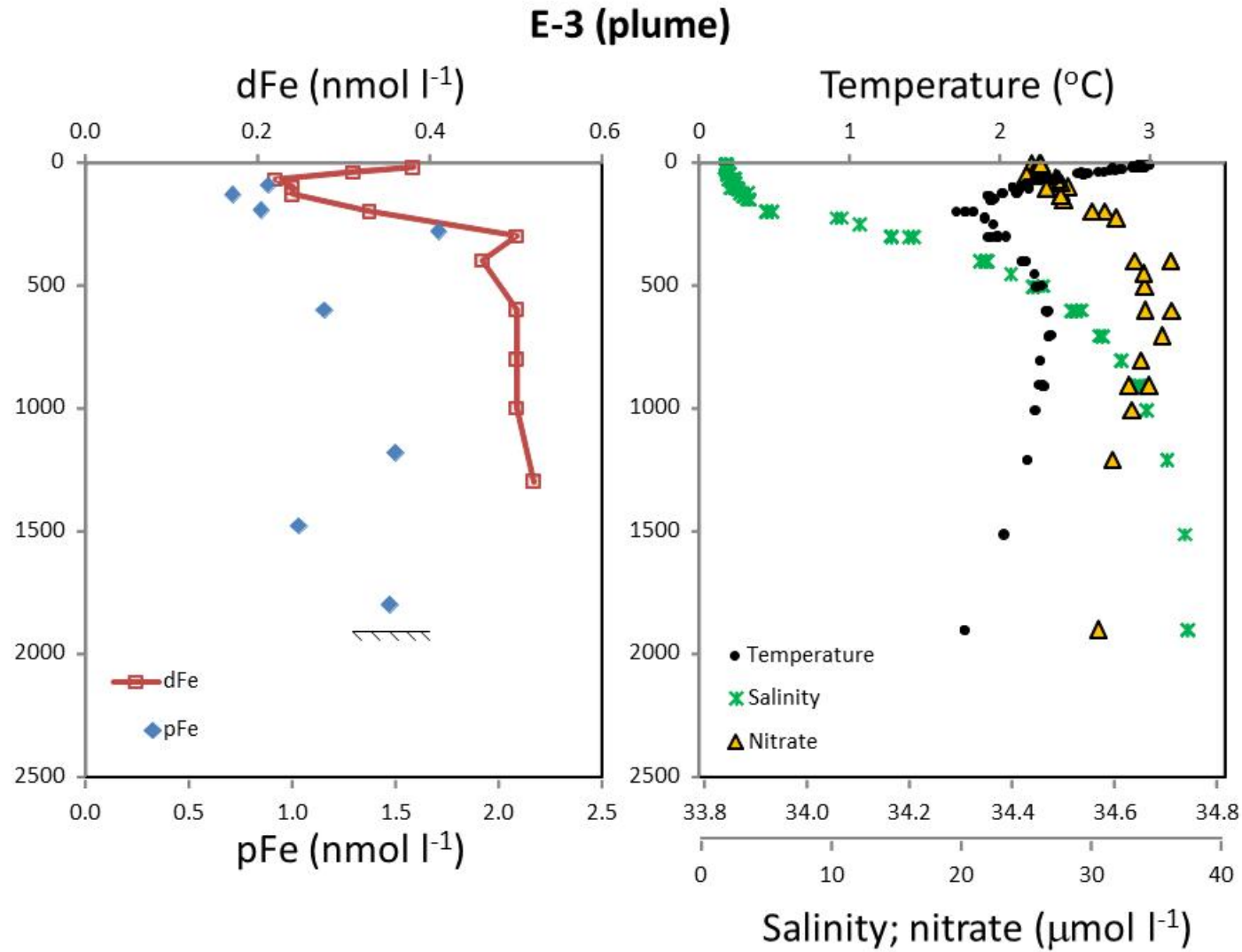


Figure 3f

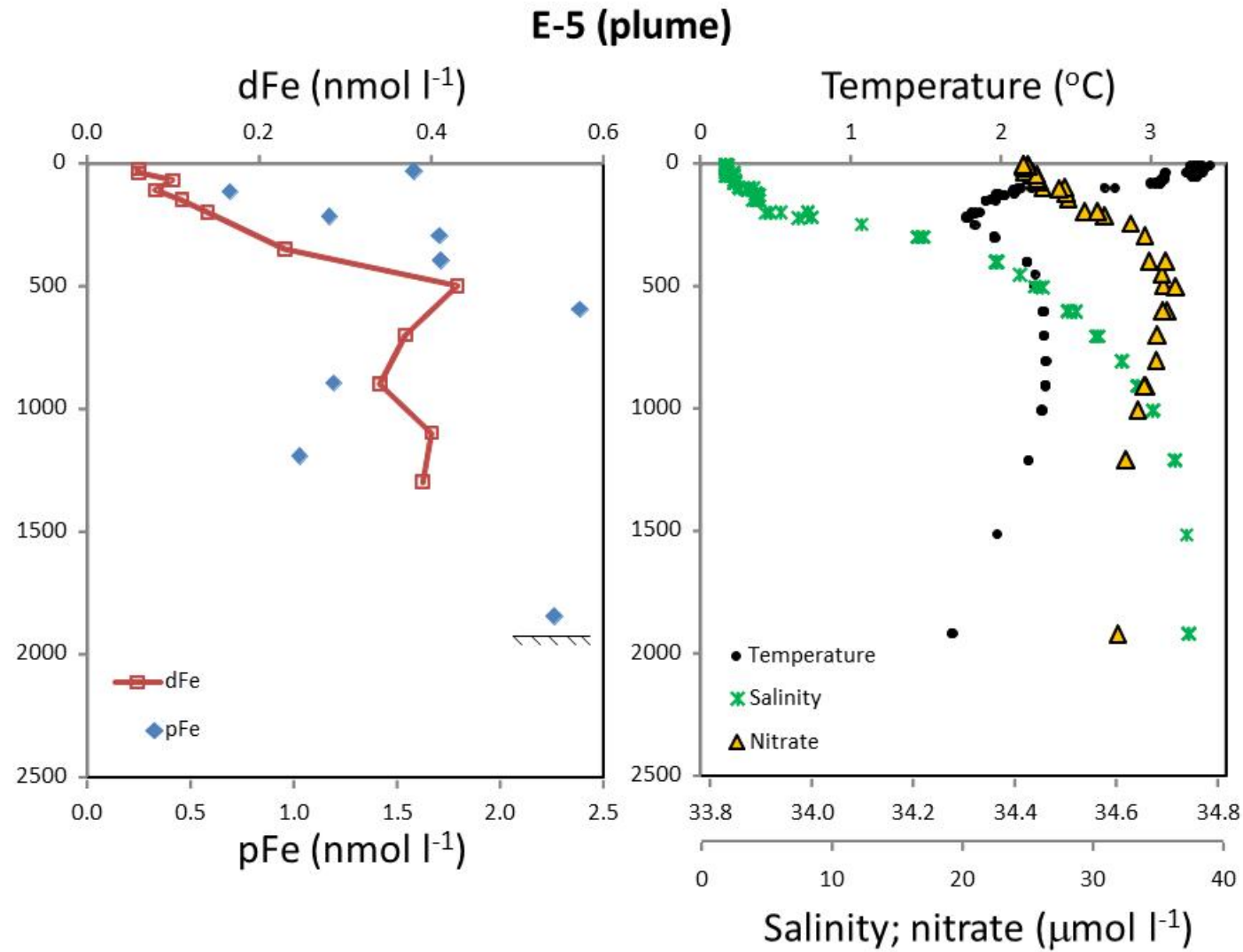
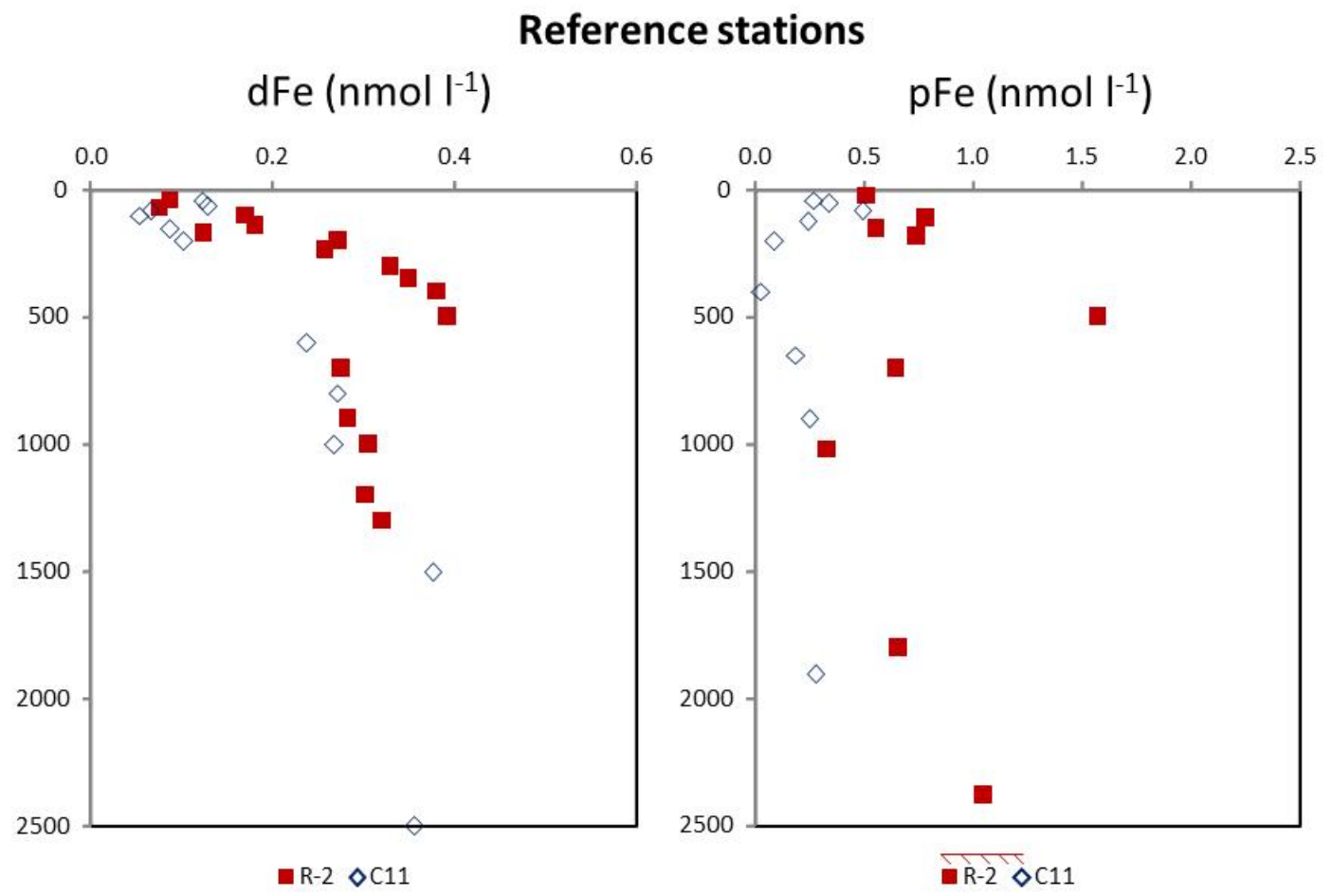
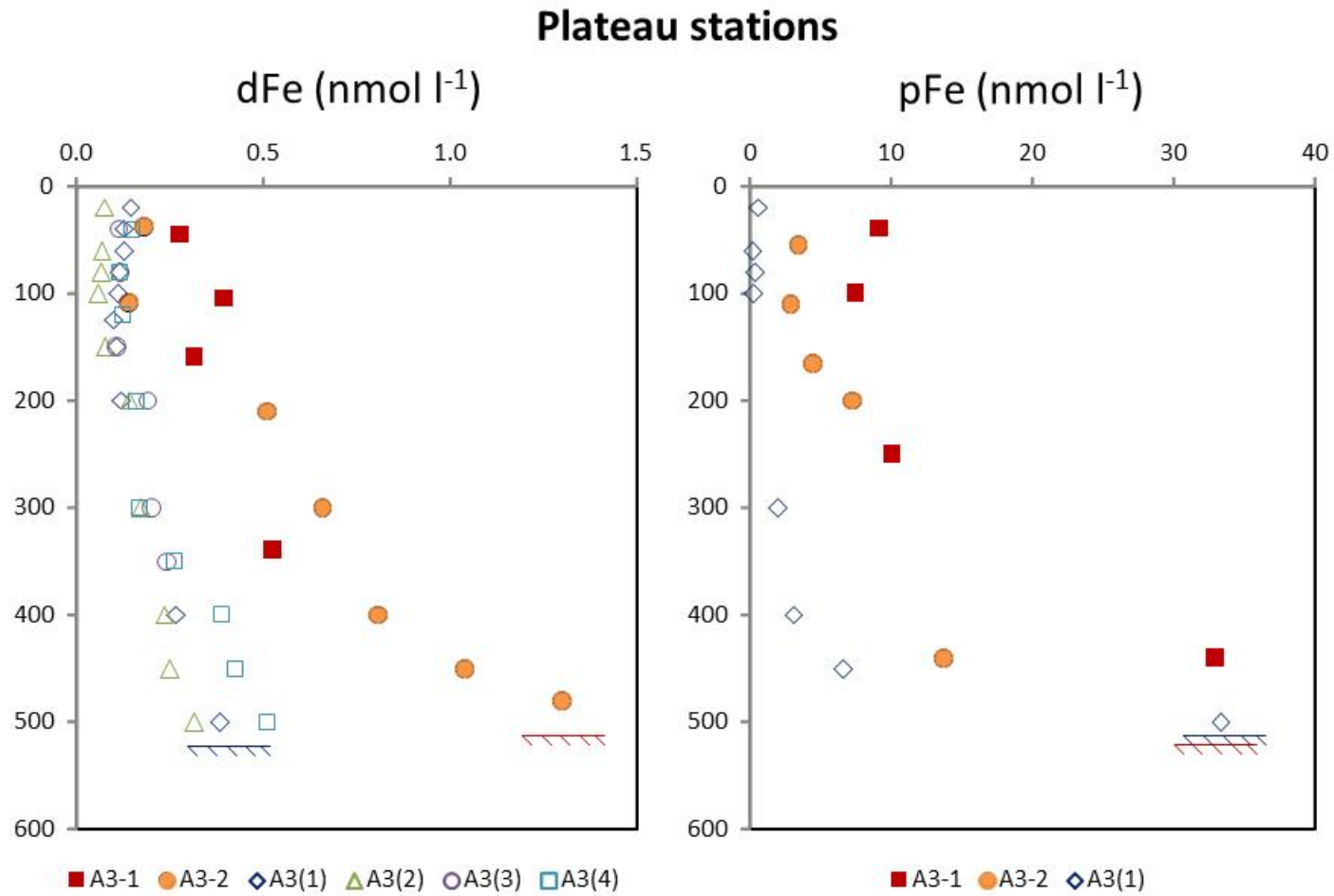


Figure 4a



1

Figure 4b



1
2

Figure 5

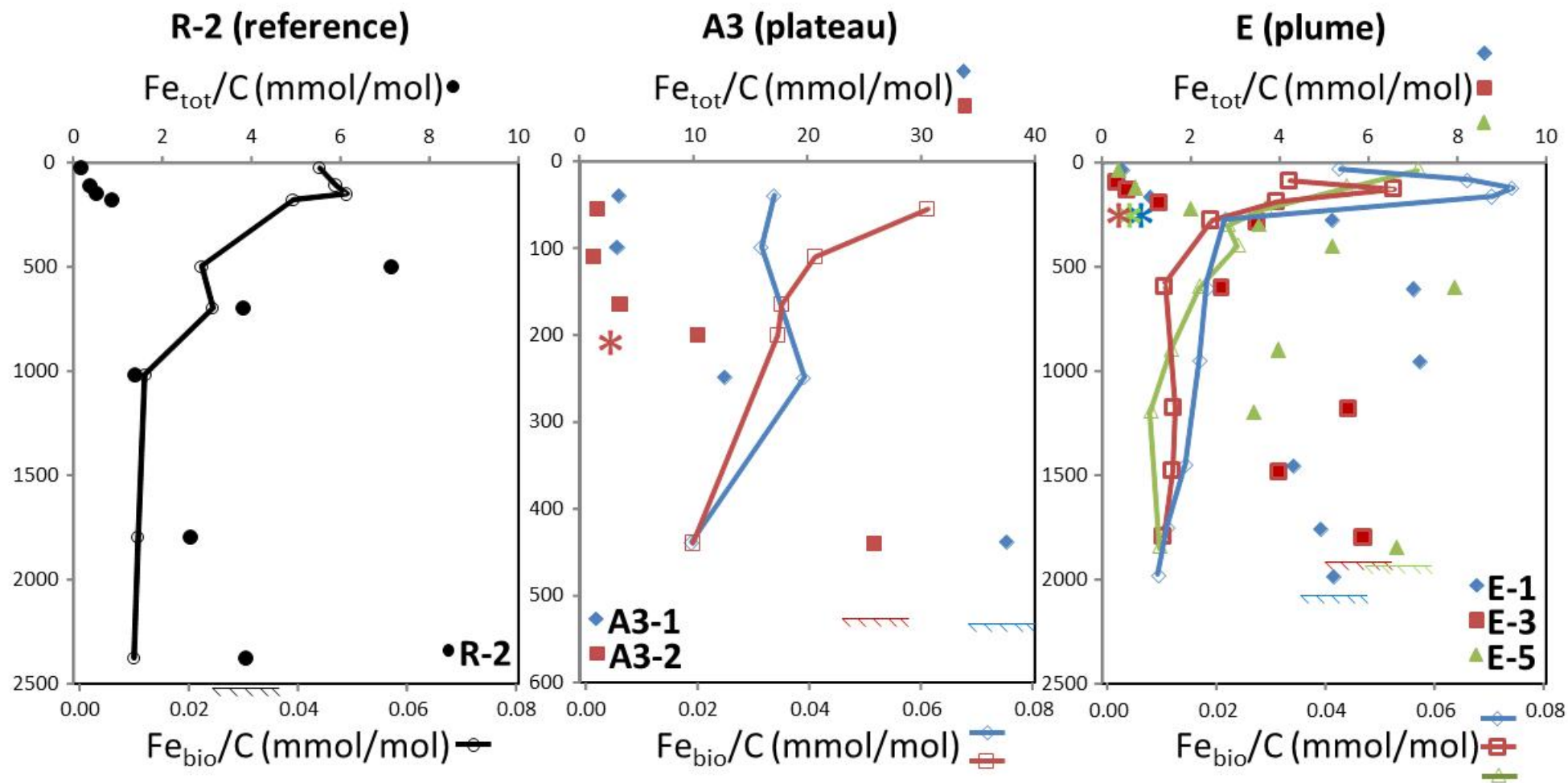


Figure 6

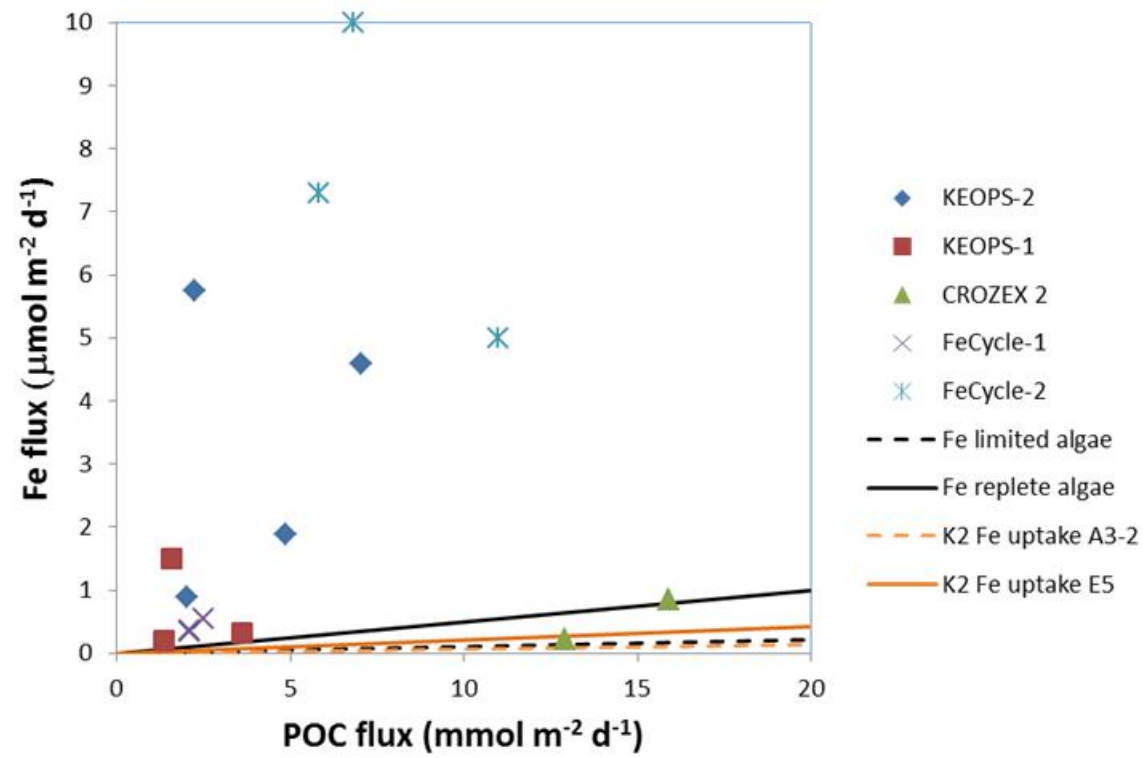


Figure 7a

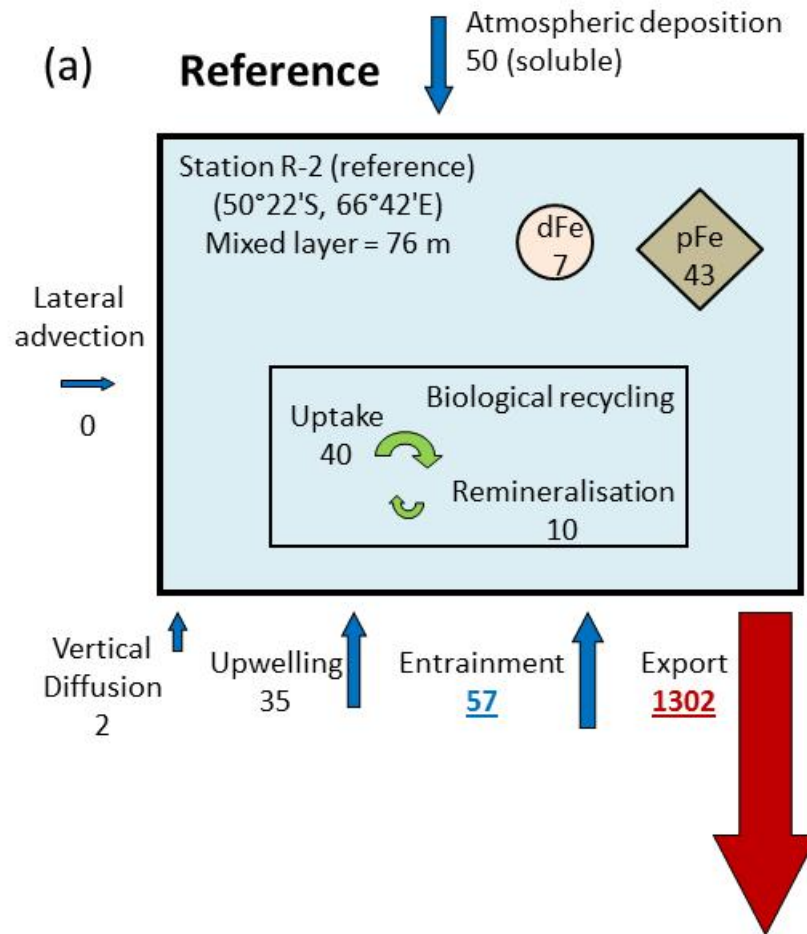


Figure 7b

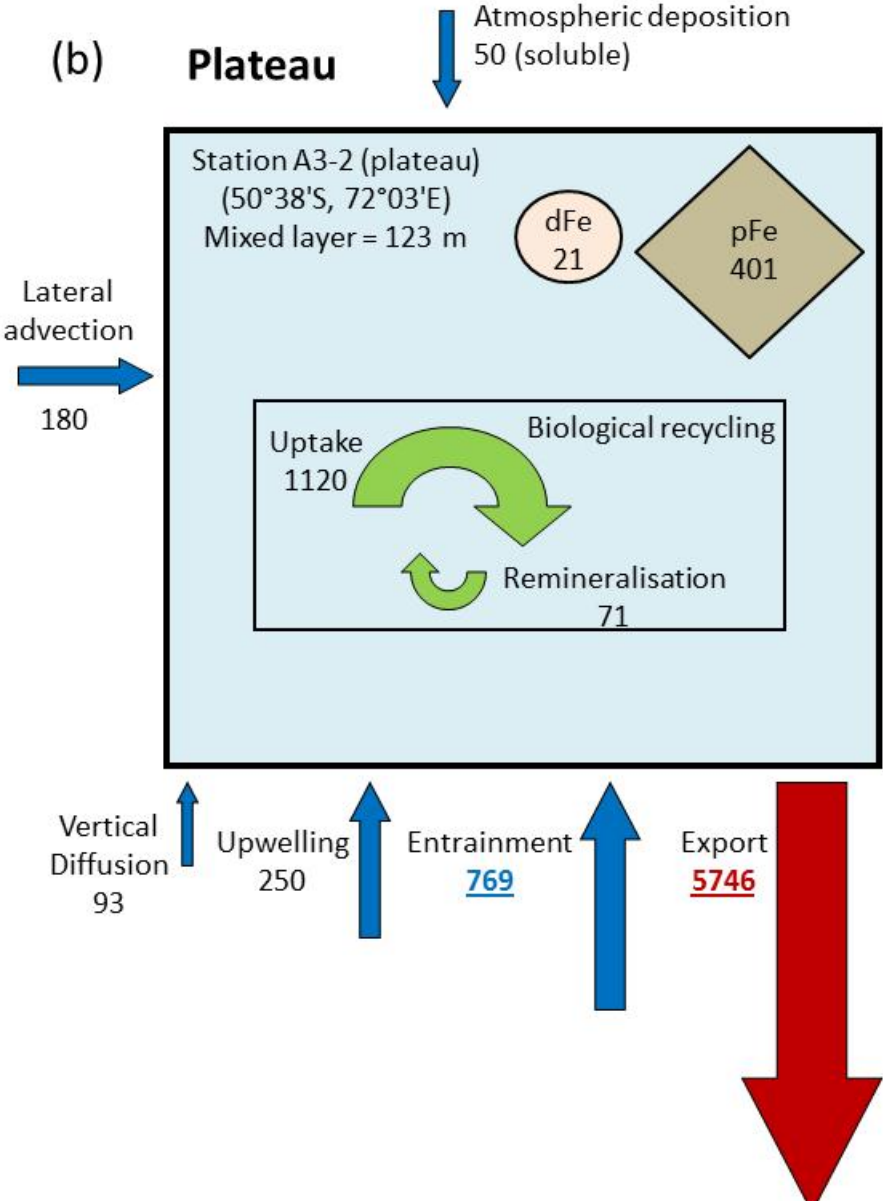
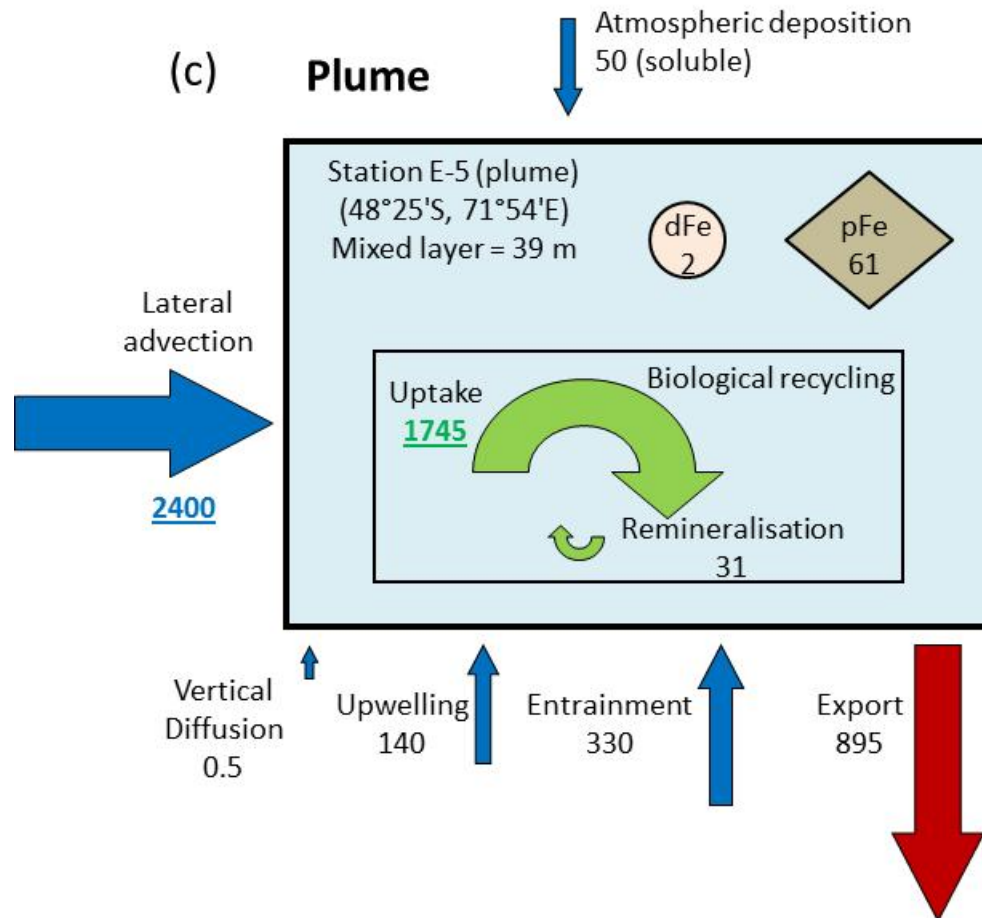


Figure 7c



1 **Supplementary material**

2 This section includes the detailed description of the method used for determination of the
3 vertical of iron supply term due to entrainment by transient (intra-seasonal) mixed layer
4 deepening. The mixed layer is subject to transient deepening due to a variety of processes.
5 Our goal here is to estimate the order of magnitude of iron entrainment into the mixed layer
6 that could be explained by these events. We assume a well-homogenized mixed layer with an
7 increase of dFe below the mixed layer (Supplementary Figure 1). When the mixed layer
8 deepens, dFe from deeper waters is introduced to the surface. The mixed layer base eventually
9 comes back to its original depth, ‘detraining’ some of the entrained dFe. The difference
10 between the original profile and the final profile is what we refer to as entrained iron. Iron
11 entrainment by a given transient event depends therefore on three parameters, namely: the
12 shape of the dFe profile (the gradient below the mixed layer); the depth of the mixed layer
13 (H); and the depth of the deepening event (H’):

$$dFe_{entrained} = \frac{H}{H + H'} \int_0^{H+H'} dFe \cdot dz - \int_0^H dFe \cdot dz,$$

14 where dFe is dissolved iron concentration, and $dFe_{entrained}$ is the amount of entrained dFe for
15 each H’ deepening event (Supplementary Figure 2).

16 To estimate the depth integrated iron amounts, we used observed dFe profiles from both
17 KEOPS cruises and associated observed mixed layer depths (Supplementary Figures 3b-3c).
18 For the plateau dFe profile, station A3 was used for both KEOPS-1 and KEOPS-2 (Figure
19 4b); for the plume dFe profile, station A11 for used for KEOPS-1 (Blain et al., 2008b) and E
20 stations used for KEOPS-2 (Figures 3d-3f). As an estimate of the order of magnitude of
21 typical H’ events in the area of the KEOPS experiment, we used the standard deviation of all
22 mixed layer estimates available in the area, computed for each month of the year from the
23 climatology of all mixed layer depth estimates. To estimate a flux, one also needs to know the
24 time frequency of the deepening events. No time series exists to document this frequency in
25 the Southern Ocean. However, we know that the mixed layer deviation H’ is related to
26 frequency of events by:

$$27 \quad [H'/std(H)]^2 = 1/2 F^{-1} \text{ (Supplementary Figure 2).}$$

28 For the purpose of quantifying an order of magnitude of entrainment, we consider here one
29 deepening event per week to a depth:

$$H' = \sqrt{7/2} \cdot std(H) \approx 1.9 \cdot std(H).$$

1 Although non-linear, deeper deepening is compensated by a smaller frequency, while
 2 shallower deepening by larger frequencies. If regular instantaneous events are concerned we
 3 have:

$$Std(H)^2 = \frac{t_0 \cdot H'^2 + t_0 \cdot H'^2 + 0 \cdot (T - 2t_0)}{T}$$

4 and thus:

$$[H'/std(H)]^2 = \frac{1}{2} \frac{T}{t_0} = \frac{1}{2} F^{-1}$$

5 If we consider all kinds of deepening events, with a Gaussian distribution, we have:

$$6 \quad f(H_0) = \frac{A}{std(H)\sqrt{2\pi}} e^{-\frac{[H_0 - mean(H)]^2}{2 std(H)^2}}, \text{ with } A \text{ being a constant.}$$

7 The frequency $F(H')$ of one event $H' = H_0 - mean(H)$, is:

$$8 \quad F(H') = \frac{f(H')}{\int_{-\infty}^{+\infty} f(x)dx} = \frac{1}{std(H)\sqrt{2\pi}} e^{-\frac{H'^2}{2 std(H)^2}}.$$

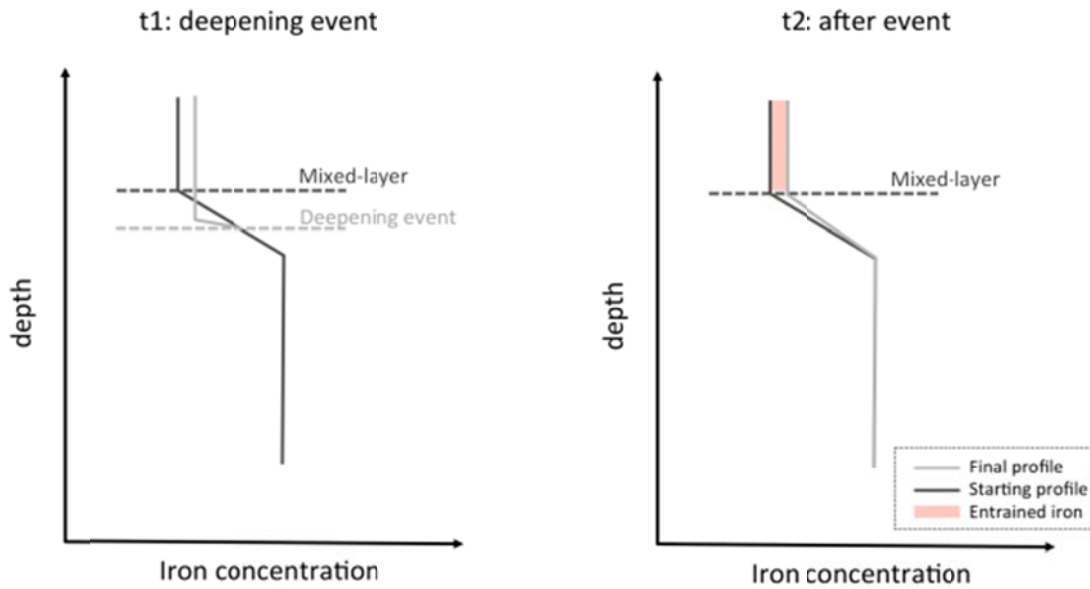
9 Thus net entrainment can be obtained by summing entrainment due to a suite of events of
 10 varying H' with: $0 < H' < 100 \cdot std(H)$, and at the associated frequency $F(H')$. We used this
 11 second approach to estimate entrainment.

12

13

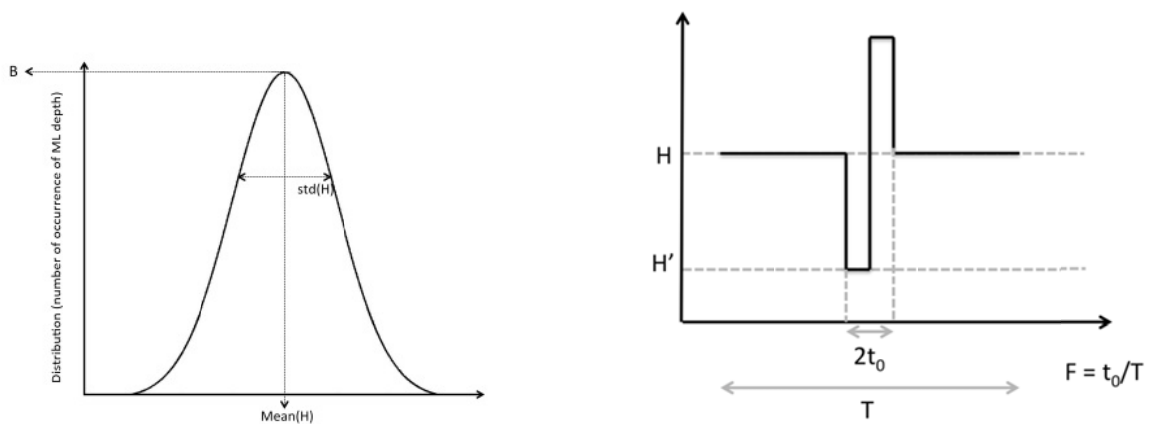
1 **Supplementary figures**

2 Supplementary Figure 1. Schematic representation of entrainment and its impact on dissolved
 3 iron concentration in the mixed layer.



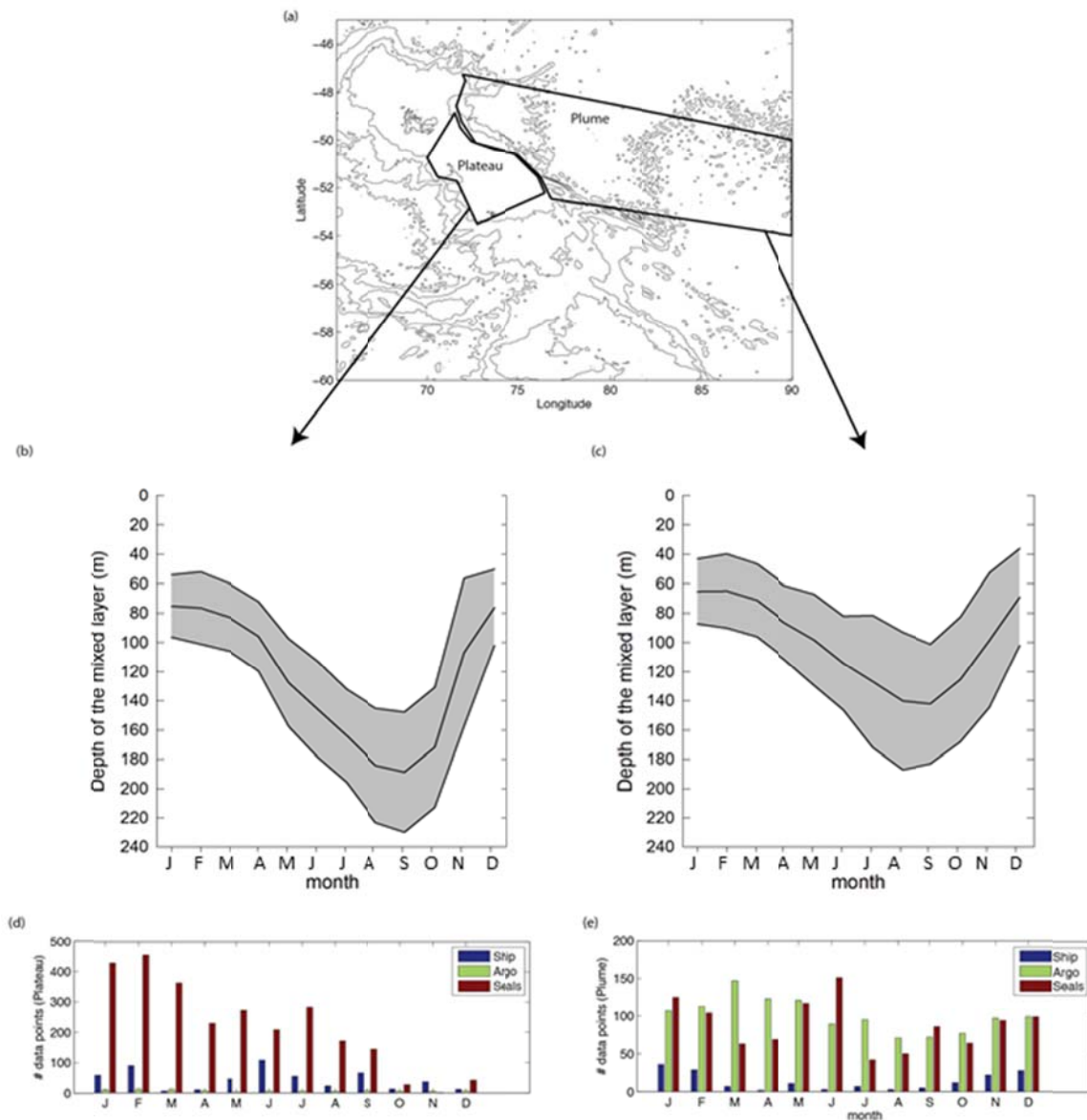
4
 5

6 Supplementary Figure 2. Plots describing the different notations used in the calculation of
 7 iron supply by entrainment. (a) Distribution of magnitudes of the mixed layer deepening
 8 events. (b) Relationships between deepening and restoration durations (t_0) and their frequency
 9 of occurrence (F).



10
 11

1 Supplementary Figure 3. Locations and origins of the vertical profiles of density used for the
 2 determination of the climatologies of the mixed layer depth above the plateau and in the
 3 plume: (a) the two regions examined; (b, c) the mixed layer depth seasonal variations (mean
 4 and standard deviations) in the plume and over the plateau from shipboard, Argo autonomous
 5 profiling float observations, and CTD sensors attached to elephant seals; (d, e) details of the
 6 available data sources for each region.



7
 8
 9